ELECTRON PARAMAGNETIC RESONANCE BIOPHYSICAL RADIATION DOSIMETRY WITH TOOTH ENAMEL

By

Rao F. H. Khan, M.Sc.

A Thesis

Submitted to the School of Graduate Studies

in Partial Fulfilment of the Requirements

for the Degree

Doctor of Philosophy

McMaster University

ELECTRON PARAMAGNETIC RESONANCE BIOPHYSICAL RADIATION DOSIMETRY WITH TOOTH ENAMEL

DOCTOR OF PHILOSPHY (2003) McMaster University

(Medical Physics) Hamilton, Ontario

TITLE: ELECTRON PARAMAGNETIC RESONANCE BIOPHYSICAL RADIATION DOSIMETRY WITH TOOTH ENAMEL

AUTHOR: Rao F. H. Khan, M. Sc. (Quaid-e-Azam University)

SUPERVISORS: Drs. Douglas R. Boreham and William J. Rink

NUMBER OF PAGES: xv, 119

Abstract

This thesis deals with advancements made in the field of Electron Paramagnetic Resonance (EPR) for biophysical dosimetry with tooth enamel for accident, emergency and retrospective radiation dose reconstruction. A methodology has been developed to measure retrospective radiation exposures in human tooth enamel. This entails novel sample preparation procedures with minimum mechanical treatment to reduce the preparation induced uncertainties, establish optimum measurement conditions inside the EPR cavity, post process the measured spectrum with functional simulation of dosimetric and other interfering signals, and reconstruct dose. By using this technique, retrospective gamma radiation exposures as low as 80 ± 30 mGy have been successfully deciphered.

The notion of dose modifier was introduced in EPR biodosimetry for low dose measurements. It has been demonstrated that by using the modified zero added dose (MZAD) technique for low radiation exposures, doses in the 100 mGy range can be easily reconstructed in teeth which were previously thought useless for EPR dosimetry. Also the use of a dose modifier makes robust dose reconstruction possible for higher radiation exposures.

The EPR dosimetry technique was also developed for tooth samples extracted from rodents, which represent small tooth sizing. EPR doses in the molars, extracted from mice irradiated with whole body exposures, were reassessed and shown to be correct within the experimental uncertainty.

The sensitivity of human tooth enamel for neutron irradiation, obtained from the 3 MV McMaster K.N. *Van de Graaff* accelerator, was also studied. For the first time this work has shown that the neutron sensitivity of the tooth enamel is approximately $1/10^{th}$ of the equivalent gamma sensitivity. Parametric studies for neutron dose rate and neutron energy within the available range of the accelerator, showed no impact on the sensitivity of the tooth enamel. Therefore, tooth enamel can be used as a dosimeter for both neutrons as well as gamma radiation. We will continue experiments to develop this endpoint as a sensitive accident or emergency tool for our response capabilities.

Acknowledgements

I'm thankful to McMaster University for providing me the opportunity to pursue my doctoral research with Medical Physics & Applied Radiation Sciences department. I'm grateful to my supervisors Drs. Douglas Boreham and Jack Rink for their guidance and support throughout my doctoral work. Their mentorship has helped me become an independent thinker and also establish a firm footing in the field of accident dosimetry. It was because of their generosity, that I have been able to attend several conferences and symposia where I presented my work in front of the nationally and internationally renowned researchers in this field. I also owe thanks to Dr. William Prestwich, who gave useful feedback about the research from time to time. I also appreciate the useful feedback of Dr. Tom Farrell on different aspects of the research.

Special appreciations are due to Dr. Fiona McNeill for her useful suggestions from time to time and helping in the experimentations regarding the Neuron Activation Analysis at McMaster Nuclear Reactor. I'm thankful to Aslam whose research on the accelerator beam proved to be a precursor of our work on neutron response categorization of tooth enamel. I would like to thank Scott McMaster and Jason Falladown for helping me run the neutron experiments at the McMaster Accelerator Laboratory.

I also take this opportunity to thank my other laboratory colleagues, Kerry Chancellor-Maddison, Beth Forrest and Karl Keizars, who made my working environment pleasant and stimulating. Thanks are due to Linda, Lorna, Mahesh, Mehran, Ryan and Sean for their help on various occasions.

I am also grateful to my parents, brothers, and sisters, back in Pakistan, for their continued support and encouragement in whole of my life particularly during the course of my Ph.D. research.

Table of Contents

List of Illustrations

List of Tables

Chapter 1

Introduction

1.1 INTRODUCTION

For many years, and especially after the Chernobyl disaster in 1986, there have been a number of radiation-related accidents in industrial radiography, radiotherapy, industrial and research irradiation facilities (Hong *et al.* 2001; IAEA 1986b; IAEA 1988; IAEA 1990; IAEA 1993; IAEA 1996c; IAEA 1996a; IAEA 1996b; Muramatsu *et al.* 2001; Sevan'kaev *et al.* 2002; Stratton 1967; Vargo 1999). Retrospective dosimetry and dose reconstruction are an important aspect of radiation related accident investigations. Dose reconstruction is the process of assessment or confirmation or revision of previous assessment of acute or chronic radiation exposure to individuals, groups or populations. Retrospective dosimetry consists of measurements conducted for dose reconstruction purposes when information provided by conventional dosimetry methods is inadequate or unavailable. Retrospective dosimetry is therefore an important element in the process of dose reconstruction (Griffith 1998). Dose reconstruction may be required in a variety of situations, such as acute accidental or deliberate exposure, suspected chronic overexposure of public groups or populations, and occupational exposure reassessment (Guo *et al.* 1998)

Retrospective dosimetry performed for dose reconstruction is important to provide input for: a) clinical prognosis, b) to help improve the understanding of the effects in man of acute and chronic exposure to high doses of radiation c) useful epidemiological support; and d) litigation and compensation purposes.

When a radiation accident from external overexposure takes place, the best possible evaluation of absorbed dose and the best possible assessments of vital prognosis are matters of urgency. Biological dosimetry, which is based on biological assays, is a necessary complement to physical and clinical dosimetry. Physical dosimetry and, particularly the reconstruction of the accident, are essential and give

important information about the dose and its distribution. However, standalone, it cannot take into account the individual's radiosensitivity and hence cannot be an exact indicator of biological consequences of the exposure. Clinical dosimetry is based on the observation of the delay, the intensity, the frequency and the duration of the early and transient neurovegatative symptoms, such as nausea and vomiting, fatigue, headache, diarrhea, hypertension, hyperthermia and blood cell counts. Although it can give interesting data, it can be perturbed by different factors associated with the exposure and the individual.

Over the past 50 years, a wide range of techniques have been employed for dose reconstruction and retrospective dosimetry. Some of them are well established for the last 30 or so years, whereas some new techniques have shown potential to act as biological markers of radiation. These can be divided into the following four categories:

a) *Biophysical techniques*, lie at the frontier between physical and biological dosimetry, and result in both dose measurement along with the complementary biological response. It is usually done either by gamma spectrometric method (Knoll 2001), Electron Paramagnetic Resonance, (EPR) (Romanyukha *et al.* 2000a), Thermoluminescence dosimetry, (TLD) (Guo *et al.* 1998), or Optically Stimulated Luminescence, (OSL) (Kubelka *et al.* 1999; Oliveira *et al.* 1991).

b) *Classical techniques* can give an estimation of the mean biological dose such as electroencephalography, (EEG) (Court *et al.* 1986), lymphocyte counting (Dehos *et al.* 1986), and unstable chromosome aberrations in lymphocytes (IAEA 1986a).

c) *Biochemical indicators*, such as amino acids, enzymes etc, can also provide vital prognosis after irradiation in mixed field (Lushbaugh *et al.* 1991).

d) *Cytogenetic techniques*, such as Fluorescence in situ hybridization, (FISH) (Darroudi & Natarajan 2000; Darroudi 2000; Edwards 2000), Micronucleus assays (Almassy *et al.* 1987; Chang *et al.* 1999), Apoptosis detection (Wang *et al.* 1999), Glycophorin A (GPA) (Jones *et al.* 2002), and Premature chromosome condensation (PCC) (George *et al.* 2002), have been in for the measurement of retrospective exposures over the past ten years.

All above mentioned techniques require a dosimeter material which could provide some kind of observable response due to radiation exposure. The available materials for dose reconstruction vary from quartz, clothes, buttons, watch glasses (Dalgarno & Mcclymont 1989) to various human tissue such as hair, fingernail, feces, urine, tooth, bones, tissues, and blood (Gerber *et al.* 1961). These materials show a

different type of response and the quantity of the response is dependent on the degree of radiation exposure. To be a useful accident dosimeter, a material should posses the following qualities:

i. The radiation dose response must be well-known for the dosimeter and easily observable.

ii. There must be no dose rate effect for the radiation under consideration, and possibly a flat energy response.

iii. It should be sensitive for both low and high exposures and useful for protracted or acute radiation exposures.

iv. The radiation damage must remain stable over a reasonably long time after radiation exposure.

v. It must be useful for the measurement of dose in a radiation field consisting of various radiation qualities.

vi. An *in vivo* dosimeter is preferable, so that individual dose measurement could be obtainable in terms of tissue dose.

vii. The dose reconstruction should possibly be non-invasive and non-destructive without sacrificing the major sample so that multiple and inter-laboratory reconstruction be possible.

As summarized in Table 1.1 most of the currently developed cytogenetic techniques (Darroudi & Natarajan 2000; Moquet *et al.* 2000) have their limitations. First they can not provide the physical measure of doses and secondly they have strong dependence on the dosimetric response of the individual (Bothwell *et al.* 2000). Accident dosimetry using biological systems, in which the quantification of chromosome aberrations or the ratio between different blood proteins can give an indication of exposure, is hampered by the individual characteristics of the victim (i.e. general health, diet, etc) and by the complexity of the techniques. These problems can be avoided by adopting a more physical approach, and both chemiluminescence and thermoluminescence of possible dosimeters, for example, have been found to be useful. The drawbacks here concern the solubility with chemiluminescence, the amount of sample required for thermoluminescence, and impossibility of taking repeated measurements with either system.

Table 1.1 Comparison of various biophysical and cytogenetic techniques on human tissues (such as blood and tooth) (Fatome *et al.* 1997; Romanyukha & Regulla 1996; Prasanna *et al.* 1997).

Category	Techniques	Detection	Preparation & analysis time	Stability
Biophysical	Gamma spectrometry	Activated trace elements	Several days	Half-life of marker
	EPR	Paramagnetic centre in bones and tooth	Several days	> 10 million years
Cytogenetic	Conventional	Dicentrics & acentric fragments	Several days	3 months
	FISH	Unstable & stable abnormalities	1 - 2 days	6 months to years
	Micronuclei	Unstable abnormalities	1 day	3 months

More recently developed biophysical dosimetry, based on EPR spectroscopy and solid samples of teeth or bones from the exposed victims, may complement biophysical dosimetry as far as accuracy, reliability, and simplification of evaluation technique is concerned. EPR based dose reconstructions are based on the assessment of radiation-induced radicals in hydroxyapatite, which is the mineral component of teeth and bones.

1.1.1 Tooth as an accident dosimeter

Dental enamel is the only tissue in the human body whose structure and composition is essentially constant with time (Aldrich *et al.* 1992; Desrosiers *et al.* 1989). The stable radical species produced in tooth (enamel, dentine and cementum) is CO_2^-, which has a reported lifetime of 10^7 years at 25 °C (Schwarcz 1985). The paramagnetic centres in hydroxyapatite are found to be thermally stable up to 200 °C (Hennig *et al.* 1981). The CO_2^- radical concentration increases linearly with dose up to 30 Gy (the region of interest for accidental doses), after which the response is still well known and it saturates at higher doses of 3 kGy (Grun & McDonald 1989; Grun 1996; Rink & Schwarcz 1994). EPR readout is non-destructive, which allows repeated signal evaluation and thus documentation of the dose information by storing the original sample (Romanyukha & Regulla 1996)

Compared to bones, tooth enamel (due to larger fraction of mineralized apatite) offers higher radiation sensitivity, and it is not subjected to metabolic deactivation of hydroxyapatite paramagnetic centres (Desrosiers 1991).

The radiosensitivity of enamel, dentine and cementum can be described by the ratios 7:3:1 respectively. This is because the dentine, like bone, contains a large organic fraction (collagen, 20%), whereas enamel has 99.5% hydroxyapatite crystals. The organic contents lead to a signal that overlaps the inorganic fraction and thus decreases the detection limit (Haskell *et al.* 1995). Because of the organic contents of tooth and bones, thermoluminescence dosimetry can not be performed (Chapman *et al.* 1979).

To date there is no reported dose rate effect observed in tooth enamel which is true for acute as well as chronic exposures. For photon irradiation from 58 to 1250 keV, no energy dependence of tooth enamel signal intensity is observed within experimental uncertainty (approximately 2%) (de Oliveira *et al.* 1999). For a known absorbed dose, a similar flat response was observed for various energy electrons for tooth enamel.

A tooth is an individual *in vivo* dosimeter, which is important due to heterogeneities of the dose pattern and variability of individual behaviors. The individualization of dose construction is an important and desirable feature (Voight & Paretzke 1996).

Except for gamma rays and electrons, a different sensitivity of tooth enamel has been seen for different radiation qualities such as proton, alpha and heavy ions (Copeland *et al.* 1996; Ivannikov *et al.* 1997; Romanyukha *et al.* 1994; Romanyukha & Regulla 1996; Romanyukha *et al.* 1996c; Schauer *et al.* 1994; Stuglik *et al.* 1994; Stuglik & Sadlo 1996; Wieser *et al.* 1994). Therefore, tooth enamel can respond to a mixed radiation field.

Dose in the tooth is close to the organ doses or effective doses for some cases, which avoids unnecessary dose conversions. Some investigators have shown that the dose distribution in the oral region can give useful information for the investigation of the orientation of a human body towards an external radiation source (Takahashi *et al.* 2001).

EPR dosimetry particularly offers the potential to discriminate between the dose components from external photons and internal β emitters, at least for short ranged β particles. This can be achieved by separate determination of the dose components from the enamel, dentine and the surrounding bone (Romanyukha *et al.* 1996b). The considerable difference from the dose constructed out of these can give strong indication of the presence of and dose contribution from the internal β emitters.

Tooth dosimetry is invasive, as tooth is required to be extracted from the individual; however, dose reconstruction could still possibly be non destructive without sacrificing the whole sample (Haskell *et al.* 2000; Yamanaka *et al.* 1993).

The sensitivity of the technique and accuracy of the results adequately complies with particular post accident scenarios. Results produced by this technique have been consistent with other independent dosimetric methods and internal standards and are reproducible at different times (Hayes *et al.* 1998a; Hayes 1999).

1.2 ELECTRON PARAMAGNETIC RESONANCE – PHYSICAL BASIS

In 1921, Stern and Gerlach observed that an atom in a magnetic field, can take discrete orientation (Wertz & Bolton 1972). Later in 1925, Uhlenbeck and Goudsmit proposed a new intrinsic property of electrons called spin. The unpaired spin in the outer shell of an atom gives rise to the paramagnetic properties of matter.

Quantum mechanically, an electron has an intrinsic angular momentum described by the spin of an electron (½ in units of ħ). In a magnetic field, the ground state energy level of an atom splits, which is based on the Zeeman effect (Schiff 1968). The electron orients itself such that only two states are possible (as in Fig. 1.1), either spin up (parallel to the magnetic field) or spin down (anti parallel to the magnetic field) given by spin magnetic quantum number, m_s, i.e. 2S+1 values ±S (+½ to –½).

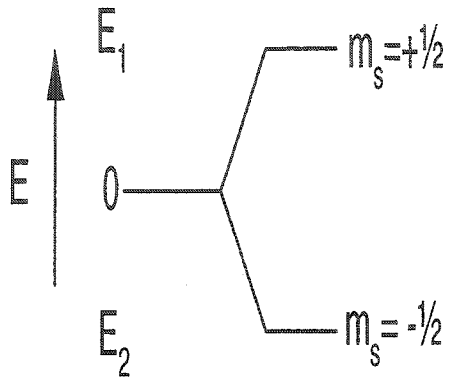

Fig. 1.1 Splitting of the ground state of an atom in an external magnetic field.

In the absence of an applied magnetic field, unpaired electrons of paramagnetic species can occupy either of the two spin states (m_s = +½, -½). However, in the presence of a strong magnetic field, H, one of these states becomes more energetically favored. A greater number of spins are found in the lower state. Simultaneous application of electromagnetic quantum of appropriate frequency ($\Delta E = h\nu$ where υ typically >2 GHz), corresponding to the energy difference between spin states $\Delta E = g_e \beta_e H$, causes a spin flip transition to higher energy state. The quantity $\beta_e = \frac{e\hbar}{2mc} = (9.274096 \pm 0.00065) \times 10^{-24} J/T$ is called Bohr magneton, and g_e is called the Landé factor. Absorption of applied electromagnetic radiation is detected by an EPR spectrometer and after suitable amplification it is displayed as the first derivative of the microwave absorption curve with respect to the magnetic field.

Absorption resonance spectra are characterized by their position, (given by Landé factor g) signal width, and intensity in the magnetic field and microwave energy absorption space. The g factor is expressed as a function of microwave frequency and the magnetic field H at resonance $g = \frac{h\nu}{\beta_e H}$, which makes a signal machine independent. The g values are defined for free radicals in atoms, molecules, and crystals and depend on their electronic structure (Fischer 1965). Table 1.2 shows typical parameters for the

signals produced in tooth. Special compounds with precisely known g values are used as standards (Knowles *et al.* 1976).

Table 1.2 Dosimetric, native and Mn^{++} standard signals and their parameters used in the study of tooth enamel EPR (Ikeya *et al.* 1986; Rossi & Poupeau 1990; Schwarcz 1985).

Species	g values (signal width)
Native	2.005 (0.9 - 1 mT)
CO_2^-	$g_{\perp}$ = 2.0018 (0.4 mT)
	$g_{//}$ =1.9973 (0.3 mT)
Mn^{++} marker:	
3rd line	2.0370 (0.14 mT)
4th line	1.9851 (0.14 mT)

1.2.1 EPR in tooth enamel

Tooth enamel consists of a small organic part, collagen and 97 – 98 % inorganic part, the biomineral hydroxyapatite $Ca_{10}(OH)_2(PO_4)_6$ (Driessens & Verbeeck 1990). During the mineralization process of biological apatites, carbonate ions are incorporated into the crystalline lattice substituting for both phosphate and hydroxyl ions, which gives rise to carbonated apatite.

Upon absorption of ionization energy by carbonated apatite, carbonates capture free electrons in the crystal matrix to form free radicals centre (Callens *et al.* 1987). The physics of defect formation in apatite is rather complicated due to a large unit cell structure and symmetry involved (Brown & Chow 1976). However, knowledge of the nature of EPR signal is a prerequisite for a systematic evaluation of the quantitative and qualitative properties of tooth enamel. Radiation induced defects in synthetic and biological apatite have been studied by various investigators and the stable radiation induced defects are ascribed to the CO_2^- radical (Callens *et al.* 1998; Ishii & Ikeya 1990).

A typical EPR spectrum is shown in Fig. 1.2. In the region of interest near g = 2, in untreated tooth enamel, there are generally two types of radical species giving rise to EPR absorption of microwave power. These are commonly referred to as native (Pass & Aldrich 1985), believed to be produced due to organic contents of enamel and radiogenic dosimetric signal arising from CO_2^- radicals.

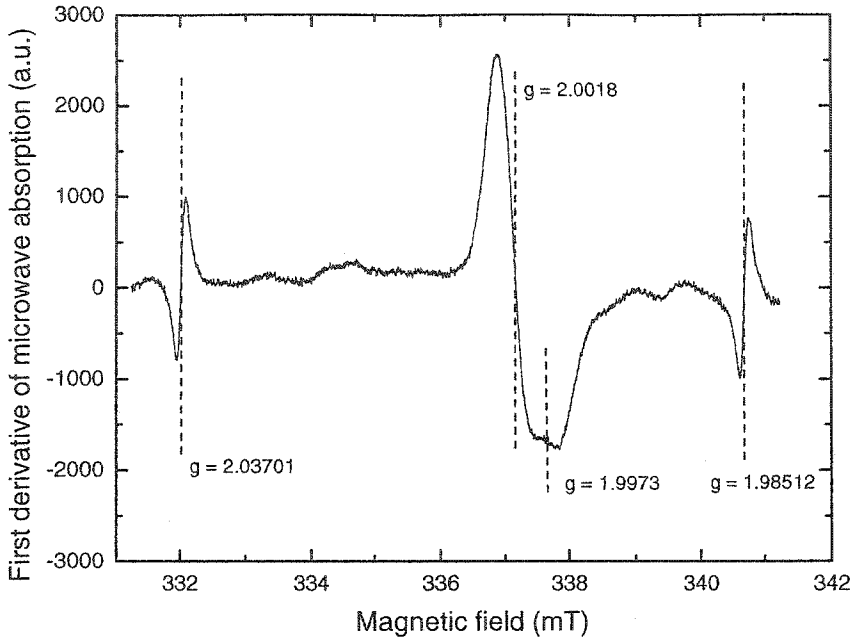

Fig. 1.2 A typical EPR spectrum from tooth enamel, where the first derivative of microwave absorption is plotted with the magnetic field intensity. Dosimetric signal (g = 2.0018 & 1.9973), and Mn^{++} standard (g = 2.0370 & 1.9851) are shown.

1.3 CHRONOLOGICAL DEVELOPMENTS IN EPR DOSIMETRY

Gordy *et al.* (1955) were the first to observe ionizing radiation dependent stable resonances in irradiated skull bone. Since the first dose reconstruction in 1968 by Brady and co workers, (Brady *et al.* 1968), EPR dosimetry developed over time essentially based on the general guideline used in geological dating (Grun *et al.* 1996; Rink 1997).

EPR dose reconstruction in A bomb survivors led to the transition from the field of geological dating and geochronology to retrospective accident dosimetry using various materials (Ikeya *et al.* 1986; Ikeya & Ishii 1989; Haskell *et al.* 1996).

The Chernobyl accident in 1986 catalyzed research in many areas of environmental and health sciences. One of these fields which received remarkable impetus was dosimetry, in particular retrospective dosimetry. The requirement of reliable retrospective dosimetry of populations exposed to the Chernobyl radiation, particularly cleanup workers, residents, evacuees, and liquidators, prompted extensive scientific

and technological investigations aimed at making EPR dosimetry usable for routine dose reconstruction. A large number of studies and applications of EPR dosimetry, found in the literature, have been published in this post-accident era (Chumak *et al.* 1998; Chumak *et al.* 1999; Chumak *et al.* 1997; Ivannikov *et al.* 1997; Romanyukha *et al.* 1994; Romanyukha *et al.* 1996a; Romanyukha *et al.* 2000b).

EPR dosimetry with tooth enamel has also proved to be a useful tool for accident dose reconstruction (Aldrich & Pass 1988; Hutt *et al.* 1996; Ikeya *et al.* 1996; Inaba 2000; Pass 1997; Rossi *et al.* 2000; Shiraishi *et al.* 2001; Shiraishi *et al.* 2002; Skvortsov *et al.* 2000; Tatsumi-Miyajima 1987), epidemiological studies, and environmental overexposures (Degteva *et al.* 1994; Degteva *et al.* 1998; Ivannikov *et al.* 2002; Mel'nichenko *et al.* 2002; Romanyukha *et al.* 2001)and has been found useful in radiotherapy dose verification (Iwasaki *et al.* 1998; Pass *et al.* 1998).

1.4 THESIS LAYOUT

This monograph consists of a series of investigations into the utility and applicability of tooth enamel in the solid state dosimetry of ionizing radiations for the measurement of accidental radiation exposure. Tooth enamel dosimetry was developed in the specialized field of electron paramagnetic resonances EPR (also called electron spin resonance, ESR) spectrometry. This methodology was evaluated for the human tooth, neutron response of the human tooth and tooth extracted from rodents (mice).

This work addresses the problems in designing the protocol for EPR dose reconstruction at low doses and small sample masses (Khan *et al.* 2002a). Under the aforementioned limitations there exist problems and uncertainties related to the measuring equipment as well as the sample configuration. The main characteristics of the research include a) sample preparation, b) cavity response determination for a given sample mass with the help of in-cavity standards, c) optimization of spectrometer/ machine parameters, d) signal anisotropy accounting, e) post-measurement spectrum processing, and f) accident dose reconstruction. Chapter 2 describes the investigations done with human tooth enamel, in development of a protocol for the dose measurement in humans for exposures as low as 100 mGy. The main objective behind this exercise was to develop an optimized set of rules for the accidental or environmental exposure evaluation in tooth enamel at McMaster University (Khan *et al.* 2002c).

After the design and testing of protocol, further investigations were carried out for the neutron response of human tooth enamel, which was hitherto unknown. Various experiments were designed to see the effect of different variables useful for dose reconstruction (Khan *et al.* 2003a). Chapter 3 describes the sets of experiments performed using the neutron beam from the McMaster *Van de Graaff* accelerator.

Chapter 4 explains the use of rodent teeth for the situations where the involvement of humans is not certain, or involving high environmental exposures (Khan *et al.* 2002a, Khan *et al.* 2003c).

Chapter 5 describes the concept of modified added dose and represents a novel change in the dose reconstruction protocol, which makes it possible to measure very low exposures without enhancing the sensitivity of the EPR spectrometers (Khan *et al.* 2003b).

The conclusion summarizes the salient features and major achievements from this research in human tooth, neutron response categorization, mice enamel dosimetry and new approach to dose reconstruction. In addition, major grey areas have been pinpointed for research and development, which may be useful for establishing the accident biodosimetry *gold standard.*

Chapter 2

EPR Dose Measurement in a Human Tooth

2.1 INTRODUCTION

The effect of ionizing radiation exposure on a tissue is the deposition of energy in the form of electron-hole pairs. The electron and hole thus formed are captured by various molecular species in the tissue which in turn lead to the formation of unpaired spins also called free radicals. In an ordinary human tissue these radicals diffuse through and produce biological effects (BEIR VI 1999). Although radicals can be produced in a variety of different tissues, in many circumstances their lifetime is too short for them to be useful as an *in vivo* radiation dosimeter (Brady *et al.* 1968; Swartz *et al.* 1965; Ostrowski *et al.* 1980). In the mineralized tissue which includes bones and teeth, the radicals thus formed can be trapped in trapping centres of the crystal structure (Becker & Marino 1966). The trapping centres are formed as a result of defects in the crystal lattice or due to the presence of impurities (Saidoh & Townsend 1975). The stable radical species as a result of irradiation have been identified as either CO_3^{3-} or CO_2^- (Callens *et al.* 1987); the CO_2^- radical has a reported lifetime of 10^7 years at 25 °C (Schwarcz 1985). Dental enamel is one of the few tissues in the human body that can essentially retain indefinitely the history of the radiation exposure mainly due to its large (~ 98 %) mineral contents. In fact hydroxyapatite paramagnetic centres in tooth enamel, unlike bones, are not subjected to metabolic deactivation (Brik *et al.* 2000). Also these paramagnetic centres created in hydroxyapatite are found to be thermally stable up to about 200 °C (Hennig *et al.* 1981).

Electron paramagnetic resonance (also called electron spin resonance) dosimetry for retrospective exposures, developed during the past two decades (Aldrich & Pass 1986; Aldrich & Pass 1988; Chumak *et al.* 1998; Dalgarno & Mcclymont 1989; Desrosiers 1991; Desrosiers & Schauer 2001; Egersdorfer *et al.* 1996; Haskell *et al.* 1997b; Ikeya *et al.* 1986; Ikeya & Ishii 1989; Ishii & Ikeya 1990; Pass & Aldrich 1985; Romanyukha & Regulla 1996; Romanyukha *et al.* 2001; Tatsumi 1986; Wieser *et al.* 2000), is based upon

the measurement of the radical species in the tooth enamel produced as a result of the ionizing radiation. The principle works on the transition of the spin state of the trapped radical in the crystal lattice, upon supply of electromagnetic energy in the form of microwave radiation in the presence of a magnetic field. All this is accomplished in a resonant cavity inside a commercially available electron paramagnetic resonance (EPR) spectrometer.

In this chapter, design and development of an accident dosimetry facility at the McMaster University is described which is based on EPR tooth dosimetry (Khan *et al.* 2002a). The main objective was to use EPR dosimetry for both low (< 300 mGy) as well as at high (> 300 mGy) radiation exposures. The boundary of 300 mGy is chosen because different kinds of problems exist in the two domains. EPR dosimetry involves a number of steps from sample collection to assessment of accidental exposure. A suitable mix of the sample preparation, in-cavity measurement and post-processing of the EPR spectrum can result in a reliable evaluation of radiation exposure with reasonably low uncertainty (Khan *et al.* 2002c).

2.2 PROTOCOL DEVELOPMENT

2.2.1 Sample collection

Human teeth are divided into two major categories: deciduous and permanent. Teeth from each of these can be divided into four groups: molars, premolars, canines and incisors. For dose reconstruction purposes, information must be available about the position of the tooth in the mouth, age of the donor, number of medical exposures (i.e. dental X rays, or CAT examinations involving head and neck, or any previous history of radiation therapy and occupational exposure of the donor).

The location of a tooth inside the buccal cavity is important for the estimation of the age of the tooth which in turn will be helpful in subtracting the natural background exposure from the accidental irradiation. If no prior information is available about the tooth, then its location in the buccal cavity is determined by the shape of cusps, enamel layer thickness, and the number of roots. The tooth selected should have a minimal amount of dental cavities or metal fillings or history of endodontic treatment. Teeth

are extracted due to either carious or periodontal disease; the mineral content and carbonate concentration can change only for a few dental diseases (Brik *et al.* 1996). However in accident dosimetry, molars and premolars may not always be available. To exploit those instances, in addition to sound molars and premolars, various types of teeth have also been considered in this research.

2.2.2 Machine parameter optimization

Machine parameter selection is an important step in the quantification of dosimetric signal. A wrong choice of parameters could degrade the shape and amplitude of the signal. In the following, all important variables have been studied to find the optimum set of parameters for spectrometer operation in order to get the maximum sensitivity and best signal discrimination. This is required to be done once and for all, if the machine configuration remains the same. For all these measurements, a high sensitivity cylindrical EPR cavity with TE_{011} mode has been used.

2.2.2.1 Microwave power selection

Microwave power represents the number of microwave radiation photons of a given frequency in the volume of the EPR cavity under the resonance condition. A high density of microwaves is able to induce more spin transitions and results in higher signal intensity. However, this does not continue to take place indefinitely, because a saturation point is approached as the populations of the two levels equalize, if the absorption rate exceeds the emission rate. The saturation behavior is different for different signals, which could be used to separate different overlapping signals. The effect of microwave power on the shape and amplitude of the dosimetric and native organic signals is therefore studied. Fig. 2.1 shows the variation in dosimetric signal intensity with microwave power, whereas the saturation of the native signal intensity as a function of microwave power is shown in Fig. 2.2.

2.2.2.2 Sensitivity of the cavity due to mass variation

The variation in sensitivity of the cavity was studied as a function of mass for enamel grains from RK02-32333435 (0.106 – 0.3 mm) dosed to 10 Gy and measured in a 5 mm diameter tube. The position of the digital Mn^{++} marker was fixed at 550 (arbitrary units) in the cavity.

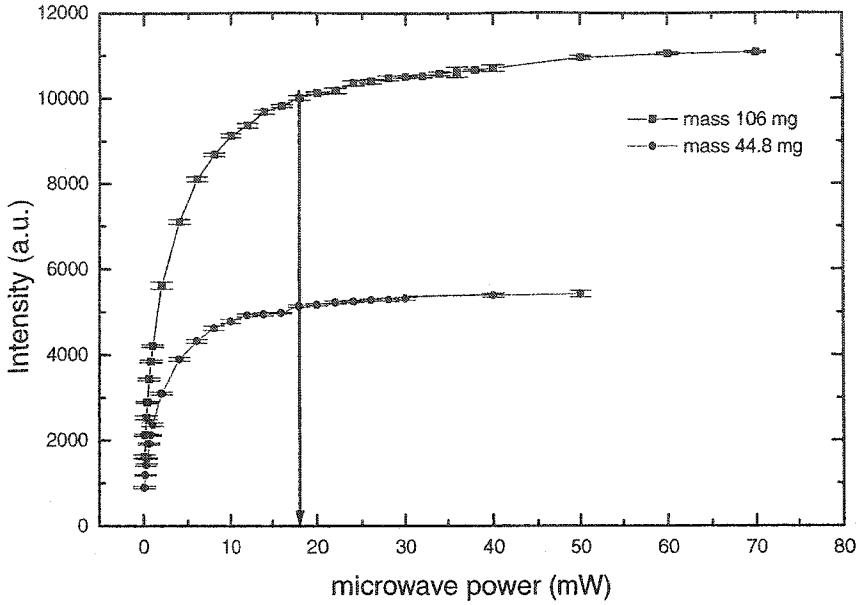

Fig. 2.1 Variation of dosimetric signal intensity (in arbitrary units) as a function of microwave power, for two different sample masses. Dosimetric amplitude continues to increase with the microwave power, as more transitions can take place. Microwave power from 18 – 25 mW can be used for signal discrimination purposes.

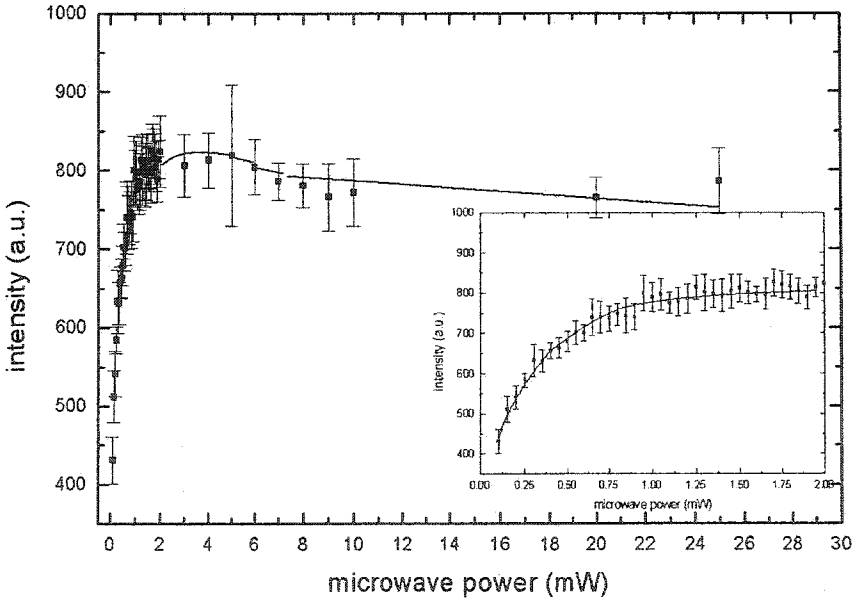

Fig. 2.2 Variation of native signal intensity (g = 2.0045, width = 0.9 mT) as a function of microwave power for a sample mass of 80 mg (modulation amplitude was chosen to be 0.5 mT). The signal saturates and its shape (not shown here) is also deteriorated by microwave power. The native signal approaches maximum from 1.5 – 2 mW as the inset shows, which is the basis of the selective power saturation technique for signal discrimination.

Fig. 2.3a shows the cavity Q factor dropping as a function of mass of the sample. Q value is the ratio of maximum microwave energy stored in the resonator to the energy loss in the cavity per microwave cycle. This ratio continues to decrease as a result of energy absorption in the sample and due to the moisture present in the sample.

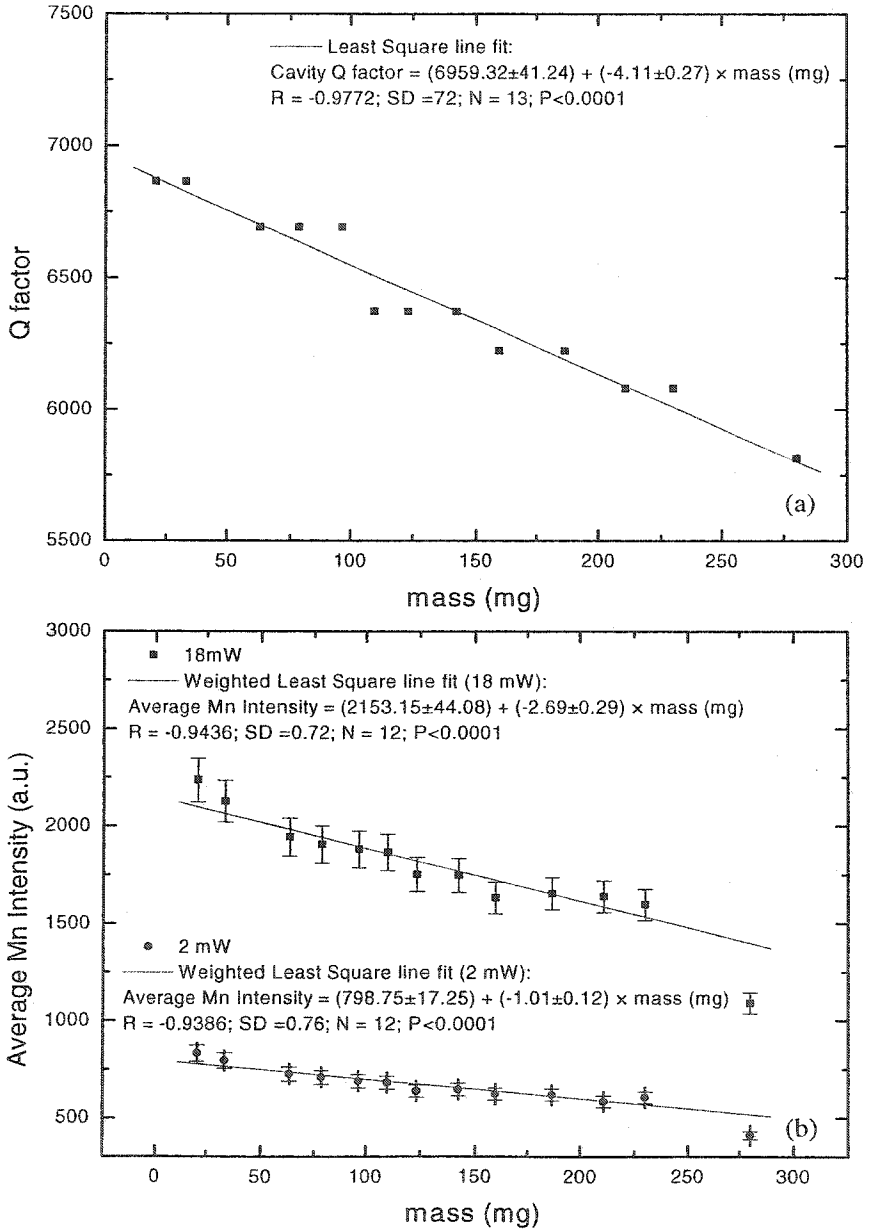

Fig. 2.3 a) Deterioration of cavity Q factor and b) intensity of average Mn^{++} marker (mean of 3rd and 4th Mn^{++} marker lines) as a function of enamel mass.

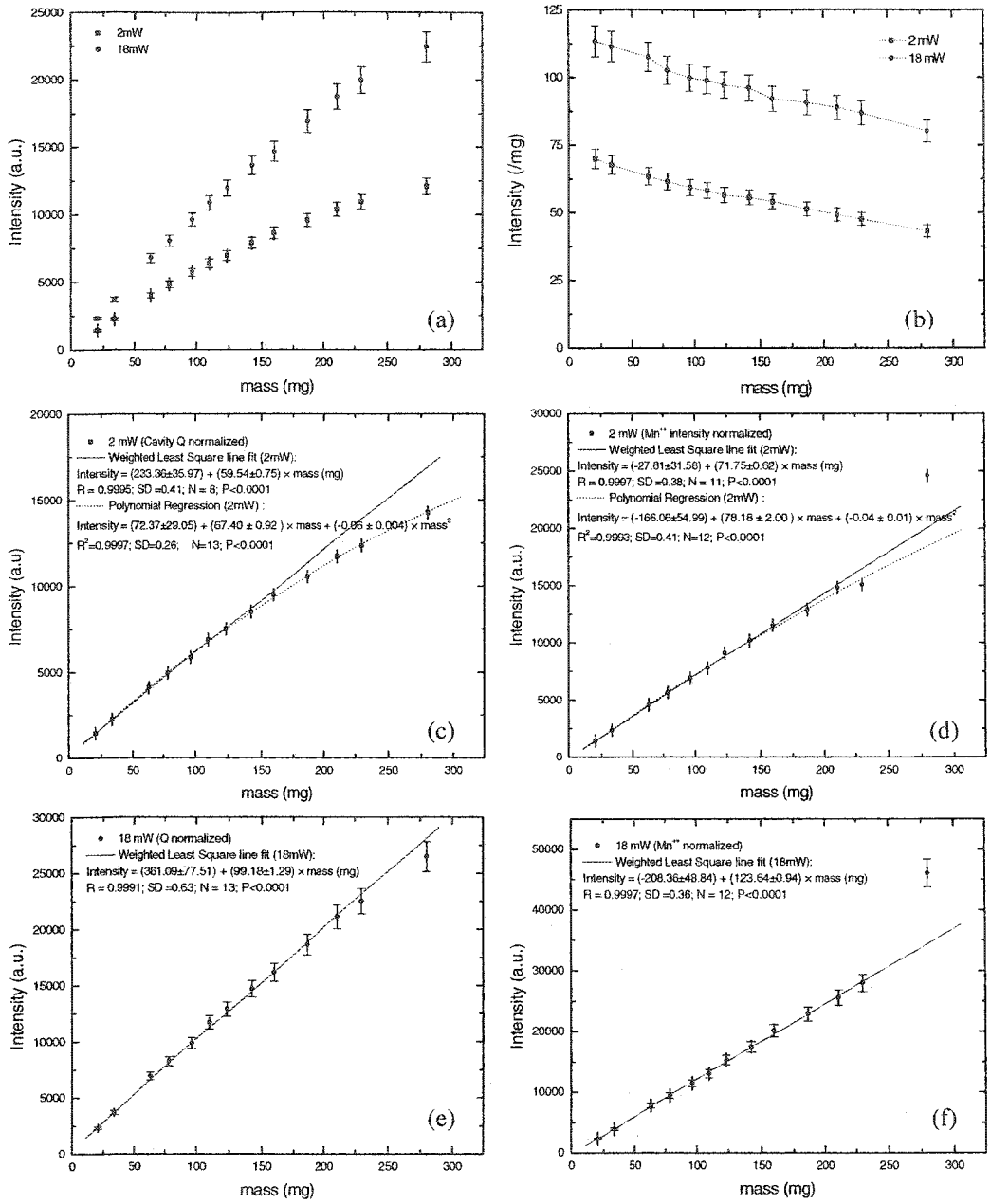

Fig. 2.4 Mass variation of a) dosimetric signal intensity at 2 and 18 mW; b) Intensity (/mg); c) Intensity (Q value adjusted) at 2 mW; d) Intensity (normalized over the average Mn^{++} signal) at 2 mW; e) Intensity (Q value adjusted) at 18 mW; f) Intensity (normalized over the average Mn^{++} signal) at 18 mW.

It has also been observed that with the decrease of Q, the intensity of the Mn^{++} marker lines also decreases (although a constant amount of which is inserted into the cavity Fig. 2.3 b). Therefore, the introduction of larger sample mass in the cavity results in a drop of both cavity Q and the intensity of in-

cavity Mn^{++} marker, even though its position is fixed (at 550 a. u.). The intensity of the dosimetric signal should correspondingly increase with the mass and it must remain constant per unit sample mass, but Fig. 2.4b shows this is true only up to mass of 75 mg. However, the intensity per unit mass when normalized either over Mn^{++} intensity or Q of cavity extends the range of constancy of dosimetric intensity per unit mass up to 150 mg (Fig. 2.5). If the intensity per mass is normalized both to Mn^{++} marker intensity and Q of the cavity, this range could be extendible up to 250 mg (Fig. 2.6), which is half the typical mass of enamel obtainable from a molar.

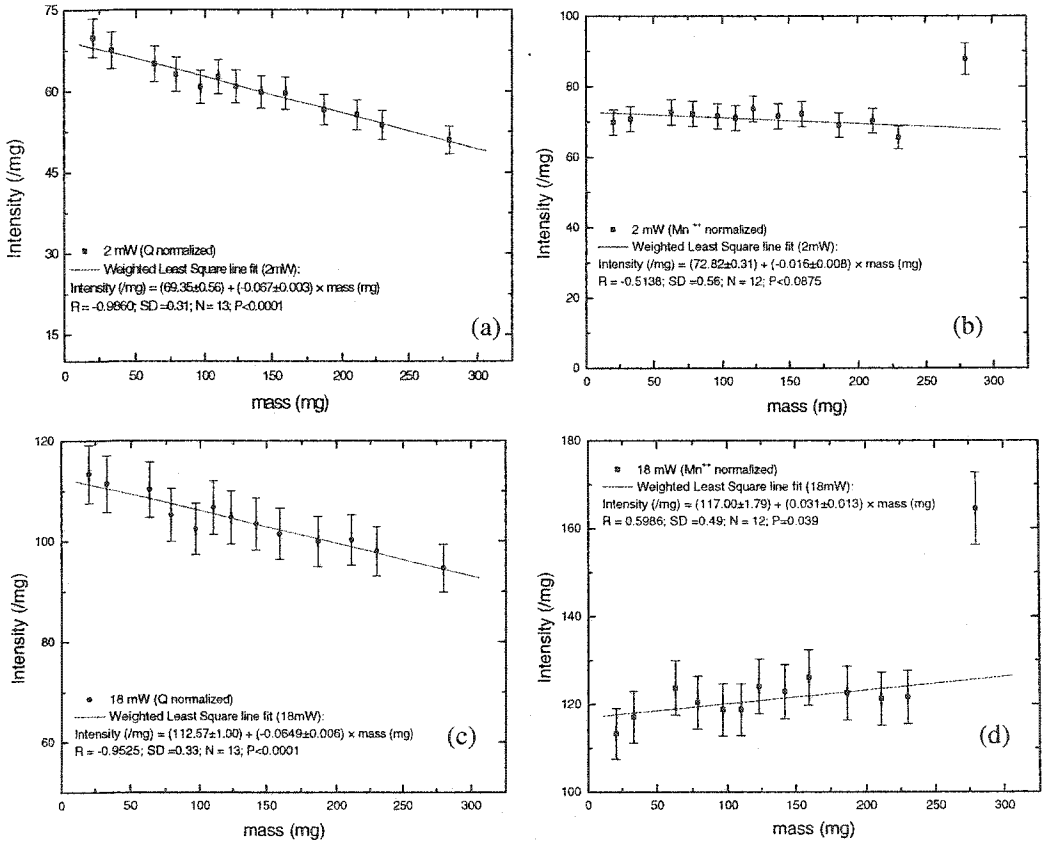

Fig. 2.5 Mass variation of intensity (/mg) a) Q normalized at 2 mW; b) normalized over average Mn^{++} intensity value at 2 mW; c) Q normalized at 18 mW; d) normalized over average Mn^{++} intensity value at 18 mW.

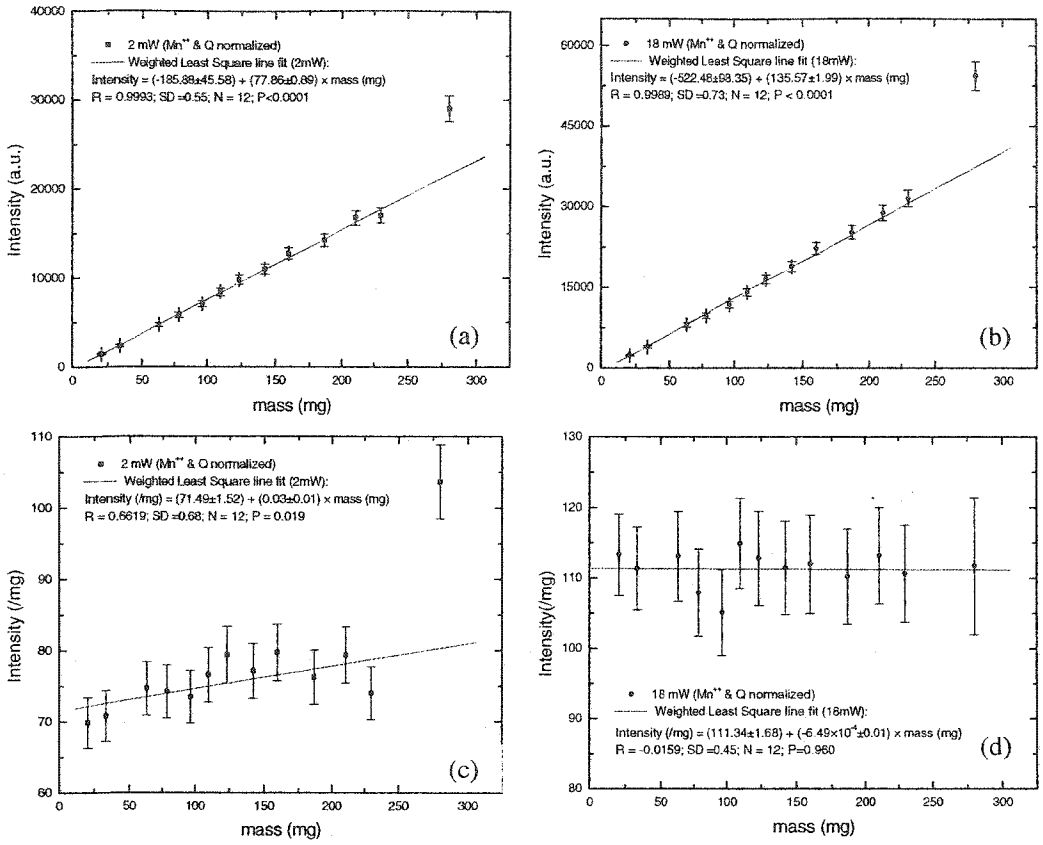

Fig. 2.6 Mass variation of a) intensity (normalized over both Q value & average Mn^{++} signal value), 2 mW; b) intensity (normalized over both Q value & average Mn^{++} signal value), 18 mW c) intensity (/mg)as a function of mass (also normalized over Q value & average Mn^{++} value), 2 mW d) intensity (/mg)as a function of mass (also normalized over Q value & average Mn^{++} value), 18 mW.

Earlier in some experiments, it was observed that the amplitude of Mn^{++} marker lines changed, when the same sample (mass being constant) with differently irradiated doses is measured, however, it just proved to be an artifact as shown in Fig. 2.7.

In summary, if the sample mass is variable or a larger mass is used which is usually the case for low dose measurement, the cavity sensitivity also decreases. However, this decrease of cavity Q can be compensated if the sample is measured with the Mn^{++} markers inserted in the cavity at the fixed position and subsequently normalized with the intensity of the Mn^{++} lines to account for the cavity Q factor change due to reasons mentioned earlier. This leads to some loss of precision due to normalization procedure.

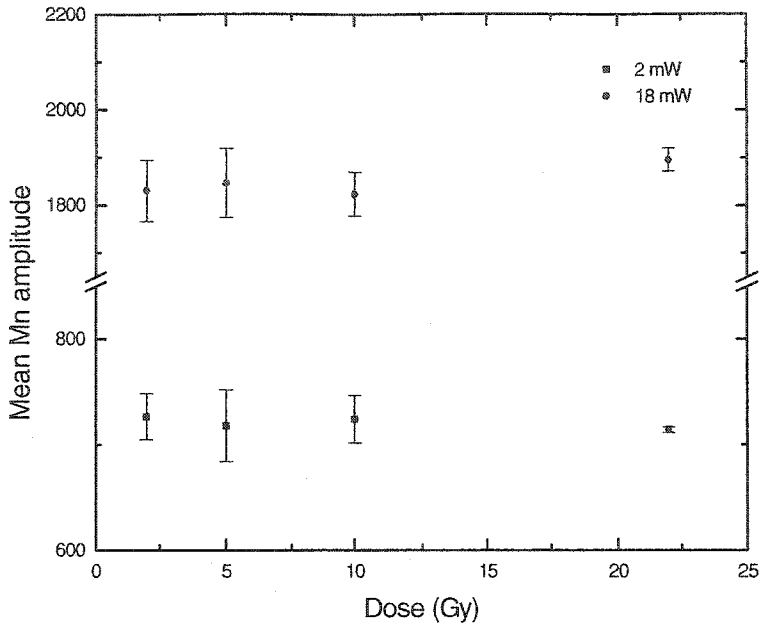

Fig. 2.7 a) Mean intensity of Mn^{++} marker (3^{rd} and 4^{th} lines) as a function of various dosed samples for the same mass (25.6 ± 0.2) mg.

2.2.2.3 *Effect of modulation amplitude*

The field modulation frequency is usually chosen around 100 kHz. The modulation width is selected to be less than the line width of the signal of interest. If it is too small the signal intensity is small. Larger the modulation width the signal becomes broader and over modulation makes it harder for two adjacent signals to be resolved. The variation in signal intensity and the effects of over-modulation are shown in Fig. 2.8. Overlapping signals could be resolved by using the small modulation widths.

2.2.2.4 *Choice of the time constant*

The time constant of the amplifier is selected to find the best signal to noise ratio. For a given scan time, the signal shape may distort and the amplitude changes with different time constants. Fig. 2.9 shows the changes in line shapes and signal intensity with the time constant, for a short scan of 3s/mT.

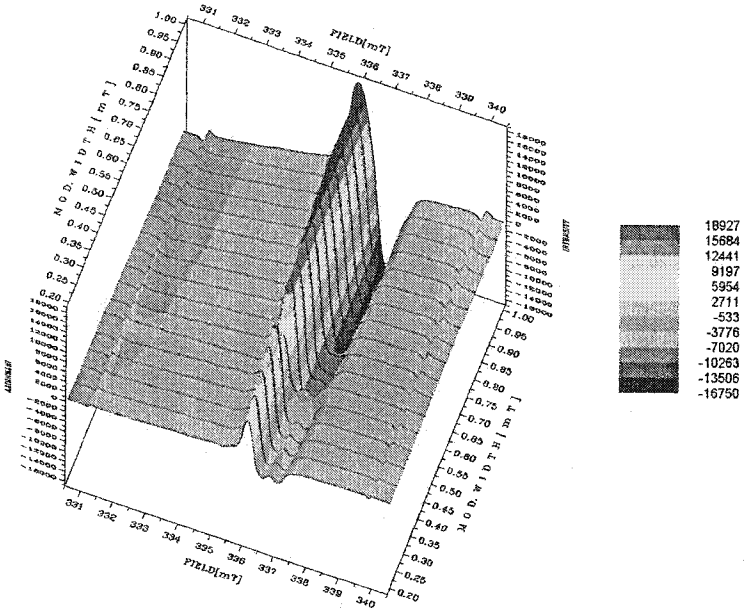

Fig. 2.8 Variation in intensity and line shape of enamel sample as a function of modulation amplitude. The line shape distorts around 0.55 mT due to over modulation of the dosimetric signal.

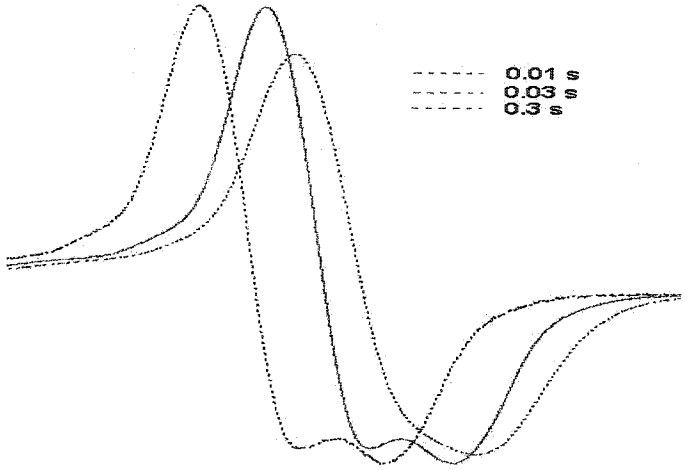

Fig. 2.9 Changes in the line shape with the time constant for a total scan time of 30s. Not only shape but also the amplitude is disturbed for larger time constant.

2.2.2.5 Amplifier gain

Amplifier noise could contribute significantly, especially for low dose measurements, if it is not properly accounted for. Fig. 2.10 shows the variation in dosimetric intensity with the amplification in arbitrary units. The linearity of the amplifier was observed up to 3000 (a.u.), above which the amplitude of

the noise becomes higher producing the supra-linear part of the line. The variation in random noise on the signal of interest (dosimetric signal) shows an increase in the noise on the dosimetric signal as a function of amplification (Fig. 2.11). The random noise was evaluated by taking a constant window of g=0.003 on three intensity contributing parts of the dosimetric signal.

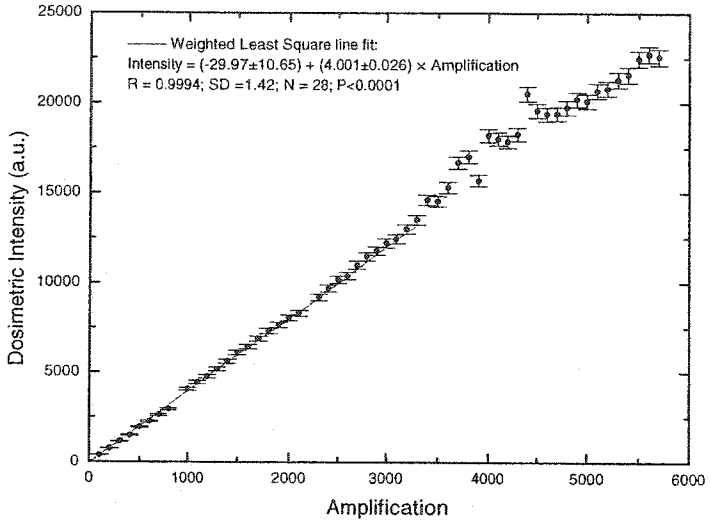

Fig. 2.10 Variation in dosimetric signal intensity as a function of gain of the amplifier. The signal intensity varies linearly with the gain of the amplifier up to 3000, after which noise contributes to the supra linear part of the plot.

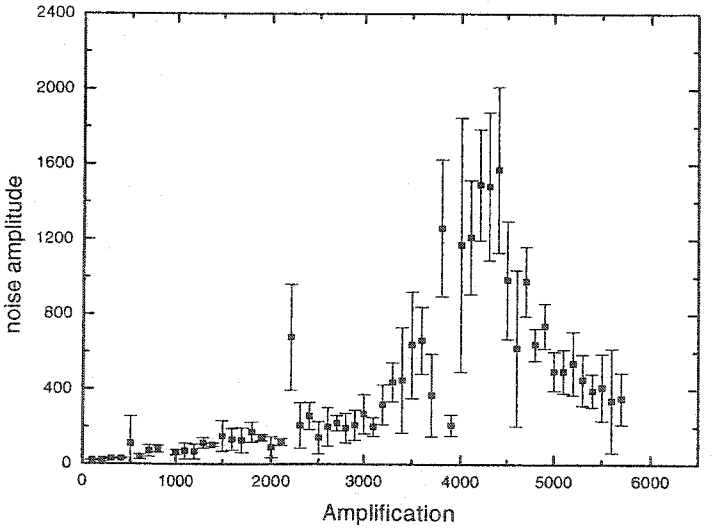

Fig. 2.11 Variation in mean random noise of the dosimetric signal as a function of gain of the amplifier. The noise amplitude remains constant below an amplifier gain < 3000, thereafter fluctuation increases. Mean noise is calculated by choosing three constant windows of width g = 0.003 on the dosimetric signal.

2.2.2.6 *Number of scans*

Larger numbers of scans have been found to improve the signal to noise ratio, this is evident from Fig. 2.12.

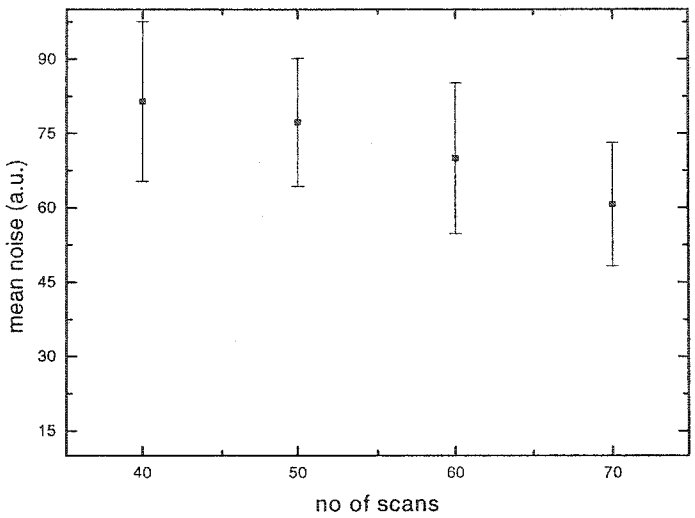

Fig. 2.12 Variation in mean random noise of the dosimetric signal as a function of the number of scans (for 18mW power, 0.5mT modulation amplitude, 0.01s time constant, and 30s per scan). Mean noise decreases with increase in the number of scans and the signal to noise ratio. Mean noise is calculated by choosing three constant windows of width g = 0.003 on the dosimetric signal.

2.2.2.7 *Spectrum scanning time*

One longer scan of 15 minutes duration (with time constant of 0.3s) was compared to the mean of 30 shorter scans of 30s duration (time constant 0.01s). Large number of shorter duration scans showed a better signal to noise ratio, than a single longer duration one.

2.2.2.8 *Optimum parameters*

The machine parameters have been optimized as a result of the experiments mentioned in earlier sections. The optimized parameters for the JEOL JES-FA 100 type EPR spectrometer with a cylindrical cavity are shown in Table 2.1.

Table 2.1 The optimized sample measurement conditions for JEOL JES-FA 100 type EPR spectrometer.

Power (mW)	2 & 18
Magnetic field (mT)	335±5
Frequency (MHz)	9442.5
Modulation frequency (kHz)	100
Modulation amplitude (mT)	0.5
Amplifier gain	800
Time constant (ms)	10
Scan time (s)	30
No. of scans	40
Mn^{++} marker position	550
Digital resolution	8192

2.2.3 Sample preparation

For this purpose teeth preserved in sodium hypochlorate were acquired from the local dental clinic. Teeth were cleaned and any apparent material like plaque was removed. Teeth were photographed, catalogued, buccal and lingual sides were identified.

2.2.3.1 Mechanical Treatment

Historically, mechanical cutting, grinding, and pulling to fracture have been found to induce free radicals in biological tissues such as bone (Marino & Becker 1968). Enamel when ground to powder exhibits a major EPR resonance near g = 2.002. Since this mechanically-induced signal coincided with that due to ionizing radiation, one could mistakenly estimate the background or baseline radical yield induced by mechanical operations. The dose equivalent to grinding, determined by comparison with irradiated enamel powder, was found to be in 20 - 60 Gy range (Polyakov *et al.* 1995). Mechanically induced radicals may be formed primarily on the particle surface in contrast to the radiation-induced radical formation which is likely to take place uniformly throughout the particle (Desrosiers *et al.* 1989). Mechanically induced radicals are found to be of two types: short-lived due to sample preparation steps and long-lived due to use of high speed dental borers around the caries. Short-lived species decay completely within 48 hours of incubation above 40 °C (Kirillov *et al.* 2002). It is also reported that vigorous mechanical

operations can lead to localized overheating of sample up to temperatures as high as 1000 °C (Ikeya *et al.* 1993). Subsequently, a similarity between the radicals formed as a result of mechanical operations and those generated by heating the enamel above 600 °C was observed (Aragno *et al.* 2001). Therefore, in the first instance mechanical treatment of tooth must be avoided and if it is necessary it should be accompanied by proper cooling of the sample.

2.2.3.1.1 Cutting treatment

Generally molars without any fillings are used however some teeth with metal fillings have also been processed. So using a dental burr, any metal filling or stains are removed from the tooth. The root was separated from the crown by using a low speed water-cooled diamond tipped thin blade saw (0.08 ''). The crown was cut into buccal and lingual halves. Later buccal and lingual halves, separately, were further divided into small pieces < 5 mm. This is necessary for the quick separation of dentine from enamel. It not only shortens the chemical treatment time but also exposes more surface area for the reagent to act. Other authors suggested division of enamel halves into small particles by gentle crushing using agate mortar and pestle. However, we have observed that no matter how soft the crushing treatment is, it results in smaller enamel and dentine particles, which are hard to separate during visual inspection and also lead to considerable loss of mass.

2.2.3.1.2 Crushing treatment

Usually no crushing operation is used until the chemical processing phase is completed. As a result of chemical processing (discussed in next section) a grain distribution of < 4 mm is achieved. To get particles of the desired distribution, sample is crushed in an agate mortar and pestle in the presence of liquid nitrogen for sample cooling. The effect of cooling is significant for smaller grain sizes < 0.106 mm while the naturally cooled (without liquid nitrogen) sample resulted in large amplitude signals around the dosimetric signal. Fig. 2.13 shows the effect of crushing on shape of dosimetric signal for an air-cooled (without liquid nitrogen) and liquid nitrogen cooled sample for grains in (0.106 – 0.3) mm range.

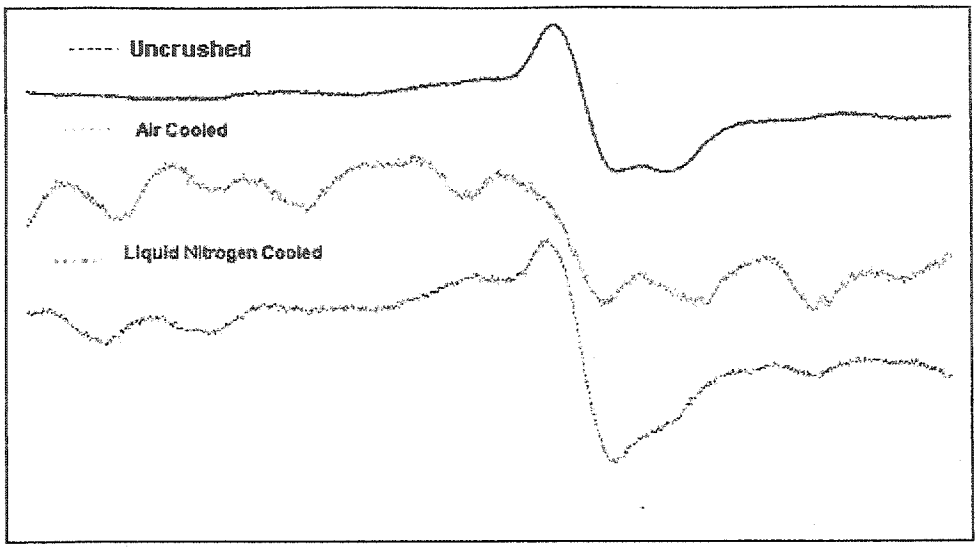

Fig. 2.13 A comparison of different mechanical treatment on the shape of dosimetric signal (first derivative of microwave absorption is plotted against the sweeping magnetic field); the top spectrum was obtained before any mechanical operation. The other two spectra shown are with and without liquid nitrogen cooling for (0.106 - 0.3) mm grain distribution. The spectrum from < 0.106 mm grains with air cooling was too off-scale to be displayed.

2.2.3.2 Chemical treatment

Due to complications produced as a result of mechanical trauma, mechanical separation of enamel – dentine is avoided. Chemical treatment is a preferable means for the separation of dentine and other undesirable organic contents from the enamel (Nakamura & Miyazawa 1997).

The sample is placed in a polypropylene tube in approximately 10 ml of freshly prepared supersaturated potassium hydroxide (KOH) aqueous solution. The sample is treated for 5 h in an ultrasonic water bath at 80°C, after which it is washed in deionized water at 80 °C for 12 h in an ultrasonic bath and dried at 40 °C for 5 h. As a result of the chemical treatment and drying, the enamel-dentine junction gets softened and therefore the dentine could be visually scraped off the enamel under a microscope. The enamel pieces are then measured in EPR spectrometer at two different microwave powers. Spectra at the two powers can be compared to see the presence/absence of dosimetric signal.

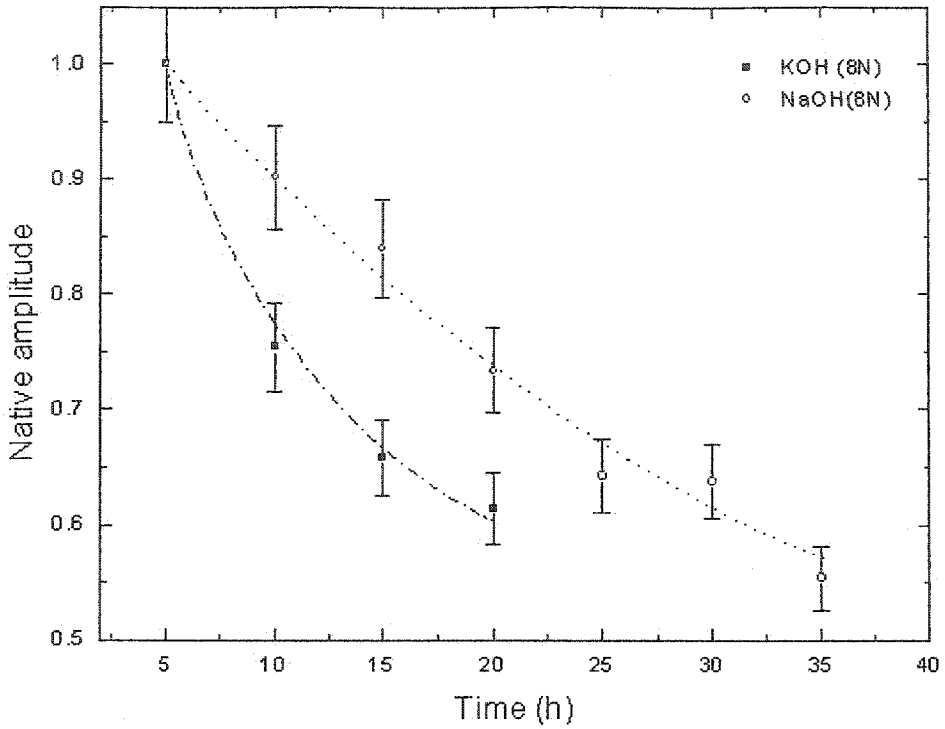

Fig. 2.14 A comparison of treatments by two common supersaturated base reagents (KOH and NaOH), treatment with sodium hydroxide is inefficient since the deterioration of the native signal amplitude as a function of chemical treatment time was a slower process. Each point is a mean of at least four different samples.

If a native signal is still present, the reagent is refreshed and the whole sequence is repeated. The process is continued till either the native signal is eliminated or maximum operation in KOH exceeds 30 h.

In the preliminary experiments, a lower concentration of KOH was compared with a supersaturated solution, which resulted in slower dissolution of the dentine; therefore, a higher concentration is preferred. In other experiments two different chemical reagents were used to see their effectiveness in removing the organic contents of tooth enamel. Fig. 2.14 shows that the treatment with KOH is a quick and efficient procedure as compared with NaOH. To check the effect of highly reactive basic treatment on the radiosensitivity of the tooth, an experiment was devised in which the tooth was divided into mesial and distal parts: mesial part was given 1 Gy of dose, both parts were chemically treated. The variation of dosimetric signal in every step was measured, and not much of a change in the intensity of the dosimetric signal as a function of treatment time was observed. The distal part (already chemically

treated) was given a dose of 1 Gy. The comparison of dosimetric intensities of both pre-irradiated and post irradiated parts of the same tooth showed an overlap within one standard deviation. Ranges of time of treatment and the alkali concentration did not lead to generation of new paramagnetic species (Sholom *et al.* 2000a).

2.2.3.3 Grain size optimization

Use of a larger grain size sample is generally avoided as the reproducibility decreases for grains larger then 1.4 mm due to increased directional dependence from the small number of enamel pieces (Haskell *et al.* 1997a). However, a sample with small grains below 0.3 mm results in a rapid drop of signal to noise ratio.

To see the effect of gamma radiosensitivity on different grain size, enamel was gently crushed and sieved into various grain size in the range 0.3 - 0.5, 0.106 - 0.3, and < 0.106 mm, and then given 1 Gy of gamma radiation dose. The results shown in Fig. 2.15 show a decreasing trend of the dosimetric signal amplitude for small grains. Based on the reproducibility of results with unirradiated spectra, there is a small reduction in radiation sensitivity with decreasing grain sizes (~ 8 %) of non-irradiated enamel. Since the signal intensity per mass is proportional to radiation sensitivity. By decreasing the size of the grains we proportionally increase the inactive volume at the surface of the samples and decrease the internal volume, where potential paramagnetic centres are located (Chumak *et al.* 1996; Sholom *et al.* 1998b).

The crushing of 100 mg of < 4 mm grain size sample usually results in 38 - 40 mg grains of 0.3 - 0.5 mm, 37 - 39 mg grains of 0.106 - 0.3 mm, and 18 - 20 mg grains of < 0.106 mm, whereas 3 - 4 mg of sample is lost.

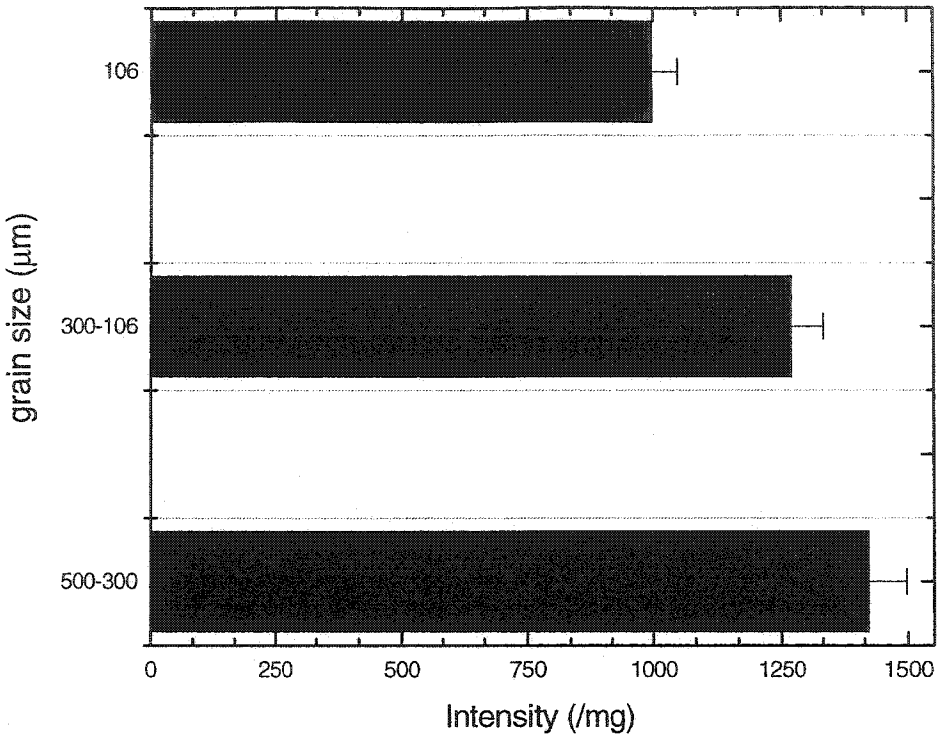

Fig. 2.15 A comparison of radiation sensitivities for different grain sizes from the same enamel sample.

2.2.3.4 Temperature effects on the shape of the dosimetric signal

Experiments were done in order to test the effect of temperature on the shape of signal during sample preparation process. Enamel samples were thermally treated from room temperature to 420 °C for 1 h in an oven.

Fig 2.16 shows the peak-peak amplitude of the dosimetric signal for various temperature, some of the signals are themselves shown in Fig 2.17. The shape and amplitude of dosimetric signal remains unchanged until 200 °C; after 240 °C a signal starts to appear and it continues to grow till 400 °C. This rise at larger temperature is due to the drastic change in water contents which is known to take place at this temperature range (Fowler & Kuroda 1986). Above 400 °C there is a probable annealing of the radicals and a new species is produced (Aldrich *et al.* 1992). In the interval from 350 – 1000 °C changes in the physical and chemical properties of the organic and inorganic matrix have been reported (Fattibene *et al.* 2001).

Therefore, any operation leading to local temperature maxima > 200 °C in enamel will degrade the dosimetric intensity.

2.2.3.5 Sample preparation revisited

Molars separated into buccal and lingual sides by using a low speed water cooled saw were further sawed into < 5 mm size. The samples were ultrasonically treated in supersaturated KOH for 5 h, then with water for 12 h, and finally dried up to 4 h at 40 °C. Enamel was visually cleaned under a microscope, and spectrum was collected at 2 and 18 mW. If required sample was crushed into 0.2 - 0.4 mm grains in the presence of liquid nitrogen.

2.2.4 In-cavity measurement

The EPR measurements were done in a cylindrical cavity with TE_{011} resonance mode. The JEOL JES-FA 100 type spectrometer was operated in the X band. The spectrometer was turned on for at least 3 hours before the measurement to minimize any fluctuation in magnetic field or current. The spectrometer was operated under the optimized conditions mentioned in section **2.2.2.8**. The current section deals with the effects produced due to extra-sample materials such as sample holders, tubes, and due to the relative position in the cavity.

2.2.4.1 Empty cavity signals

For low dose measurements, signals arising from the extra-sample elements must be measured and accounted for. The interfering signals can come from the cavity, sample holder and empty tube itself, which could be significant at low exposure measurements. Before any further signal processing, the composite spectrum from the empty cavity, empty EPR tubes in the same position under the identical conditions must be measured and then subsequently removed. Fig. 2.18 shows a typical empty tube spectrum at two different microwave powers.

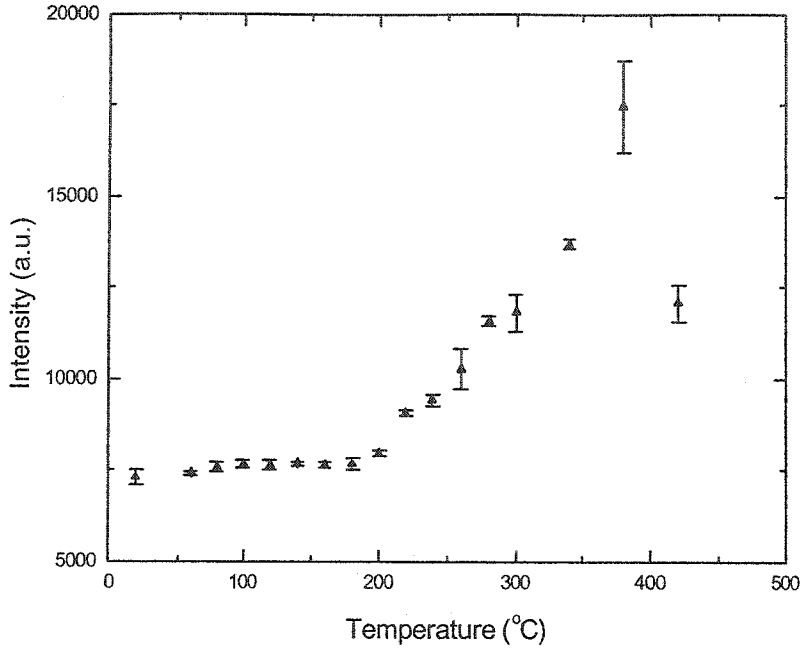

Fig. 2.16 Effect on dosimetric signal intensity as a result of heating in an oven for 1h at different temperatures. Peak-peak amplitude of the dosimetric signal is shown as a function of temperature.

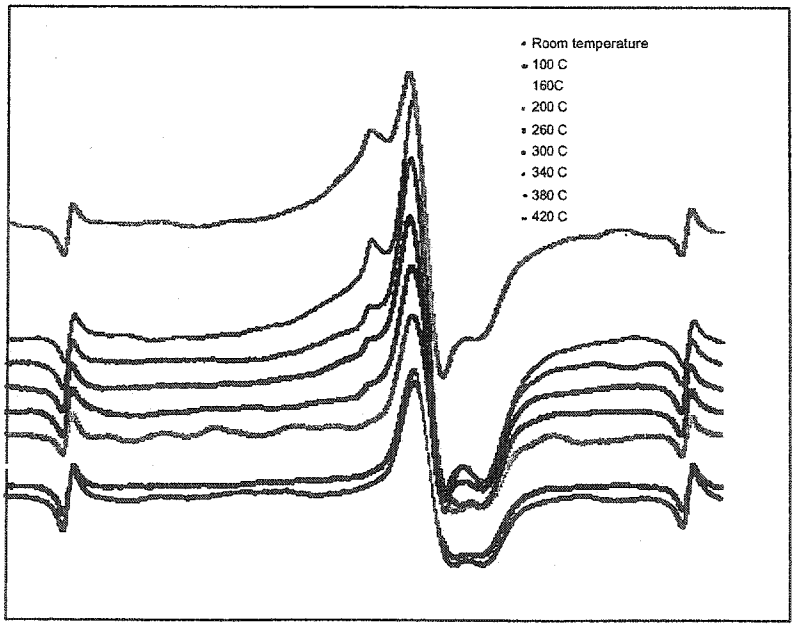

Fig. 2.17 Effect on shape of the dosimetric signal (first derivative of microwave absorption is plotted against the sweeping magnetic field) as a result of sample heating for 1h in an oven. Above 200 °C the shape of the dosimetric signal changes due to interference from a signal produced next to the dosimetric signal.

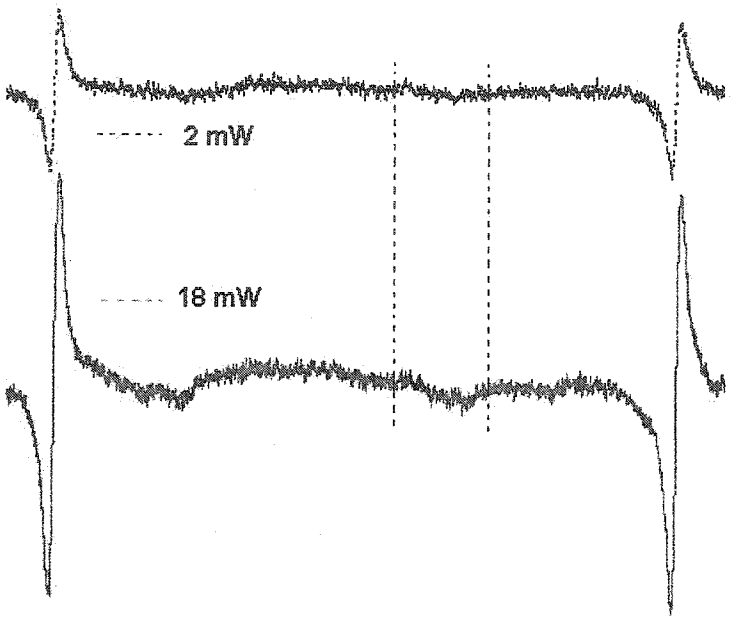

Fig. 2.18 EPR empty cavity spectrum at two different microwave powers. Region between the dotted lines is the place where the dosimetric signal should fall in the presence of a sample.

2.2.4.2 *Effect of sample tubes types and diameter*

In the first instance the effect of various diameter tubes on the dosimetric signal sensitivity was studied. A comparison of three different diameter tubes made from clear quartz and suprasil (synthetic quartz) for a large sample mass of 280 mg is given below (Table 2.2). A tube with 5 mm diameter produces best results despite the fact that cavity Q was higher for a 3 mm diameter tube.

Table 2.2 Variation in dosimetric signal amplitude for various diameter tubes. Data is given for a mass of 280 mg with 10 Gy dose (0.106 - 0.3 mm) measured under the same conditions as mentioned in section **2.2.2.8**.

Tube diameter (mm)	Sample height (mm)	Cavity Q factor	Dosimetric amplitude (a.u.)	Mn^{++} marker (a.u.)
5	14.37	5239	20919 ±1045	825
4	22.45	5815	12094 ± 34	968
3	65.18	6864	11954 ± 77	1298

However for a smaller sample, the results in Table 2.3 favor a 3 mm tube inside the 4 mm diameter tube compared to the single 5 mm inner diameter tube. This fact is demonstrated by using two different techniques:

1. *Mathematical averaging*; this involves measurement of dosimetric amplitude of the individual spectrum and then their subsequent averaging.
2. *Spectral averaging*; first averages all the rotated spectra of a sample and then measures the amplitude of the averaged spectrum.

The results obtained by both types of averaging (as shown in Table 2.3) are within the same range and favor the use of multiple tubing for a small sample mass.

Table 2.3 Sensitivity of the dosimetric signal in various tubes for a sample of mass 81.3 mg.

Tube diameter (mm)	**Dosimetric amplitude (*mathematical averaging*) (a.u.)**	**Dosimetric amplitude (*spectral averaging*) (a.u.)**
5	4028.25±113.24	3968.82 ±111.57
3 in 4	4329.75 ±63.44	4268. 02± 262.54

These results were further explored in another experiment, again a combination of 3 mm in 4 mm produced better results (Fig 2.19). Therefore, the measurement inside multi-tube arrangement leads to an increase in signal to noise ratio and thus provides increased sensitivity. Although no physical explanation is available, however it is believed that in some way this configuration leads to focusing of microwave power density onto the sample itself. Also the noise, by putting one tube in another, does not accumulate and remains in the same range; therefore, 3 in 4 mm tube provides a good combination to be used for higher sensitivity.

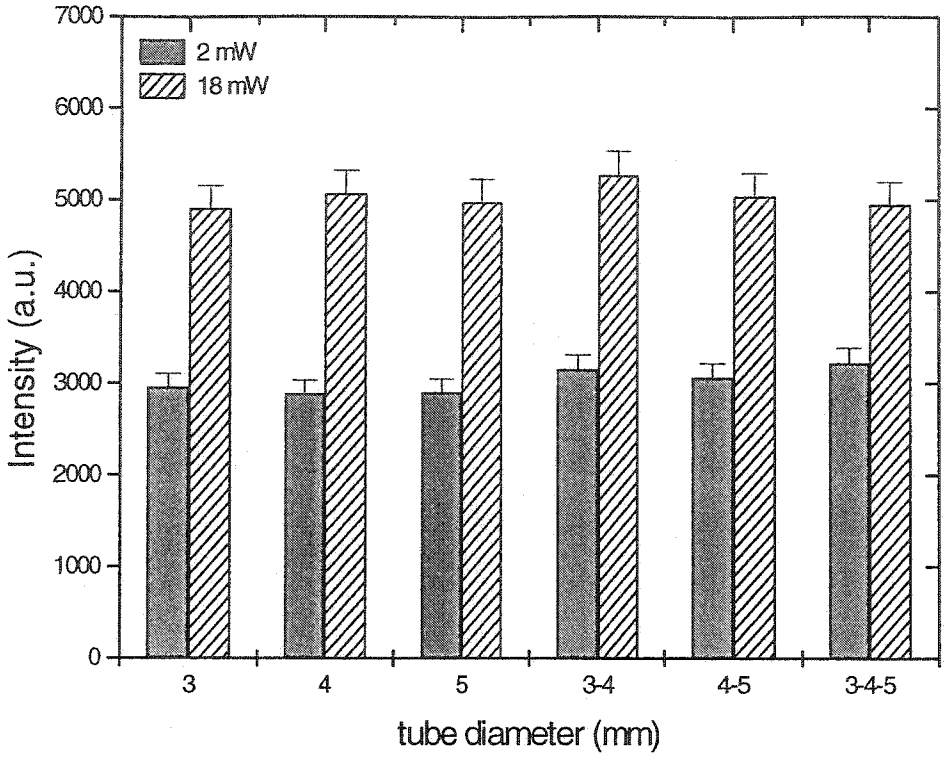

Fig. 2.19 EPR tubes of various outer diameters have been used to find the maximum sensitivity, either as a single or combined (a mass of 43.9 mg sample with height of 10 mm in the smallest diameter tube was used). A 3 mm tube inside 4 mm tube provides the best sensitivity, if the sample height does not exceed the most sensitive volume of the cavity.

2.2.4.3 Optimal positioning

The sensitivity of the cavity could change if the sample mass lies outside the active volume of the cavity. This was determined by using a 20 Gy dosed sample of mass 5 mg in a 4 mm tube. The sample tube in a marked reproducible position was pulled up from the bottom of the cavity in small steps of 1 mm. Fig. 2.20 shows that the sensitivity of the cavity drops on both sides (up and down) of the cavity centre. However, for a sample of height 10 mm, the decrease in amplitude is only ±5% around the centre.

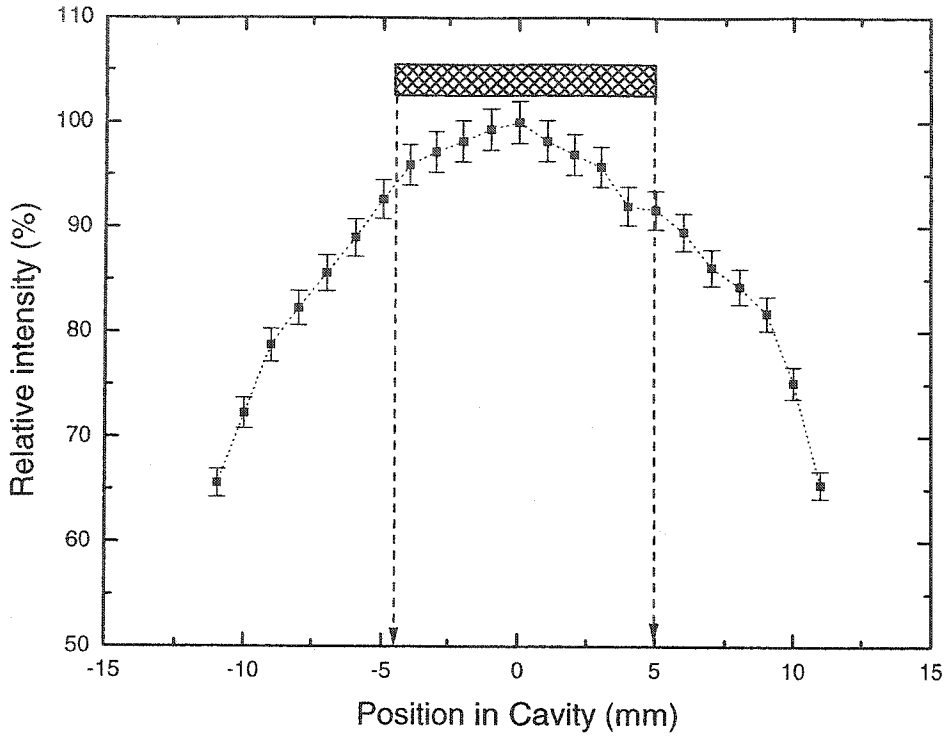

Fig. 2.20 Search for the maximum sensitive volume in the EPR cavity, zero on the abscissa represents the centre of the cavity (at a depth of 45 mm from the teflon sample tube holder). Approximately 95% sensitivity of the sample can be found for a sample height of 10 mm distributed around the cavity centre.

2.2.4.4 Dosimetric signal anisotropy considerations

For a sample crushed to 0.1 - 0.3 mm grain size with small mass (< 50 mg) can not approximate the powder distribution, which could cause anisotropy of the radiation signal. Some studies have shown that due to anisotropy the intensities of the $g_{//}$ and $g_{\perp}$ signals of tooth enamel can vary by as much as 50% (Aoba *et al.* 1982). Therefore, anisotropy of the dosimetric signal can cause a major artifact in the amplitude determination. To account for the dosimetric signal anisotropy, traditionally three techniques exist; a) using single large enamel piece to get reproducible positioning (Grun *et al.* 1996); b) recording several spectra for one sample with repeated shaking and changing of sample orientations, followed by averaging of the EPR dosimetric response method c) averaging spectra while rotating the sample with goniometer, such that a powder distribution can be approximated for grain size as large as 0.45 mm (Hayes 1999).

First method is useful for big enamel chips with very high amplitude dosimetric signals, generally encountered in EPR dating. However for low exposure samples where chemical treatment is used to remove organic contents, the grain size is small which will make it impossible to put enough sample with same position in the field. Third method has been found to produce good reproducible results. However, it has some problems inherent to goniometry. A modified form of the second method is described in the following.

The effect of anisotropy on dosimetric signal was studied for various grain distributions. The sample was rotated at various angles and spectrum was collected. Also a comparison was made with the spectrum collected after the sample was shaken. Table 2.4 shows that either the results from rotation or shaking were found to be reproducible within the uncertainty. After the same number of trials (either rotation or sample-shaking) the peak-peak amplitude of dosimetric signal in the 1.4 mT region surrounding both $g_{//}$ and $g_{\perp}$ parts of the signal was measured (e.g. Fig. 2.21).

Table 2.4 Dosimetric signal anisotropy for four different samples having different radiation doses and sample masses; in column 2 the data are the mean of at least 10 shaking and subsequent spectrum measurements; column 3 data show the rotation in 360° range where at least ten spectra were collected without disturbing the sample.

Grain size (mm)	Shaking	Rotation
< 0.106	1.548±0.072	1.531±0.049
0.106 – 0.3	1.453±0.050	1.476±0.039
0.3 – 0.5	0.399±0.020	0.409±0.049
< 4	0.473± 0.026	0.452±0.031

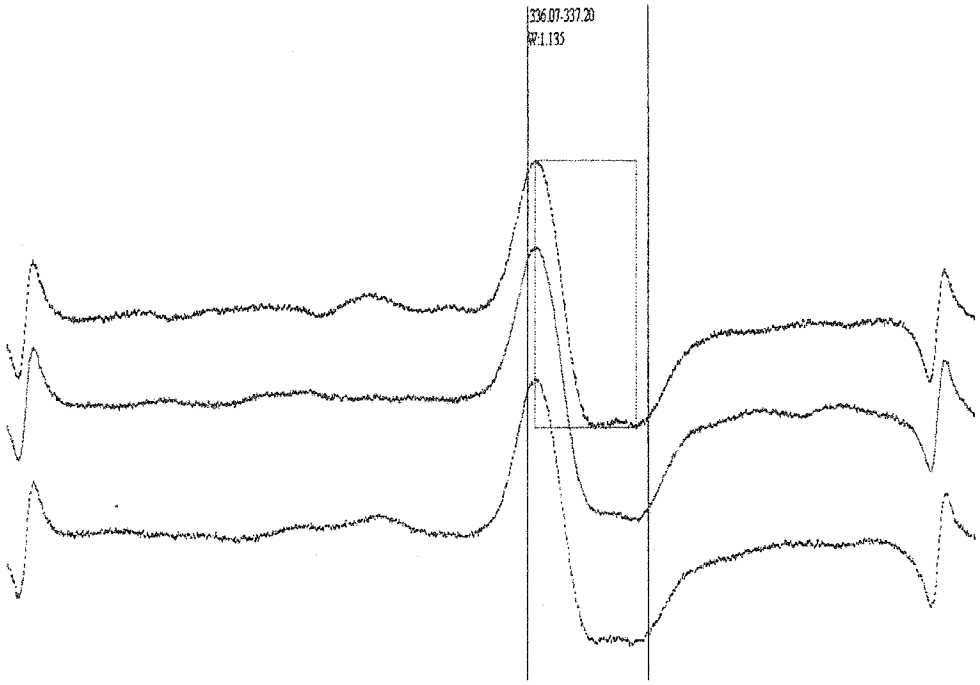

Fig. 2.21 Three spectra obtained from the same sample at different orientations are shown. Measurement of peak-to-peak amplitude of the dosimetric signal is done within a fixed window of ~ 1.4 mT surrounding both components of the g tensor (as shown). Signal anisotropy leads to a rise or fall of either of the two components, at various angular orientations in the cavity.

Sample shaking or manual rotation changes the cavity Q because of a change in the boundary condition from different grain distribution. Therefore, during the signal intensity measurement the change in the cavity Q was taken into account for each measurement by positioning in cavity Mn^{++} marker at a fixed location. Corrections are done by dividing the dosimetric signal intensity with the average intensity of the 3^{rd} and 4^{th} lines of the Mn^{++} marker. The position of Mn^{++} could be fixed in the cavity for any number of measurements. The precision of measurement can be improved by taking a large number of trials, that result in a low standard deviation and hence less uncertainty.

Thus, in the absence of goniometer, small angle manual sample rotation after each measurement can also be used to correct for the anisotropic contribution from the dosimetric signal. Therefore, each sample is rotated at full 360^0 angular range in 30^o steps and corrections are made by either averaging the

spectrum or taking the maximum dosimetric signal intensity in 360^0 angular range. This procedure is however laborious and both machine and time intensive.

2.2.4.5. Optimal sample positioning

Prior to sample measurement, empty EPR tube spectrum should be collected with the tube inserted at the same depth around the cavity centre for the rotations. The average empty EPR tube spectrum must then be evaluated. The in-cavity sample measurements must ensure that the height of sample must not exceed ±5 mm from the cavity centre. The sample measurement must involve a complete 360^0 rotation in steps of 30^0 to account for dosimetric signal anisotropy, with in-cavity Mn^{++} marker sitting in a fixed location.

2.2.5 Laboratory irradiation and dosimetry

In EPR dosimetry, an additional calibrated amount of radiation dose is needed in various stages between measurements which require an irradiation facility providing controlled doses to sample. A low dose rate ^{137}Cs gamma cell was first calibrated using the Farmer dosimeter with a thimble ionization chamber. The choice of this facility was made because of its availability and the absence of any significant undesirable up or down dose (due to shutter speed). Farmer dosimeter was pre-calibrated (AAPM 1983) against one of the secondary standards (IAEA 1971), and provides dose within 5 % uncertainty at 95 % confidence level. At a given distance from the source the fluence varied within 3 - 4 % of the mean value (of the reference line from the source to the centre of the rack), for all distances from the source. The fluence away from the ^{137}Cs source behaved according to Inverse Square law of radiation. However, the placement of the radiation rack was chosen at a distance of 80 cm away from the source to achieve uniformity over the selected area. Due to requirement of uniform buildup and backscatter of the dose from all three dimensions, (for charged particle equilibrium condition at all interfaces), a special irradiation rack was designed. The design consisted of uniformly distributed flat-bottom cylindrical pits of diameter 12 mm and depth 6 mm each having separation of 3 mm between them, machined into a 2″ thick acrylic sheet. The top opening of the sample pits after filling with the sample can be covered with a 3 mm thick acrylic sheet

to provide uniform buildup from the top (Shimano *et al.* 1989). A top view of the irradiation rack is shown in Fig. 2.22.

Samples of approximately 100 - 200 mg placed inside small polyethylene vials are inserted in the pits, inside the thick acrylic sheet. The Farmer dosimeter is then placed in its designated slot, which is designed such that the central active region of the 0.6 cc ionization chamber coincides with the sample's thickness at the fixed distance away from the source. The samples are then exposed at a rate of 4.275 Roentgen /minute (10.97×10^{-4} C/kg-minute). Temperature and pressure corrections are made for the Farmer chamber for the irradiation conditions. The exposure thus measured is the dose to air which could be converted into the equivalent dose to enamel by taking the mass attenuation coefficient ratio of the enamel to air at the calibrated cesium energy (ICRU 1989).

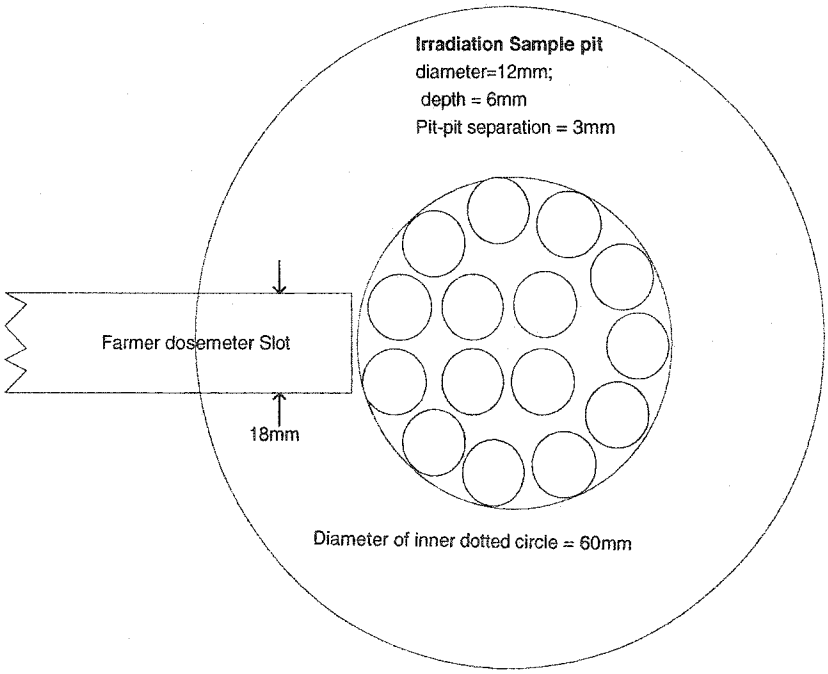

Fig. 2.22 Top view of the acrylic irradiation rack designed for ^{137}Cs irradiation of the tooth enamel powder. Samples placed inside small vials are sunk into the 12 mm diameter machined holes, and distributed evenly in a 60 mm diameter circle. The pits are covered by a 3 mm thick sheet of the same material, for uniform dose distribution inside the sample.

2.2.6 Spectrum adjustment and post-processing

For accurate dose measurements, spectrum adjustment or dosimetric signal unfolding is a crucial step, especially for low exposures. This is because the collected spectrum may consist of various composite signals like the native signal or those produced during sample preparation. The spectrum can also get contaminated due to noise originating from cavity itself, amplifier, sample holder or sample tubes. The contribution of signals having extra-sample origin is removed from the sample spectra, by collecting the empty EPR tube spectrum under the same conditions (same EPR cavity parameters) and their subsequent subtraction from the sample spectra (Hayes 1999). Fig 2.23 shows a composite spectrum consisting of both dosimetric and native signals.

For both the high and low dose regime, different post-processing is used. At higher exposures the dosimetric signal can be distinguished easily so a simple technique is used. For low exposures considerable amount of spectra processing and simulation is involved before a true dosimetric intensity is measured.

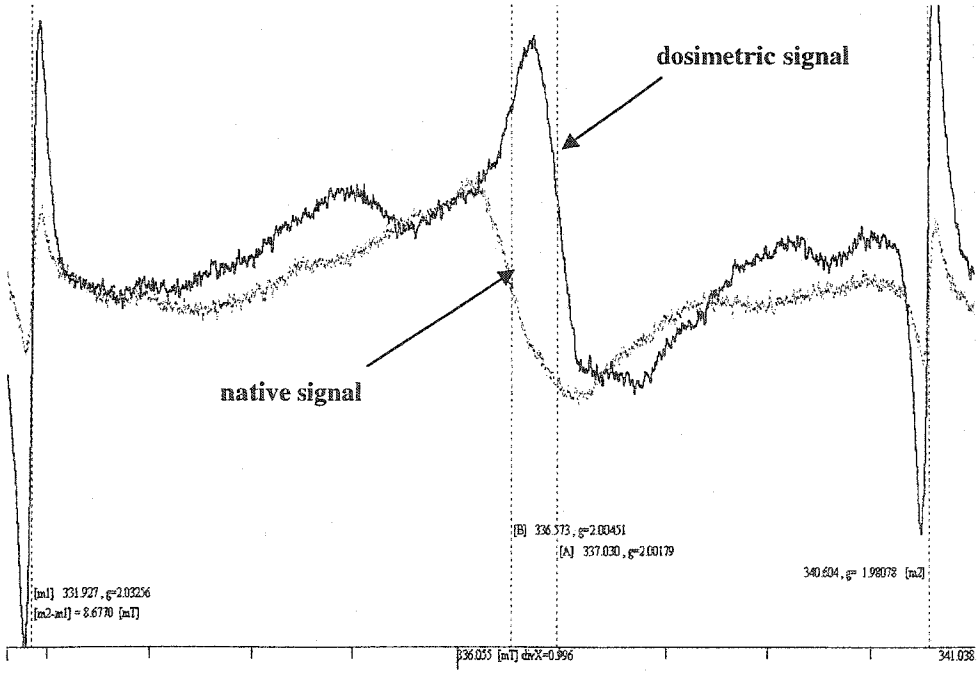

Fig. 2.23 Positions of both dosimetric (~300 mGy) and native organic signal are located by using the fixed Mn^{++} marker's 3rd and 4th lines.

2.2.6.1 *High dose signal unfolding*

At high dose levels, the contribution to radiogenic signals near the g = 2 region arise mainly from the native signal, which could be removed by using selective power saturation technique (Ignatiev *et al.* 1996).

In the selective saturation method, the spectrum of zero added dose (ZAD) sample is collected at low power ~ 2 mW where the dosimetric signal intensity is at its lowest whereas the intensity of the native signal is at maximum (section **2.2.2.1**). This is later subtracted from all differently dosed spectra collected at relatively higher power (i.e. 18 mW) where the native signal has certainly saturated (~18mW where the dosimetric signal has the maximum response but still unsaturated). Since the native signal conserves isotropy, only one measurement for ZAD at 2 mW is used for subtraction. The steps are described as:

- The ZAD 2 mW signal is aligned with the ZAD 18 mW spectrum (for 0^{o} orientation) with the help of Mn^{++} marker lines.
- Mn^{++} lines are stripped off the 2 mW ZAD spectrum prior to subtraction from ZAD 18mW spectrum (for 0^{o} orientation).
- The process is repeated for other orientations of ZAD 18mW spectrum.
- The ZAD 18 mW spectrum from all the orientations is averaged to account for the dosimetric signal anisotropy.
- The signal is smoothened out by using 31 point digital smoothening filter.
- The peak to peak amplitude of the dosimetric signal is measured and it is normalized with the amplitude of the Mn^{++} lines marker.
- The whole process is repeated with ZAD 18mW spectrum replaced by multiply-irradiated dose spectra.

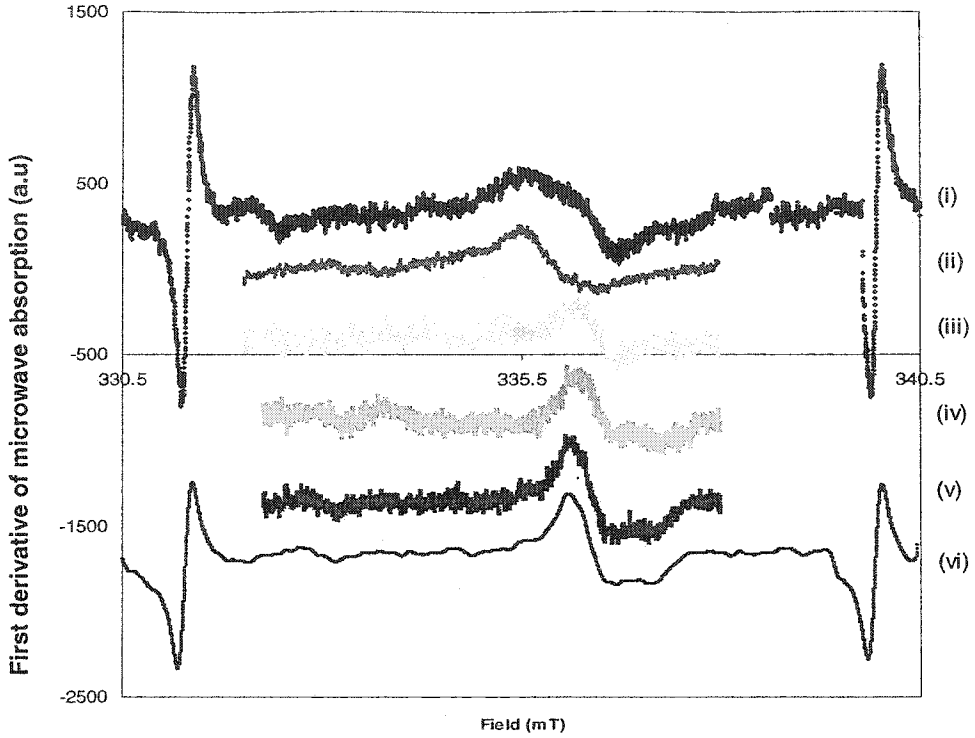

Fig. 2.24 EPR signal adjustment: the top spectrum (i) is 300 mGy composite 18 mW spectrum containing both dosimetric and native signals (at 0° orientation); (ii) signal from ZAD 2 mW spectrum; (iii) 300 mGy, 18mW spectrum after ZAD 2 mW spectrum; (iv) 700 mGy, 18 mW spectrum after 2 mW ZAD subtraction (v) 1 Gy, 18 mW spectrum after subtraction of 2 mW ZAD spectrum and (vi) 1 Gy, 18 mW spectrum after digital smoothing with a 31 point filter, to remove minor ripples. Spectra were translated for better visibility.

2.2.6.2 Low dose signal unfolding

The selective saturation method ceases to be valid for very low doses and small sample mass, when the amplitude of the low power ZAD signal contains a dosimetric signal. Subtraction of which may lead to loss of the dosimetric signal intensity from the high power and therefore incorrect results.

The methodology used in this case consists of separate simulation of both native and dosimetric components in g = 2 region by using the simulation parameter described in Table 2.5.

Table 2.5 Simulation parameters for both dosimetric and native signals.

Signal	g value	Width (mT)	Position
Native signal	2.0045	0.9	336.57
Dosimetric	2.0018	0.23	337.03
	1.9973	0.39	337.42

The shape of the native signal I_n, is first of all simulated using equation 2.1 as a combination of both Gaussian and Lorentzian components (Koshta *et al.* 2000).

$$I_n(H)=\alpha(H)+A_n(\gamma\times\frac{\sqrt{3\sigma}}{\pi}\frac{H-H_T}{[0.75\sigma^2+(H-H_T)^2]^2}-(1-\gamma)\times\frac{8(H-H_T)}{\sqrt{2\pi\sigma^3}}e^{-\left[\frac{2(H-H_T)^2}{\sigma^2}\right]}) \quad (2.1)$$

Where H_T is the position of the local maxima of the peak, σ is the peak width and γ is the relative weighting for the Lorentzian part of the signal (these parameters are also listed in Table 2.5). A_n is the amplitude scaling factor of the native signal. The factor α is usually zero, but it is used only when the spectrum has a positive or negative slope, α could be added or subtracted to the total native intensity, the choice is based on the sloping up or sloping down of 3rd and 4th lines of the Mn^{++} marker.

$$\alpha(H)=\frac{(i_{IV}-i_{III})}{(H_{IV}-H_{III})}\times(H-H_{III})+i_{III} \quad (2.2)$$

Where i_{III} and i_{IV} are the corresponding intensities of 3rd and 4th lines of Mn^{++} marker positioned in field space at H_{III} and H_{IV} respectively.

Fig. 2.25 shows the fitting of the typical native signal data with the function described by equation 2.1. The dosimetric signal is accurately modeled using a superposition of three Gaussian first derivative functions. Each Gaussian is characterized both by peak intensity A_i, position H_{Ti} and the width σ_i while A_o is a constant. Once the shape is determined by using the position and width of each Gaussian, constrained Levenberg –Marquardt nonlinear fitting is performed where only the peak intensity is allowed to vary (Bevington & Robinson 1992).

$$I_d(H) = A_o + \sum_{i=1}^{3} A_i \frac{8(H - H_{T,i})}{\sqrt{2\pi\sigma_i^3}} e^{-\left[\frac{2(H-H_{T,i})^2}{\sigma_i^2}\right]} \tag{2.3}$$

Fig. 2.26 shows the simulation of the dosimetric part of the spectrum.

Various steps for the dosimetric signal reconstruction are delineated as follows (some of them are shown in Fig. 2.27):

- The collected empty EPR tube spectrum is aligned with the ZAD 18 mW spectrum (for 0° orientation) and after removing Mn^{++} marker lines, empty EPR tube spectrum is subtracted from ZAD 18 mW spectrum (for 0° orientation).
- The native simulated signal amplitude is empirically estimated from the low field wing shape of the mixed signal (Ignatiev *et al.* 1996). At the same time the slope of baseline shift is determined i.e. α given by equation 2.2
- The native signal along with the baseline shift is simulated for ZAD 18 mW spectrum (for 0° orientation) and amplitude is found.
- The process is repeated for other orientations, and an average amplitude parameter is estimated, a true native spectrum is constructed.
- The true native simulated spectrum is subtracted from all the given ZAD and multiply-irradiated spectra.
- Average spectra for all different orientations are calculated for both ZAD and multiply-irradiated spectra.
- Dosimetric signal fitting is performed on average spectra, and peak to peak amplitude of the dosimetric signal is then evaluated from the functional fit and is normalized with the sample mass and the intensity of the Mn^{++} lines (and Q if a larger mass is used).

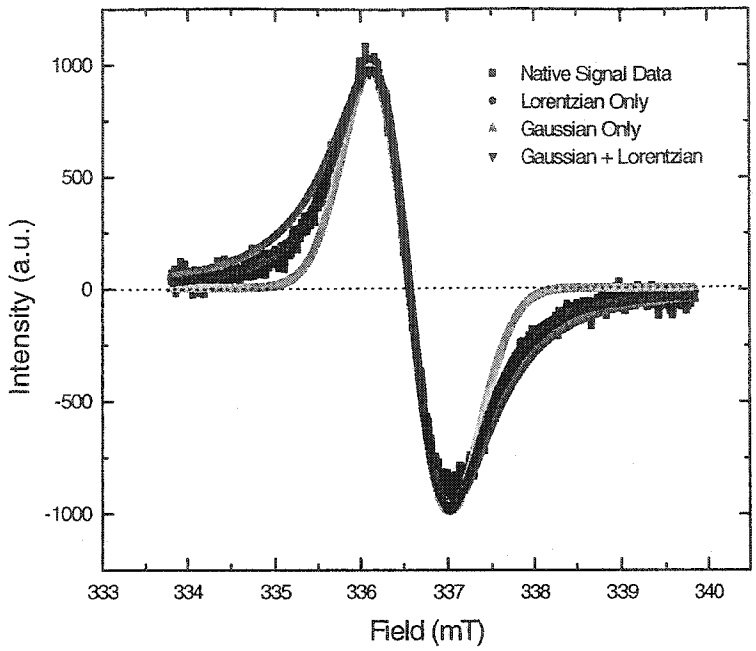

Fig. 2.25 Native signal simulation: comparison with other fitting signals is also shown. A weighted combination of Gaussian-Lorentzian works well for most native signal shapes.

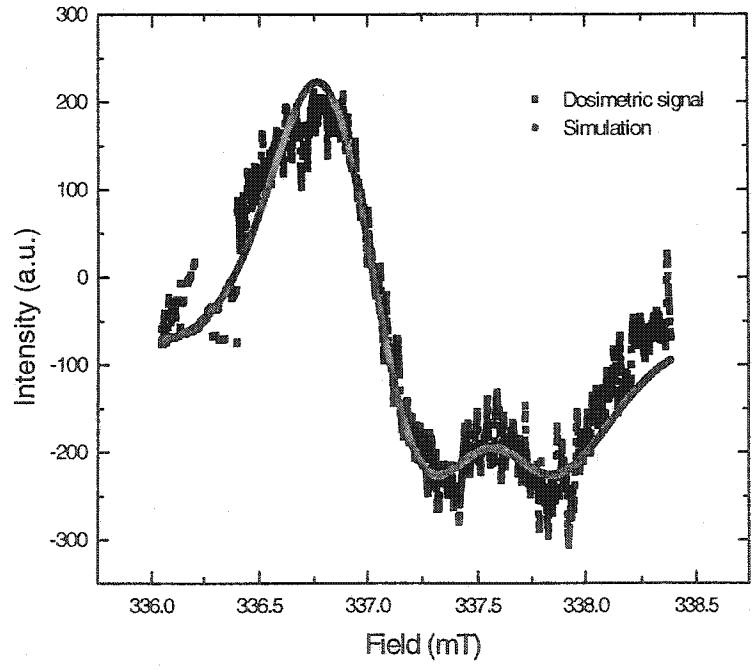

Fig. 2.26 Dosimetric signal simulation involves fitting the dosimetric signal with a combination of Gaussians.

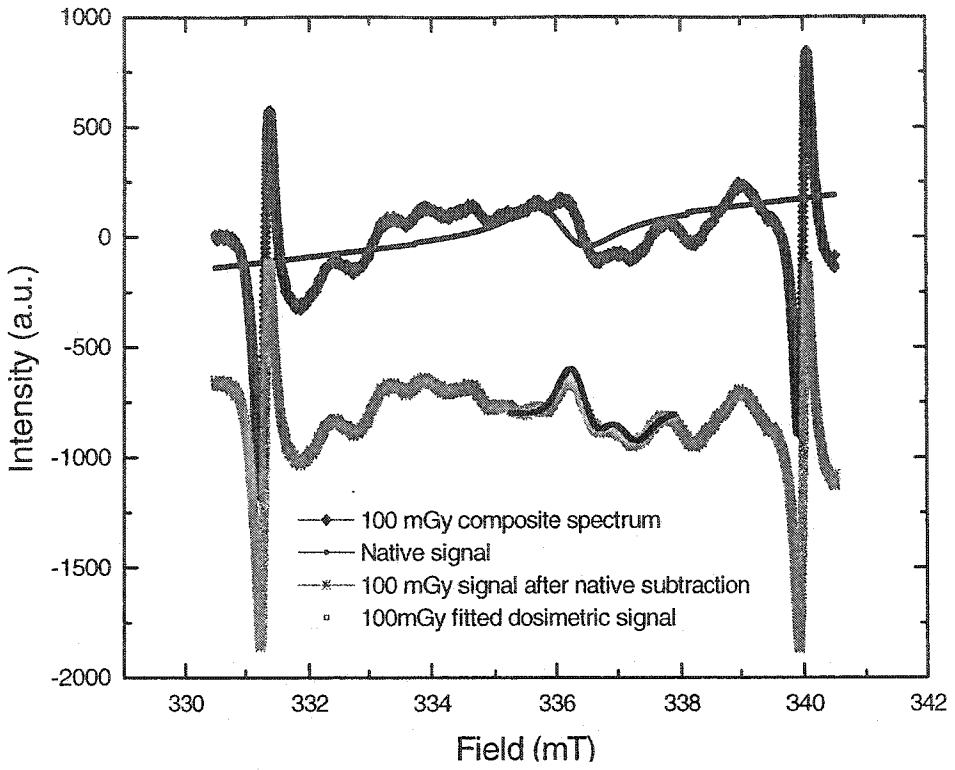

Fig. 2.27 Low exposure, dosimetric signal unfolding procedure for 100mGy dosimetric signal. Base line shifted native signal shape and amplitude are determined from the 100 mGy composite spectrum. The simulated native signal is subtracted from the composite 100 mGy spectrum. The 100 mGy dosimetric signal after native subtraction is simulated using equation 2.3.

2.2.7 Dose evaluation

Usually two methods are used for the dose reconstruction: i) calibration curve method and ii) added dose method. In calibration plot, the sample itself is not given any laboratory dose (also called nondestructive method) rather exposure corresponding to radiogenic signal from the sample is evaluated from the generic calibration line. Generic calibration plot is constructed by giving multiple doses to the samples prepared from a large pool of teeth. However, some degree of variation of radiation sensitivity in individuals and also within the same individual have been reported. The variability of radiation sensitivity of enamel in different samples from adults showed that for doses of few kGy the radiation sensitivity of back teeth was 7% and 14% for front teeth (Ivannikov *et al.* 2001). Therefore generic curve is not a good representative of the tooth under study, and could cause larger uncertainty in dose measurement. But if a

large population screening is desired, a generic calibration curve is a quick and robust method. It can also be used for the relative sensitivity comparison for various radiation qualities as will be discussed in section **3.2.10**.

For accident dosimetry, involving a few individuals, individual radiation sensitivity of the teeth must be determined. The dosimetric signal response is plotted against the added doses, the data is fitted with the weighted least-square-line; from the intersection of the backward-extrapolated line with the dose axis, the previous radiation dose is determined, and this technique is called the additive dose method. Fig. 2.28 shows the typical dose reconstruction from the added laboratory irradiations. Similar individual responses were performed for various individual samples and retrospective radiation exposures were determined. These are listed in Table 2.6.

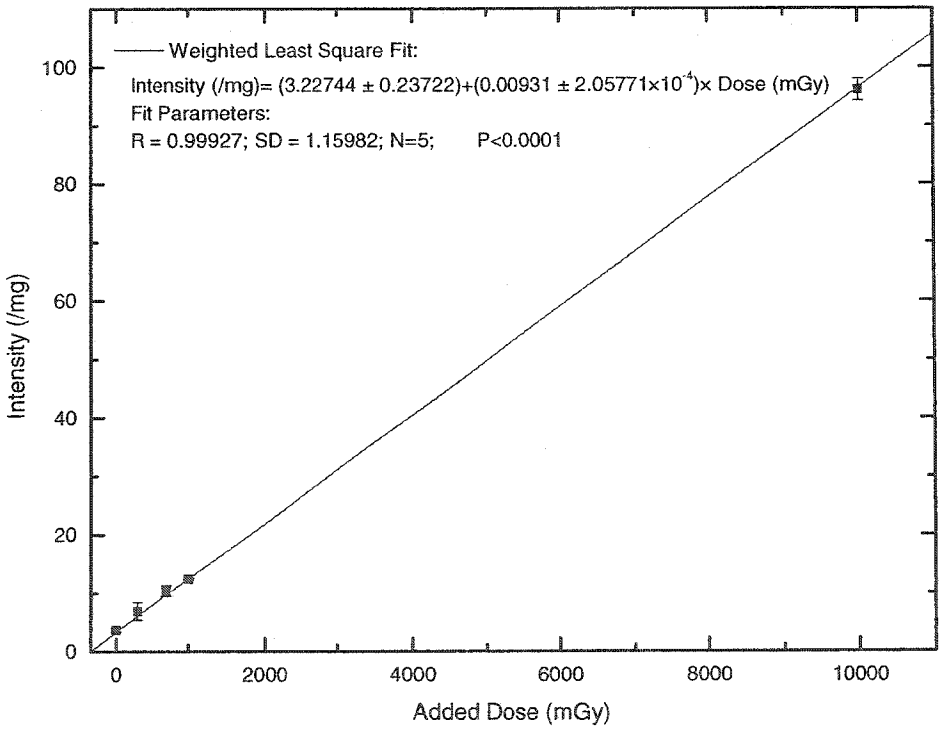

Fig. 2.28 Dose constructed using a backward extrapolation method, for the sample RK01-11 one of several samples for which the dose was reconstructed.

Table 2.6 Laboratory samples in which dosimetric signal due to retrospective exposures were observable, dose reconstructed are listed in column 5.

Sample number	Tooth type	Treatment	Mass (mg)	Retrospective constructed dose (mGy)
RK01-11	Incisor, sound	2NKOH treatment for (20h)	68mg	346.66±26.61
RK01-01	Molar, sound	2NKOH at 60C for (20h)	200 mg	80.21±30.29
RK01-46	Premolar, sound	8NKOH treatment for (20h)	170mg	222.88±54.70
RK01-47	Premolar, sound	8NKOH treatment for (20h)	123mg	88.13±11.27
RK01-21	Molar, sound	8NKOH treatment for (25h)	376mg	253.63±36.32
RK01-32	Incisor, sound	8NKOH treatment for (30h)	143mg	356.14±17.37
RK01-33	Molar, carious	8NKOH treatment for (30h)	302mg	456.04±28.89
RK01-34	Canine, cavity	8NKOH treatment for (25h)	228mg	364.34±27.96
RK01-35	Canine, whole big cavity	8NKOH treatment for (25h)	67mg	207.54±65.40
RK02-36	Molar, carious	8NKOH treatment for (35h)	224mg	361.50±41.77
*RK01-38	Molar, carious	8NKOH treatment for (10h)	121mg	76.29±30.14

* For this tooth the sample was prepared by avoiding the carious part

2.2.8 Accidental radiation dose

EPR measurement provides the total dose accumulated in the tooth; this could be a summation of exposures involving accidental, environmental, professional and dental X ray.

$$D_{EPR} = D_{acc} + D_{X-ray} + D_{Env,prof} \tag{2.4}$$

Where D_{acc}, is the dose due to a radiation accident, D_{X-ray}, is dose due to X ray exposures, and $D_{Env,prof}$, is the dose due to environmental and professional exposures.

2.2.8.1 X ray exposure separation

This step is necessary to separate out any dental X ray contribution from the accidental radiation dose. In standard dental practice, a dose of ~ 1.9 mGy (tissue dose) per dental exposure at the entrant surface of the cheek is estimated (Suleiman *et al.* 1999). For a 1 mGy entrant dose of a lower kV_{pp} X ray due to high mass energy absorption coefficients of hydroxyapatite with respect to tissue, with wisdom tooth formed between age of 9 and 10 years and standard dental exposure of 1 per year, a tooth could easily receive exposure from 0 - 100 mGy (Hayes *et al.* 2000b; Shimano *et al.* 1989). This is based on the observation that diagnostic X rays used in dentistry has a typical energy in the range 40 - 50 kV_{pp} they

preferentially penetrate the exposed side of the tooth (i.e. buccal) compared to gamma radiation which produces radicals uniformly throughout the tooth volume (Aldrich & Pass 1986). Therefore, buccal side must be separately treated from the lingual side of the tooth.

2.2.8.2 Environmental and professional exposures

An average exposure of 1 - 2 mGy per year (or 10 - 12mR/h) (UNSCEAR 1993) could be assumed, unless the complete residential history of the victim is known (Lamarsh 1983). The dose component due to environmental exposure will be a multiple of annual exposure with tooth age. Tooth age is the result of subtraction of the average age of formation of tooth (for a given position) from the age of person at the time of measurement (Ivannikov *et al.* 2000).

The professional component of dose is added only when the individual belongs to radiological or nuclear industry and the annual exposure record is available in the form of films or thermoluminescent dosimeters.

2.2.9 Protocol testing

Three samples each were irradiated in a laboratory controlled experiment. Teeth were halved in mesial and distal parts; only mesial part is given a gamma radiation dose 100, 300 and 700 mGy. The dose was reconstructed by using the designed protocol (given in sections **2.2.2.8**, **2.2.3.5**), and the results are summarized in Table 2.7. For the exposures ~ 700 mGy signal discrimination was done by power saturation method (section **2.2.6.1**), whereas for 300 and 100 mGy laboratory doses, signal was evaluated by procedure mentioned in section **2.2.6.2**.

Table 2.7 Laboratory measured and EPR reconstructed radiation doses.

Dose (mGy)	Measured EPR dose (mGy)
700 ±35	720.30 ± 42.81
300 ± 15	350.21 ± 89.23
100 ± 5	140.15 ± 49.38

2.3 DISCUSSION

Electron spin resonance dosimetry requires extremely careful sample preparation prior to the dose reconstruction process. Any miscalculation during a step can either lead to improper assessment of paramagnetic species or contaminate the dosimetric signal and results in either overestimation or underestimation of the dose constructed.

For sample preparation premolar and molars are always a preferred choice due to higher enamel contents, and also they are least affected by the sunlight induced paramagnetic centres which make a big contribution towards dosimetric signal in incisors and canine (Liidja *et al.* 1996). It has been shown that one full day of sunshine could lead to a signal with equivalent gamma radiation dose of 209 mGy in tooth enamel (Sholom *et al.* 1998a). However, acidic etching of the surface directly exposed to sun (buccal) can reduce the contribution from the sunlight.

A cylindrical cavity with TE_{011} mode, rather than a rectangular one with TE_{102} mode, produces higher signal sensitivity. All the measurements were done in X band (9.5 GHz) microwave. Although higher frequencies of K-band (25 GHz) and Q band (35 GHz) can give better resolution of signal with different g factors, they result in poor signal reproducibility due to difficulty in precise sample setting. Differential power measurement during chemical processing could reduce chemical processing time. This could be important if a large number of samples are to be processed for population or epidemiological studies.

According to the Curie law the signal sensitivity should improve for low temperature measurements, and a sharp line width must result due to the increased relaxation time. High sensitivity also results due to reduced microwave loss (as the moisture is frozen). The difference in the spin population between lower and higher energy level increases at low temperature leading to the enhancement of the signal intensity. However, in our case liquid nitrogen measurement for the tooth enamel failed to produce the signals observable at room temperature. Other authors have attributed the disappearance of signals like CO_2^- due to prevention of hindered rotation at low temperature (Ikeya *et al.* 1993).

In the current sample preparation procedures mechanical treatment was limited and it was used only with appropriate sample cooling e.g. sample was divided into small pieces by using low speed water cooled diamond tipped saw. By treating the sample with the supersaturated potassium hydroxide aqueous solution the organic contents of the enamel could be reduced (Romanyukha *et al.* 2001). The KOH treatment was preferred over the NaOH treatment as it was observed that the deterioration of native signal amplitude was much more efficient for supersaturated KOH (also shown in Fig. 2.14). This ceases to be valid for the carious teeth, unless the carious part is completely removed (Sholom *et al.* 2000b). In some of our samples, it was found that the reagent completely removed the native signal, which was also observed by other authors (Ivannikov *et al.* 2001; Romanyukha *et al.* 2000a).

To reduce the dose uncertainty contribution arising from the dosimetric signal due to large particle anisotropy, the sample is crushed into smaller pieces. However, it has been observed that the origin of mechanically generated radicals is due to inefficient heat removal during the grinding operations. In the current protocol, we have tried to cool the sample by using liquid nitrogen along with gentle crushing. The signal was measured at various times after crushing in the presence of liquid nitrogen. This was necessary to observe the presence or otherwise of crushing induced signals as the sample comes back to room temperature. The sample is then sieved into 0.2 - 0.4 mm, which have reasonable sensitivity to radiation. The surface radicals formed as a result could be reduced by etching the enamel in 5 % HCl, similar results were obtained by use of phosphoric acid by others (Fattibene *et al.* 1998).

A comparison of our technique with other laboratories shows that this eliminates multiple crushing of the enamel grains, which can produce undesirable signals in the spectrum. This is because as a result of extensive ultrasonic treatment ~ 15 – 25 h in KOH and 26 – 60 h in water, the grain size is reduced to < 4 mm. The temperature stability of dosimetric signal remains valid up to 200 °C, therefore the sample drying temperature was chosen to be 40 °C, well below the limit.

Since glass tubes and ordinary silica material give EPR signals, they may not be suitable for sample measurement, juxtaposed to this is the positioning of the tube inside the cavity. Therefore, optimized measurement conditions were chosen (given in Table 2.1). Inside the cavity, a sample filled to a

height of 10 mm was found to produce the most sensitive results, around the centre of the cavity. That is why a larger amount of sample failed to produce most sensitive results due to greater height in small diameter tubes (Table 2.2).

The anisotropy due to finite sized particles was accounted for by manual rotation. Since this method involves rotation prior to spectrum collection and fixed position of in cavity Mn^{++} marker, the change in boundary conditions on the cavity electromagnetic field produced due to sample rotation can be overcome by retuning the cavity in between rotation and measurement. The amplitude of Mn^{++} marker represents the changed cavity Q value (which is based on the argument provided in section **2.2.2.2**). This technique is less capital intensive as compared with the goniometry, where the constant rotation alters the tuning characteristics of the cavity, and therefore results in the smearing of the signal's g values. To fix this problem, a field-frequency lock or NMR gauss meter is used, which could easily cost tens of thousands of dollars (Haskell *et al.* 1997b). The advantage of goniometry is the more mechanized process and less human intervention whereas either rotation or shaking is laborious.

To produce the uniform dose across the sample, a sample irradiation rack was designed; the sample positioning reproducibility was ensured by attaching it to the fixed stand. The combined effects of positioning and ion chamber uncertainty lead to an estimate of 5 % in total dose uncertainty. The choice of calibrated doses although should not matter, because the dosimetric response of the tooth enamel is linear, however it has been observed that the selection of additional dose points both near and far apart improves the uncertainty associated with the reconstructed dose (Hayes *et al.* 1997). The distributions of added dose values as shown in Fig. 2.28 were selected keeping in view the uncertainty of measurement.

The process of additional laboratory irradiation could lead to production of some short-lived transients, which may influence the intensity of the radiation induced signal (Oduwole & Sales 1994). These signals, if not taken into consideration, can produce error in dose approximation up to 15% in routine EPR dosimetry. Some laboratories use a method wherein annealing the samples at 95 °C for 2 h can remove the transients (Sholom *et al.* 1998b). In the current protocol approximately 48 h of heat treatment is

provided to the post-irradiation sample at 80 °C. This was done to remove transients of added doses, and the water contents of the enamel which may lead to some loss of dielectric field inside the cavity.

The post-processing part of the protocol differs for low and high exposure. This results in quick and simple dose evaluation for high exposure samples, whereas low exposure samples require a lot of sample processing, spectrum fitting and consequently a longer time.

The added laboratory dose method for dose reconstruction has the disadvantage of being destructive method, which would make it impossible for re-measurement of zero added dose. However, this also avoids any uncertainty due to tooth's individual radiosensitivity and also provides the individualization of radiation dose compared to general calibration method. The additive dose method for dose construction could be used in a non-destructive way, when only a small aliquot of original sample is given a large dose, and major sample is preserved (Hayes *et al.* 2000b), and therefore dose response is reconstructed.

From the results presented in Table 2.6; it could be seen that the doses constructed out of incisors are higher than expected; which could be due to the reason that incisors were exposed to sunlight. In the front tooth enamel, solar light induces an EPR signal with the same properties as the radiogenic signal. The depth of exponential distribution of solar induced paramagnetic centres was determined to be about 0.3 mm (Sholom *et al.* 1998a). Such a thick layer of enamel can not be removed by surface etching. Special investigations have revealed that the inner side of the front teeth had no solar component; however the amount of enamel would be very small for reliable dose reconstruction, due to special structure of the incisors.

Also observed from Table 2.6 are the high exposures constructed out of the teeth containing dental carries, which is in accordance with the observations by several other authors. It is well-known that tooth disease induces changes of chemical composition, dimensions, orientations and other properties of crystallites in tooth enamel. In carious teeth the quantity of carbonate groups can increase from 5 - 15%. Because the radiation defects in tooth enamel, which have been used for dose reconstruction, are associated with carbonate groups, it can be a cause of increased radiation sensitivity in carious teeth (Brik *et al.* 1996).

However, if the caries are excised tooth sample can be carefully prepared. For example, by avoiding the caries (i.e. in case of sample RK02-38), the dose measurement could be performed with low uncertainty.

If doses from X ray and environmental exposure are properly taken into consideration then accidental dose to the enamel can be constructed. The dose to the whole body and various other tissues can be evaluated from the knowledge of the accident and the positions of the individual involved, with respect to the radioactive source (Takahashi *et al.* 2001).

2.4 CONCLUSION

An EPR based technique for accident dosimetry using human teeth has been described. Radiation doses to the human tooth enamel have been successfully reconstructed in three different dose ranges < 100 mGy, 100 – 300 mGy, and 300 - 700 mGy with uncertainties ranging from 5 to 40%. Using the EPR spectrometer in the optimized configuration, the noise arising from the cavity could be controlled and by using multiple tube measurement, maximum dosimetric signal sensitivity could be achieved. Q value normalization and digital Mn^{++} marker alignment helps increase the reproducibility of measurements. Undesirable signals produced due to sample preparation could be avoided by limiting mechanical treatment, and liquid nitrogen cooling during the sample grinding. The dosimetric signal anisotropy could be accounted for by using manual rotation of the sample inside the cavity, in the presence of a fixed positioned in cavity Mn^{++} standard. Uniform calibrated doses could be delivered to sample through a customized 3D irradiation rack design (section **2.2.5**). Post processing of spectra involves fitting the functions for both native and dosimetric signal in the low dose range (section **2.2.6.2**), while at higher doses (section **2.2.6.1**) selective power saturation results in quick dose reconstruction.

Chapter 3

Neutron Response of Tooth Enamel

3.1 INTRODUCTION

Electron paramagnetic resonance (EPR) dosimetry of teeth involves the measurement of paramagnetic centre formed as a result of ionizing radiation exposure. The quantification of the centre provides a measure of the radiation dose an individual is exposed to and is an accurate measure of accident dose. This technique has been extensively used and developed over the past ten years to account for the radiation dose to the population and accident victims (Aldrich & Pass 1988; Chumak *et al.* 1997; Ikeya *et al.* 1986; Schauer *et al.* 1993).

Most research and development in the field of EPR dosimetry has involved exposures involving only photons (e.g. ultraviolet, X, and gamma rays). There are very few instances when the studies involved either higher or intermediate linear energy transfer (LET) radiation. This is also because most of the accidents involved the exposure to photonic radiation, but in practice there exist several situations when the exposure also includes non-photonic radiations. For example, a high LET accidental exposure may take place in or around a nuclear facility e.g. Tokai Mura accident (Inaba 2000), Chernobyl reactor site, Three Mile Island or during safety criticality exercises (Stratton 1967; Vargo 1999). High LET radiation exposure also occurs in extra-terrestrial environments, in manned space missions or high altitude aircraft flying.

If tooth enamel is to be utilized as a good radiation dosimeter for all practical radiation exposure scenarios, it becomes essential to categorize its response to all other kinds of radiation qualities usually encountered. The most common type of accidental radiation fields includes electrons, photons, and neutrons either individually or in the form of mixed fields. Except for neutrons, the response of tooth for photons and electrons has been very well studied. Radiations like alpha particles, protons and heavily charged particle ions have very short range in solids (4 MeV α particles have a range of 0.04mm in tooth).

Thus they can not deposit energy inside the oral cavity unless they get incorporated internally and thus deposit their energy. In tooth enamel, Lyons (1987) studied the EPR response per unit dose for alphas in the energy range of 2 to 14 MeV; for higher energy the enamel response was higher, however a linear EPR response was found with respect to incident alpha track length. Response of human bone powder was studied for proton and other heavily charged ions by several authors (Copeland *et al.* 1996; Stuglik *et al.* 1994; Stuglik & Sadlo 1996). Very high LET ions ($_{12}C^{6+}$, $_{59}Co^{25+}$ ions) have been found to have approximately 15 - 25% effectiveness of the ^{60}Co gamma rays in inducing the EPR dosimetric signal in bone powder. Also it was found that the high LET radiation produces the same EPR signal as gamma radiation. Therefore, without an appropriate correction, any dose estimate solely based on the intensity of the induced EPR signal will underestimate the contribution from the very high LET radiation.

For the purpose of dating and archeological age estimation, on very few instances neutron irradiation was performed. In one case, neutron irradiation was done by using fast neutrons from a research reactor for the additive dosimetry purposes (Garrison *et al.* 1981). Whereas in another case, the additive irradiation effect was not observed when a dose was given from a ^{252}Cf source to estimate the age in granite sample (Ikeya *et al.* 1993). Since additional laboratory irradiation with calibrated gamma radiation sources was simple and well-established, neutron irradiation was never needed and hither to fore remain unexplored.

Alanine was probably the only radical based dosimeter which was explored for both neutron and gamma irradiation. It was observed that stable radicals of same type result from the irradiation of both neutrons and gamma rays in alanine, and they produced same EPR signal (Katsumura *et al.* 1986). However, the effectiveness of neutrons in terms of radiation sensitivity for different energies varied from 0.4 – 0.68 of that of gamma radiation (Simmons & Bewley 1976).

As pointed out by several authors, there is no published information available about the neutron response of human tooth enamel (Desrosiers & Schauer 2001; Haskell *et al.* 1997b). Further research in this regard is required, because the success of EPR dosimetry lies in the correct prediction of biological consequences. However in some studies it was suggested that tooth enamel is not very sensitive to neutrons

based on the dose response to 14 MeV neutrons and ^{252}Cf spectrum (Tatsumi 1986). The sensitivity of tooth enamel to neutron exposure was estimated as 0.03 of its sensitivity to γ exposure (Bochvar *et al.* 1997; Tatsumi 1986).

The unavailability of the neutron response studies could be mainly due to two reasons: 1) the neutron response of enamel was believed to be very low even for highly biologically significant doses of neutrons. Therefore, the signal was expected to have very low amplitude and if the tooth enamel already consisted of the native signal, the signal due to neutron dose could never be revealed accurately. 2) Unavailability of neutron sources largely devoid of any gamma ray contamination.

The first problem could be circumvented by using an optimum sample preparation protocol that not only minimizes or eliminates the native signal but also avoids production of any new species of radicals due to local overheating in enamel. Romanyukha and colleagues have shown that high-temperature supersaturated basic chemical treatment can remove or degrade the native signal from the tooth, (Romanyukha *et al.* 2001). Also others have demonstrated that the native signal removal could be accomplished by using a combination of physical and chemical treatment with hydrazine (Ivannikov *et al.* 2001). We have also observed complete removal of the native signal in some of tooth samples (section **2.3**). This has opened the way for the quantification of low dose response for high LET radiation like neutrons and protons.

Table 3.1 is a list of generally available neutron sources, of these only charged particle accelerated sources and photo-neutron sources qualify as clean sources; the remainders contain a high degree of gamma rays contamination. However, for photo-neutron sources, low neutron yield is a major disadvantage; only one in 10^5 gammas interact with the target material to produce a single neutron. Therefore, these types of sources are not practicable. Whereas, a 1 mA beam of deuterons accelerated by a potential of 100 – 300 kV will produce about 10^9 neutrons per second from a thick deuterium target. However, small quantities of bremsstrahlung photons and gamma rays are produced both due to other competitive reactions in target and neutron interactions in extra-target material or engineering structure. This necessitates the accelerator beam

characterization which will yield the information about the contribution of neutron and gamma radiation components to the total dose.

Table 3.1 Commonly available neutron sources for physics research (Knoll 2001).

Sources	Typical targets	Energy range	Quality
Fission sources:			
Induced fission	$^{238}U/^{235}U/^{239}Pu$	0.253eV -18 MeV	dirty
Spontaneous fission	^{252}Cf	0.253eV – 8MeV	
(α ,n) Sources:			
^{9}Be- sources	^{239}Pu; ^{241}Am; ^{244}Cm	0.253 eV – 10MeV	dirty; high neutron yield
^{7}Li-sources	^{241}Am	> 1MeV	
^{10}B or ^{11}B-sources	^{241}Am	2 - 4MeV	
Photo-neutron sources	^{9}Be; ^{2}H	monoenergetic	low neutron yield
Accelerated charged particle sources:			
^{2}H	^{9}Be; ^{2}H; ^{7}Li	monoenergetic; energy varies from reaction to reaction	yield based on beam current and cross-section
^{1}H			

In summary, this chapter addresses the problem of neutron dose response determination in human tooth enamel, using the accelerator-based neutron source. Using the accelerator beam, different experiments were designed to develop understanding about the types of paramagnetic centres and sensitivity of tooth enamel for the neutron. Finally, the tooth enamel neutron response was evaluated in terms of gammas. This efficiency can serve as the basis for correcting retrospective doses in tooth enamel for exposures involving mixed neutron-gamma radiation fields.

3.2 PROCEDURE & EXPERIMENTAL DESIGN

3.2.1 Sample preparation and measurement

Teeth free from any dental caries or disease were collected from a local dental clinic. The crowns were separated from the root, and halved into mesial and distal parts by using a low speed water-cooled diamond saw. The mesial part of the sample was placed in a polypropylene tube and given 5h of ultrasonic treatment in 10ml of supersaturated potassium hydroxide aqueous solution at 80°C. The sample was then

washed in an ultrasonic bath for 12 h, dried and the EPR spectrum was then measured (Khan *et al.* 2002). The whole chemical treatment procedure was repeated until the native signal was eliminated or its amplitude ceased to decrease further. The cleaned sample was crushed in an agate mortar and pestle and sieved into 0.3 – 0.5 mm, and 0.106 – 0.3 mm distribution as required in various experiments. The enamel powder was then placed in 4 mm inner diameters suprasil (synthetic quartz) low noise EPR tube. The EPR measurements were performed in a cylindrical TE_{011} cavity with the JEOL JES-FA 100 type spectrometer operating in the X-band under the conditions mentioned in section **2.2.2.8**. The spectrometer was warmed up for at least 3 hours before measurements to minimize any fluctuation in magnetic field or current. The sample was measured several times at various angular rotations inside the cavity. Based on the specific experimental requirements, the previous dose history and the native signal of the teeth were accounted differently and will be described with the relevant experiments. After spectrum subtraction, the peak to peak amplitude of the dosimetric signal was measured. For a known sample mass (100 mg), the dosimetric amplitude was normalized with the intensity of the 3rd and 4th line of the Mn^{++} markers; which will hereafter be called *dose response*. The EPR dosimetric signal anisotropy due to angular rotation results in the uncertainty of the dose response. Similarly *neutron (or gamma) radiation sensitivity* is defined as the neutron (or gamma) radiation dose response per gray of a neutron (or gamma) absorbed dose.

3.2.2 Neutron irradiation and dosimetry

Tooth samples were irradiated with the neutron beam at the 3 MV McMaster K.N. Tandem Van de Graaff accelerator facility at a distance of 5 cm away from the proton target. The neutrons were produced from $^{7}Li(p, n)^{7}Be$ reaction by bombarding protons (proton current ~ 41 - 61 μA) accelerated to a terminal voltage of 2.25 MV on a thick lithium metal target. The neutron dose was measured at 2 m away from the proton target by using Anderson and Braun neutron remmeter (Tracerlab, Model NP-1 portable monitor). The monitor, colloquially called snoopy, consists of a unique polyethylene moderator assembly, a BF_3 detector, and associated electronics. The incident neutrons, moderated and thermalized by the polyethylene assembly, are counted by the stable BF_3 proportional counter due to $^{10}B(n, \alpha)^{7}Li$ reaction. The snoopy dosimeter was pre-calibrated, and has good gamma radiation discrimination. The dosimeter response

required a uniform irradiation, so it was placed at a larger distance from the accelerator target, which also avoids the detector saturation at higher dose rates (Pejovic-Milic 1998). The inverse square relationship for the neutron beam was tested by placing the detector at various distances prior to experimentation. The dose rate at 2 m away from the lithium metal target was 1 rem/h. The dose equivalent was then converted to the absorbed dose, D, to the tissue by using the $H = D \times Q$, where H is the dose equivalent for tissue and Q is the radiation quality factor for neutrons. Unless mentioned otherwise, for various experiments proton energy of 2.25 MeV (mean neutron energy 280 keV) was used. The corresponding radiation quality factor was found both experimentally and theoretically and tabulated as Table 3.2 (Aslam *et al.* 2003b). The gamma radiation yield of the target was measured by using a tissue equivalent proportional counter (TEPC) and it was < 1% of the neutron dose (Aslam *et al.* 2003a).

Except for the whole tooth halves, all neutron irradiations were done by placing the powdered samples in polypropylene vials (wall thickness ~1mm) in front of the accelerator beam (Fig. 3.1). The total uncertainty in dose measurement arises from three fixed sources: dose rate from dosimeter (relative error ~ ±0.05), duration of irradiation (relative error ~ ±0.016), and sample positioning in front of the beam (relative error ~ ±0.04).

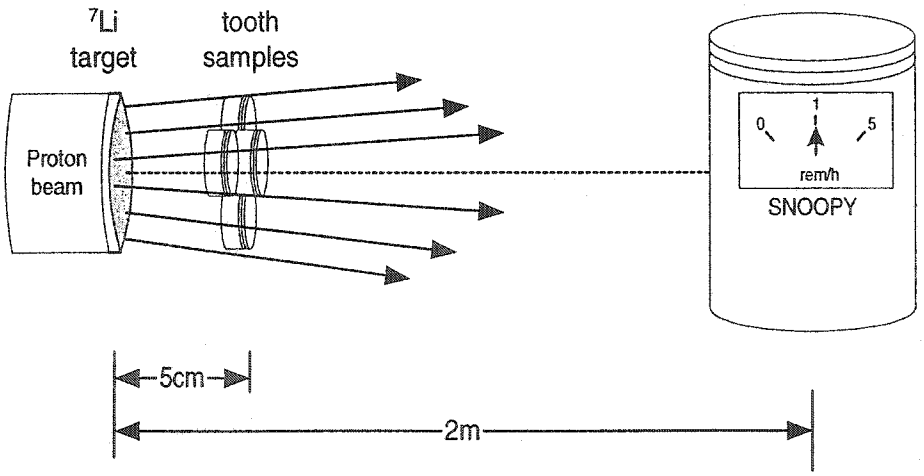

Fig. 3.1 Irradiation configuration of the tooth samples in front of the neutron beam generated by the McMaster K.N. *Van de Graaff* accelerator.

Table 3.2 Radiation quality factor and mean neutron energies used for neutron experiments (Aslam *et al.* 2003a; Aslam *et al.* 2003b).

Proton energies (MeV)	Mean neutron energy (keV)	Neutron quality factor
2.15	167	12.00
2.25	280	13.2
2.35	387	13.2
2.45	450	13.3

3.2.3 Experiment 1: Tooth enamel dose response

Chemical treatment of molar sample RK02-27 resulted in < 4 mm grains which were then measured in the EPR cavity. The sample was then given different doses of neutrons, and remeasured. The dosimetric signal intensity was found by subtracting the undosed spectrum from the neutron dosed spectra for given doses.

3.2.4 Experiment 2: Dose response for various grain sizes and whole tooth

Chemically processed tooth enamel powder with grain size 0.3 – 0.5 mm (samples N4 & N5), 0.106 – 0.3 mm (samples N1 & N2), < 4mm (RK02-27) and mesial halves of the whole tooth samples (RK02-49, RK02-50, RK02-53, RK02-54, and RK02-55) were measured in the EPR spectrometer. The sample N4, N5, N1, N2, RK02-27 and distal halves of RK02-49, RK02-50, RK02-53, RK02-54, RK02-55 were then irradiated in the neutron beam for different times and the spectrum was collected. The dosimetric signal intensity was found by subtracting the corresponding undosed spectrum from the neutron dosed spectra for each sample. While for the whole samples, the unirradiated mesial spectrum was subtracted from the corresponding irradiated distal parts, after normalizing it for mass, to evaluate the dosimetric signal intensity.

3.2.5 Experiment 3: Response for various grain sizes from the same tooth

Samples RK02-68 and RK02-636465 crushed and sieved into 0.3 - 0.5, 0.106 - 0.3 and < 0.106 mm distribution and the spectrum was collected. The samples were given neutron dose of 9.09 ± 0.70 Gy

and post irradiation spectrum was measured under the identical conditions. The dosimetric amplitude was evaluated by subtracting undosed spectrum from the neutron irradiated one.

3.2.6 Experiment 4: Effect of crushing on the dosimetric signal

The distal half of RK02-86 was given neutron dose of 14.02 ± 1.08 Gy. The chemical processing resulted in grains distribution < 4 mm and the sample was subsequently measured in EPR spectrometer. Peak to peak intensity was measured after subtracting undosed spectrum obtained from the corresponding mesial half from the neutron irradiated distal grains. The sample was gently crushed and sieved into three grains distribution 0.3 - 0.5, 0.106 - 0.3 and < 0.106 mm, spectrum was collected and peak to peak intensity was measured.

3.2.7 Experiment 5: Pre- and Post-chemical processing dose response

The distal half of the sample RK02-54 previously irradiated with 12.32 ± 0.89 Gy, was chemically treated and dosimetric amplitude was measured. The sample was then given two additional neutron doses of 6.16 ± 0.48 Gy each and the EPR spectrum was measured. The dosimetric signal amplitude was measured after subtracting the EPR spectrum from the unirradiated mesial half.

3.2.8 Experiment 6: Dosimetric signal stability with chemical processing

The distal halves of the whole tooth were given known neutron doses and the samples were later chemically processed as mentioned in section **3.2.1**. The spectrum was collected at 5 h intervals for 40 h of chemical treatment. The dosimetric signal was found by using the power saturation of the spectrum at 2 and 18 mW.

3.2.9 Experiment 7: Build-up layer effects

Sample RK02-27-waxed with grain distribution < 4mm and N45-waxed with grain size 0.3 – 0.5 mm, were mounted behind a layer of 4 mm thick paraffin wax (C_{25} H_{52} density 0.93 g/cm^3), and another aliquot of RK02-27-bare (without any wax layer in front) were placed in the neutron beam. The spectrum

was measured and dosimetric signal intensity was found by subtracting the corresponding unirradiated spectrum for the given sample.

3.2.10 Experiment 8: Gamma radiation dose response

The mesial parts of samples (RK02-49, RK02-50, RK02-53, RK02-54, and RK02-55) were chemically processed, mixed, and crushed into grain size 0.3 – 0.5 mm. The spectrum was collected to look for any previous radiation history. Approximately 100 mg of powder was placed in small polypropylene vials and given multiple known laboratory gamma radiation dose in the specially-designed perspex rack providing both charged particles build up and backscatter for uniform dose distribution in the sample. The dosimetric intensity was found by subtracting the unirradiated spectrum from the gamma irradiated spectrum. A calibration curve was generated from multiple irradiations of the sample from a ^{137}Cs source with air exposure rate of 4.25 Roentgen per minute (10.97×10^{-4} C/kg-minute). The dosimetry was done using Farmer dosimeter (more pertinent details are provided in section **2.2.5**). The air dose was then converted into the tissue dose by using the ratio of mass energy absorption coefficients for the given energy (Attix 1986).

$$D_{tissue} = D_{air} \times \frac{(\mu_{en}/\rho)_{tissue}^{662keV}}{(\mu_{en}/\rho)_{air}^{662keV}} \tag{3.1}$$

The dose calibration curve was then translated to pass through the origin for direct reference to neutron amplitude and corresponding dose.

3.2.11 Experiment 9: Post neutron irradiation gamma radiosensitivity of enamel

Distal halves of the samples RK02-53, RK02-54 and RK02-55 previously given neutron doses and chemically processed (in experiment 2) were given ~1 Gy of gamma radiation dose along with their mesial undosed halves. Spectrum was collected for both post neutron dosed and no neutron dosed halves. The peak to peak intensity of dosimetric signal due to gammas only, for neutron dosed sample, was found by subtracting the pre gamma radiation dosed spectrum from the post gamma radiation dosed spectrum. Similarly, for no neutron dosed distal half, undosed spectrum was subtracted from the gamma radiation

dosed spectrum and intensity arising from gamma radiation only, was measured. The process was repeated for all three samples.

3.2.12 Experiment 10: Neutron radiosensitivity with dose rate

Various distal halves of the samples were given neutron absorbed dose with samples placed at 5 cm away from the accelerator target Table 3.3. Teeth were then processed and spectrum was collected, dosimetric signal intensity was evaluated after subtracting the corresponding undosed mesial spectrum from neutron dosed distal spectrum.

Table 3.3 Samples used for studying the effect of neutron irradiation dose rate on neutron sensitivity. Neutron dose rate was obtained by dividing the equivalent dose rate, measured using an Anderson and Braun rem meter, by the quality factor given in Table 3.2 (at 2.25 MeV beam energy).

Neutron dose equivalent rate at 200 cm (rem/h)	Dose rate at 5 cm (Gy/h)	Samples	Irradiation time (h)	Cumulative dose (Gy)
0.5	0.6	RK02-72, RK02-73	8	4.8
0.75	0.9	RK02-66, RK02-67	6	5.4
1	1.2	RK02-53, RK02-55	4	4.8
1.3	1.6	RK02-68, RK02-69	3.5	5.6
2	2.4	RK02-70, RK02-71	2	4.8

3.2.13 Experiment 11: Neutron radiosensitivity with mean neutron energy

Various distal tooth halves were irradiated with different energy neutrons at the fixed distance of 5cm away from the accelerator target (Table 3.4). Teeth were then processed and spectrum was collected, dosimetric signal intensity was evaluated after subtracting the corresponding undosed mesial spectrum from the distal half. A typical spectrum subtraction process is shown for sample RK02-78 in Fig. 3.2.

Table 3.4 Samples used for measuring changes in neutron sensitivity with mean neutron energy.

Mean neutron energy (keV)	Samples	Total dose (Gy)
167	RK02-76, RK02-77	4.89± 0.38
280	RK02-72, RK02-73	6.16± 0.48
387	RK02-74, RK02-75	6.58± 0.51
450	RK02-78, RK02-79	7.22± 0.56

3.3 RESULTS AND DISCUSSION

Gamma irradiation of tooth results in the formation of electron and hole pairs. The dosimetric signal in the enamel matrix is produced because of capturing of electron hole pairs by carbonates sites. Therefore, in theory, any ionizing radiation having the penetrability in the tooth should produce a dosimetric signal. It must be noted that although neutrons and gamma rays are neutral radiations, their initial mechanism of interaction is completely different. Gamma rays interact with the atom (or specifically with the extra-nuclear electrons) the interaction probability increases with charge number (Z) of the atoms. On the other hand, neutron interactions almost entirely take place with the nuclei and thus depend on mass number (A) of the nuclide. These nuclear encounters result in the formation of charged particles which in turn produce the dosimetric signal as shown in Fig. 3.3. The dosimetric signal due to neutrons in tooth enamel is located exactly in the same place as the dosimetric signal due to gamma irradiation i.e. $g_{//}$ = 1.9973, signal width 0.4 mT and $g_{\perp}$= 2.002, signal width 0.3 mT. This means that like gamma rays, the neutron interactions in enamel lead to the formation of the same kind of radicals i.e. CO_2^- or CO_3^{3-}, which give rise to the same g value signal in an EPR spectrometer. Other authors have found that in alanine dosimeters neutron irradiation yields a similar response (Katsumura *et al.* 1986).

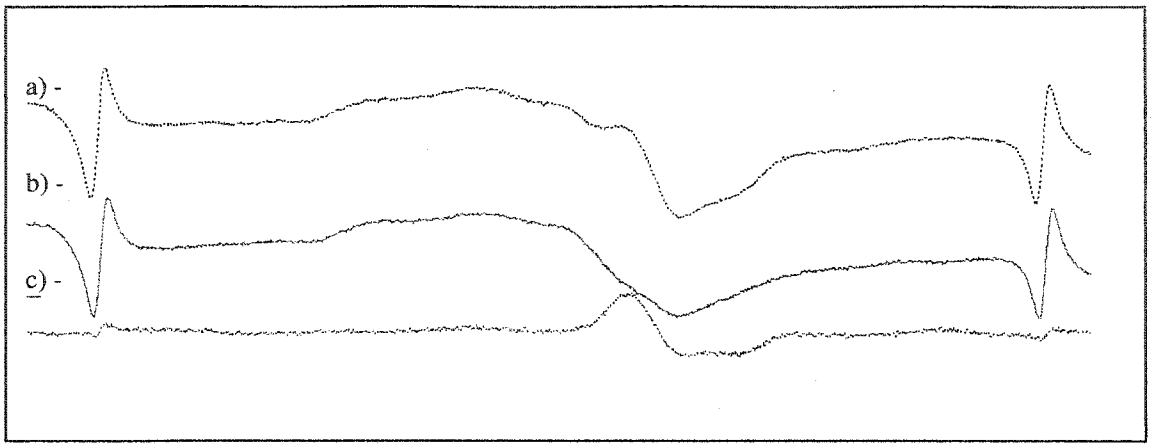

Fig. 3.2 Dosimetric signal measurement process for RK02-78, a) spectrum obtained as a result of neutron irradiation of distal half; b) spectrum obtained from undosed mesial half for a given mass, and c) spectrum results from mesial subtraction from distal. The spectrum is then smoothed and the peak-to-peak amplitude of the dosimetric signal is measured.

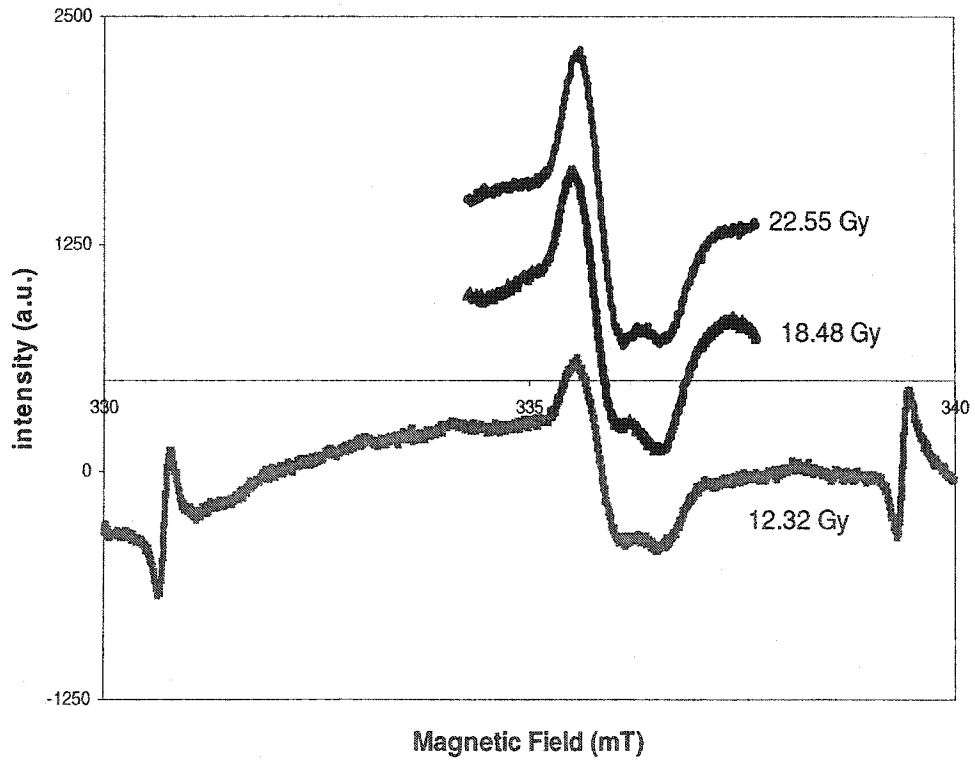

Fig. 3.3 Neutron dose response for the RK02-27 sample (grain < 4mm); first derivative of microwave absorption is plotted against the applied magnetic field.

The production of dosimetric signal due to both neutron and gammas at the same g value reported, in our earlier work (Khan *et al.* 2002b), has implications for biophysical dosimetry using tooth enamel for mixed radiation exposures. Unless the dose from the either components is known independently, the dose estimate based on the amplitude of total signal intensity will underestimate the true physical dose. This necessitates either the separation of neutron and gamma radiation doses using the spectral properties of the signal; or some secondary accident dosimeter which is sensitive for one radiation quality but not for the other. Further investigations on possible methods to separate out neutrons from gammas will be discussed in later part of this section.

Experiment 1 was designed to measure the dose response of the tooth enamel as a function of added neutron doses. Fig. 3.4 shows that for the sample RK02-27 the neutron response increases linearly with the dose. It implies that the radiation damage builds up continuously with the neutron dose at dose rate of 1 rem/h at 2m from the target, for mean neutron energy (280 keV). The neutron sensitivity of the above mentioned sample remains constant up to 35 Gy, except for the first dose point. This means that multiple neutron irradiations of the same sample do not alter the neutron sensitivity of the tooth enamel.

Experiment 2 was performed to see the effect of dosimetric signal induction in different grain sizes, and the whole tooth samples. The increased sensitivity was also observed for the whole tooth samples; which have a mean neutron sensitivity of 34.70 ± 4.80 /Gy-100mg (Table 3.5); compared to 4mm grain sample RK02-27 it is 23.23 ± 3.74 /Gy-100mg (calculated after taking mean of multiple neutron irradiations of the same sample). It appears that the neutron sensitivity may decrease for smaller grains. The results with various grain distributions remain inconclusive due to high signal anisotropy; however, in general, increased neutron sensitivity in larger grains is observed. The uncertainties in small grain size arise primarily from various sources, smaller sample mass, crushing procedure, dentine grains left in the enamel, low exposure (especially for N2 sample), and spectrum subtraction procedures. Further experimentations are required to explore the grain size effect for grains < 0.5 mm on the neutron sensitivity of tooth enamel. Sholom *et al.* (1998) have demonstrated a direct dependence of gamma radiosensitivity on grain size. They ascribed the lower sensitivity due to the grain surface area effects and showed that these effects could

systematically offset a correct dose by 10% for 0 – 0.075 mm. Table 3.5 also shows that there seems to be no major neutron sensitivity difference between incisors and molars for neutrons, which is also true for gamma rays.

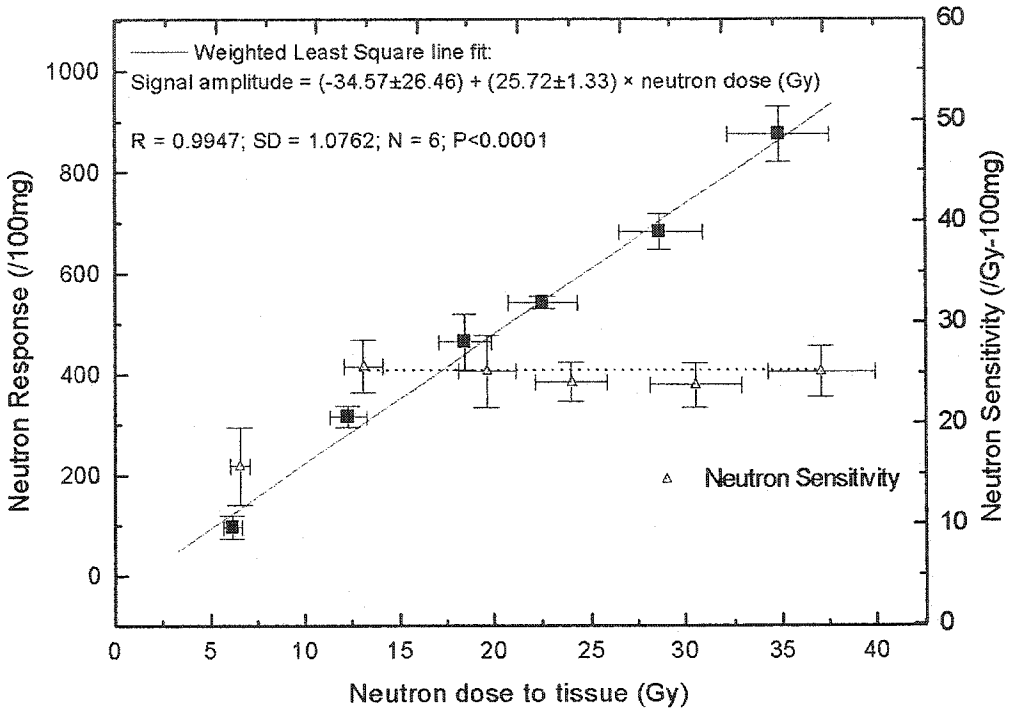

Fig. 3.4 Variation in neutron response (▪) and neutron sensitivity (Δ) with the dose to tissue; except for the first point the dose response of tooth enamel is linear. The data are obtained by multiple irradiations of the RK02-27 sample.

To avoid the signal variation from one sample to another, experiment 3 was done with the same sample. It was observed from Table 3.6 that there is a drop in response for grains in the range 0.106 – 0.3 mm compared with 0.3 - 0.5 mm (mean of neutron response and neutron sensitivity approximately c.a. 42 % lower in smaller grains). Moreover, consistent with previous experiment the response of < 0.106 mm grains is still low and includes higher uncertainty arising from dosimetric signal anisotropy, sample crushing, and spectrum subtraction.

Table 3.5 Neutron sensitivities for different grain sizes and distal halves of the whole teeth.

Sample no.	Grain size (mm)	Neutron dose (Gy)	Neutron response (/100mg)	Neutron sensitivity (/Gy-100mg)
N2	0.106 - 0.3	2.04 ± 0.16	70.29 ± 23.61	34.45 ±11.87
N3	0.106 - 0.3	6.16 ± 0.48	11.75± 23.38	1.91 ± 3.80
N4	0.3 - 0.5	6.16 ± 0.48	67.53± 14.63	10.96 ± 2.52
N5	0.3 - 0.5	4.10 ± 0.32	39.25 ± 50.97	9.57 ± 12.45
RK02-27	< 4 mm	6.16 ± 0.48	96.93 ± 22.56	15.74 ± 3.86
RK02-49	Incisor, whole	6.16 ± 0.48	238.52 ± 62.99	38.72 ±10.65
RK02-50	incisor, whole	6.16 ± 0.48	249.01 ± 77.28	40.42 ± 12.93
RK02-53	incisor, whole	6.16 ± 0.48	177.59 ± 37.60	28.73 ± 6.47
RK02-54	molar, whole	12.32 ± 0.95	396.74 ± 12.26	32.20 ± 2.68
RK02-55	molar, whole	16.39 ± 1.27	548.23 ± 12.26	33.44 ± 2.69

Table 3.6 Mean values of neutron sensitivity and neutron response for different grain sizes from the same tooth sample are presented in columns 3 and 4.

Grain size (mm)	Neutron dose (Gy)	Neutron response (/100mg)	Neutron sensitivity (/Gy-100mg)
< 0.106	9.09 ± 0.07	38.00 ± 41.01	4.18 ± 4.51
0.3 - 0.106	9.09 ± 0.07	110.32 ± 25.60	12.13 ± 2.82
0.3 - 0.5	9.09 ± 0.07	192.54 ± 31.81	21.18 ± 3.50

Table 3.7 shows the effect of crushing on the dosimetric intensity. From 0.5 mm to 0.106 mm grain size, there is no significant effect (0.3 - 0.5 mm overlaps with the 0.106 - 0.3 mm response within one standard deviation) of crushing on the dosimetric signal. Whereas, below 0.106 mm that there is an apparent sensitivity increase seen, which is most probably due to crushing induced radical production in this range.

In earlier experiments, except for the whole tooth samples, all other samples were chemically processed and then given a neutron dose. To determine whether a pre- and post-chemical treatment neutron irradiation has any impact on the neutron sensitivity of the enamel, neutron response was tested in

experiment 5. Table 3.8 shows that post chemical processing neutron irradiation does not seem to change the neutron sensitivity of the enamel (within ca. 10%).

Table 3.7 Effects of crushing operations on the dosimetric amplitude of the EPR signal for the RK02-86 sample.

Grain size (mm)	Neutron response (/100mg)
< 4	419.86± 20.99
< 0.106	627.59 ± 31.37
0.106 - 0.3	411.88 ± 20.57
0.3 - 0.5	400.86 ± 20.04

Table 3.8 Pre- and post-chemical processing irradiation effects on tooth enamel.

Neutron dose (Gy)	Cumulative neutron dose (Gy)	Neutron response (/100mg)	Neutron sensitivity (/Gy-100mg)
	Dose before chemical processing		
12.32 ± 0.89	12.32 ± 0.89	396.74 ± 12.26	32.20 ± 2.52
	Dose after chemical Processing		
6.16 ± 0.48	18.48 ± 1.33	542.76 ± 13.02	29.37 ± 2.23
6.16 ± 0.48	24.64 ± 1.77	697.97 ± 36.35	28.33 ± 2.52

Experiment 6 tested the effect of high temperature base treatment on the neutron induced dosimetric signal as a function of chemical treatment time. Fig. 3.5 shows that for two molar samples (RK02-54 & RK02-55) the neutron response remains approximately constant (within ca. 20%) during the course of chemical treatment. This remains true for an incisor sample where the native signal was eliminated after 25 h of chemical treatment.

Experiment 7 was designed to mimic a possible accident situation wherein the tooth would be residing inside mouth and the cheek would provide a dose build up, a layer of ~ 4mm of hydrogenous material (paraffin wax) was used. Table 3.9 shows that for both irradiations, there was no significant neutron sensitivity difference for either bare or waxed sample (i.e. RK02-27). Similar behavior was seen

for N45, this data also confirms a lower neutron sensitivity trend for the smaller grains compared with the larger ones. Although a significant increase in neutron sensitivity was expected for the wax covered sample due to higher hydrogenous contents. This was because some authors have reported an increase in neutron sensitivity in α-alanine with increase in paraffin contents (Katsumura *et al.* 1986).

The neutron sensitivity was determined in terms of gamma radiosensitivity by using Fig. 3.6 (experiment 8). It has been observed that the equivalent neutron sensitivity, for mean neutron energy of 280 keV, on average, is approximately 10 % of the gamma radiosensitivity, which is higher compared with the expected 3 % response evaluated for grains < 0.3 mm (Bochvar *et al.* 1997). Since neutron radiosensitivity of human tooth enamel is much less than gamma radiosensitivity, it could be predicted that the neutron dose range of linearity should exceed the gamma radiation dose range (which saturates at higher gamma radiation dose ~ 3 kGy (Rink 1997))

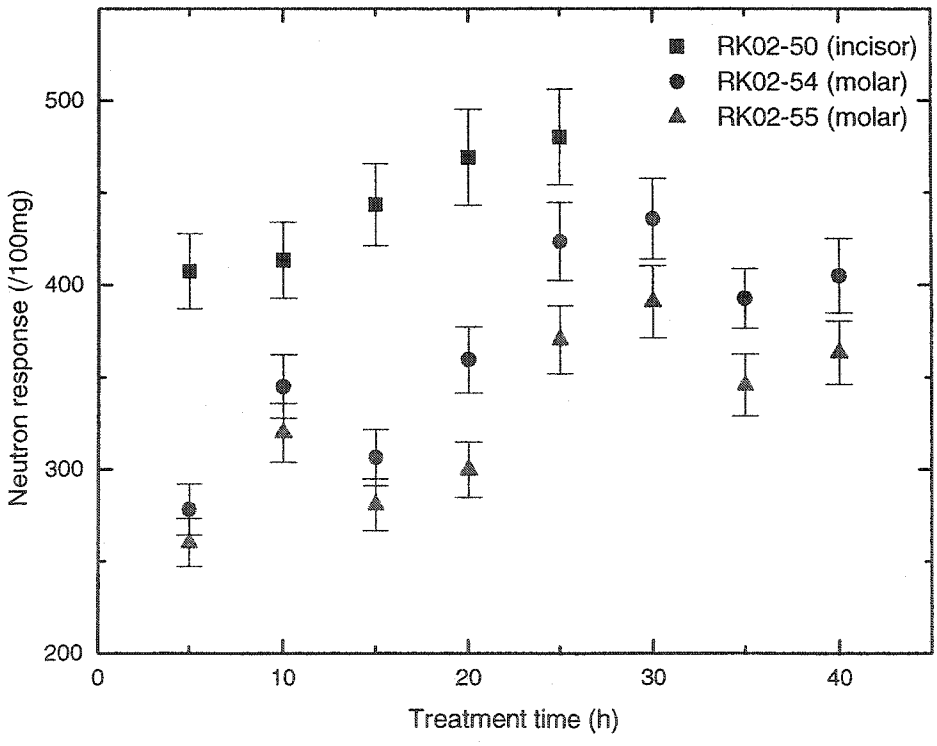

Fig. 3.5 Variation in the neutron response (/100mg) of human tooth as a function of chemical treatment. Relative error bars of ~5 % are added to the data points.

Table 3.9 Effect of 4 mm wax layer on tooth enamel, bare and waxed samples are compared. Neutron sensitivity for smaller grained waxed samples is also studied.

Sample	Cumulative dose (Gy)	Signal intensity (a.u.)	Neutron sensitivity (#/Gy-100mg)
RK02-27-bare	6.16 ± 0.48	435.73 ± 108.69	22.70 ± 5.93
	12.32 ± 0.95	1035.86 ± 170.88	26.99 ± 4.92
RK02-27-waxed	6.16 ± 0.48	355.21 ± 57.90	18.51 ± 3.34
	12.32 ± 0.95	1020.11 ± 111.65	26.58 ± 3.56
N45-bare	6.16 ± 0.48	197.14 ± 241.37	10.27 ± 12.55
N45-waxed	6.16 ± 0.48	117.76 ± 136.73	6.14 ± 7.14
	12.32 ± 0.95	295.61 ± 147.70	7.70 ± 3.89

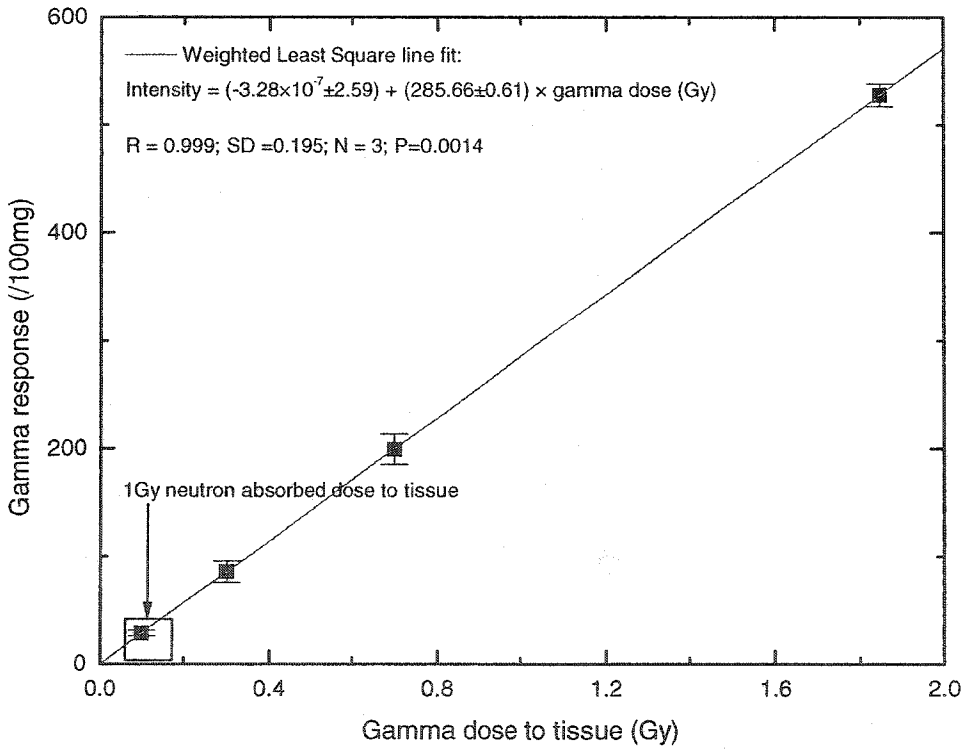

Fig. 3.6 Adjusted gamma radiation dose calibration curve passing through the origin; the amplitude of the neutron curve will give the corresponding gamma radiation dose to the tissue. The neutron radiosensitivity of the enamel lies in the gamma radiation dose range shown by a small box on the plot.

Low radiosensitivity for neutrons or any other high LET radiation compared with gamma radiation has been well known in organic materials such as alanine. This tendency has been reported for radical formation in bio-organic compounds and for G values of Fricke dosimeters and Courmasine dosimeters.

Lower sensitivity for neutrons could be due to smaller hydrogenous contents of enamel which are usually responsible for energy transferring mechanisms for neutrons via elastic recoils.

It was earlier thought that the neutron irradiation of the tooth will enhance or decrease the gamma radiosensitivity of the tooth, because the irradiation with high LET radiation like neutrons will produce new localized sites for free radicals to reside. To test this hypothesis, experiment 9 was performed. Data in second and third column of Table 3.10 show that the gamma radiation signal amplitude in both halves is more or less the same. This reveals no apparent enhancement or reduction of gamma radiosensitivity after neutron irradiation.

The dosimetric signal intensity induced due to neutron irradiation was followed and remeasured at different days; the intensity was reproducible within one standard deviation (Fig. 3.7). The constancy of neutron induced signal has implications for the EPR accident dosimetry using tooth enamel. Therefore, tooth enamel still remains a useful biophysical dosimeter involving neutron exposures.

Table 3.10 Effect of post neutron irradiation gamma radiosensitivity on tooth enamel, the same mass has been used for mesial and distal halves.

Sample	Pre-neutron dosed mesial intensity	Undosed distal intensity
RK02-53	1989.5 ± 64.15	1884.43± 154.62
RK02-54	1003.36 ± 130.47.	966.06 ± 20.65
RK02-55	1015.84 ± 216.76	1281.97 ± 73.95

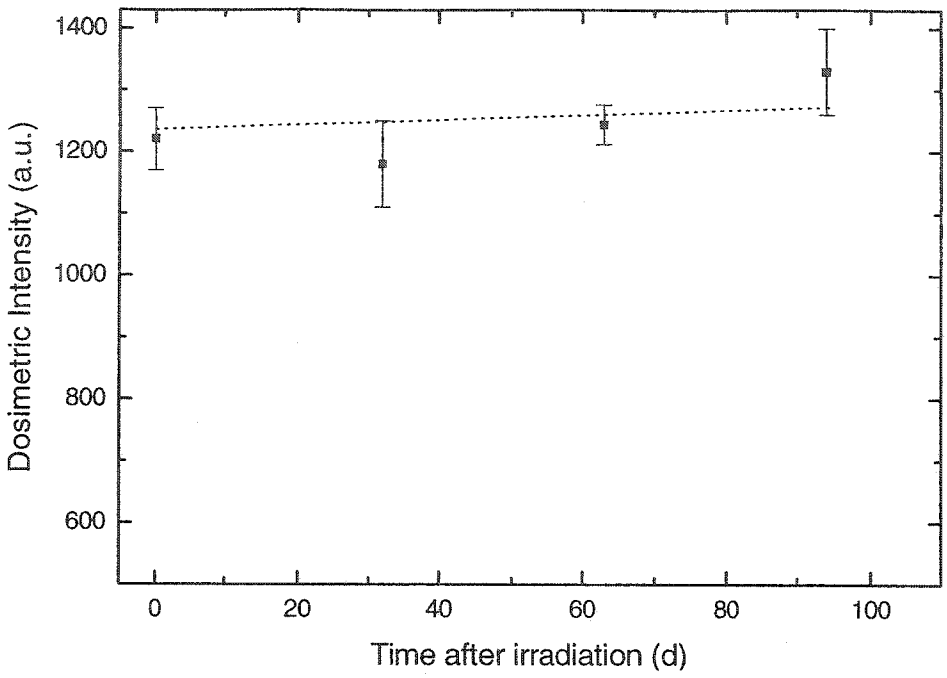

Fig 3.7 Stability of dosimetric signal as a function of time after irradiation (days).

Experiment 10 was designed to see the effect of both low and high dose rates available from the McMaster K.N. accelerator. Results from Fig. 3.8 show a constant neutron response as a function of dose rate. Tooth halves were irradiated in pairs for each dose rate and the same study was repeated to average out the uncertainties due to sample positioning and inter-tooth sensitivity variations. It was expected that for high dose rate the sensitivity of neutron will decrease, due to large radical formation and their subsequent recombination before EPR measurement. However, it was not observed in these experiments, this could be due to the fact that the spread in dose rates practically available from McMaster accelerator were not very high.

Fig. 3.9 shows the effect on neutron sensitivity as a result of the change in mean neutron energy for samples (listed in Table 3.4). This was accomplished by changing the proton current on the target.

No effect of neutron energy was observed in the energy range available at McMaster K.N. accelerator facility. It is still expected that the neutron sensitivity would be different at lower energy near the thermal. However, in practice it would be hard to obtain a neutron spectrum near thermal energies devoid of accompanying gammas.

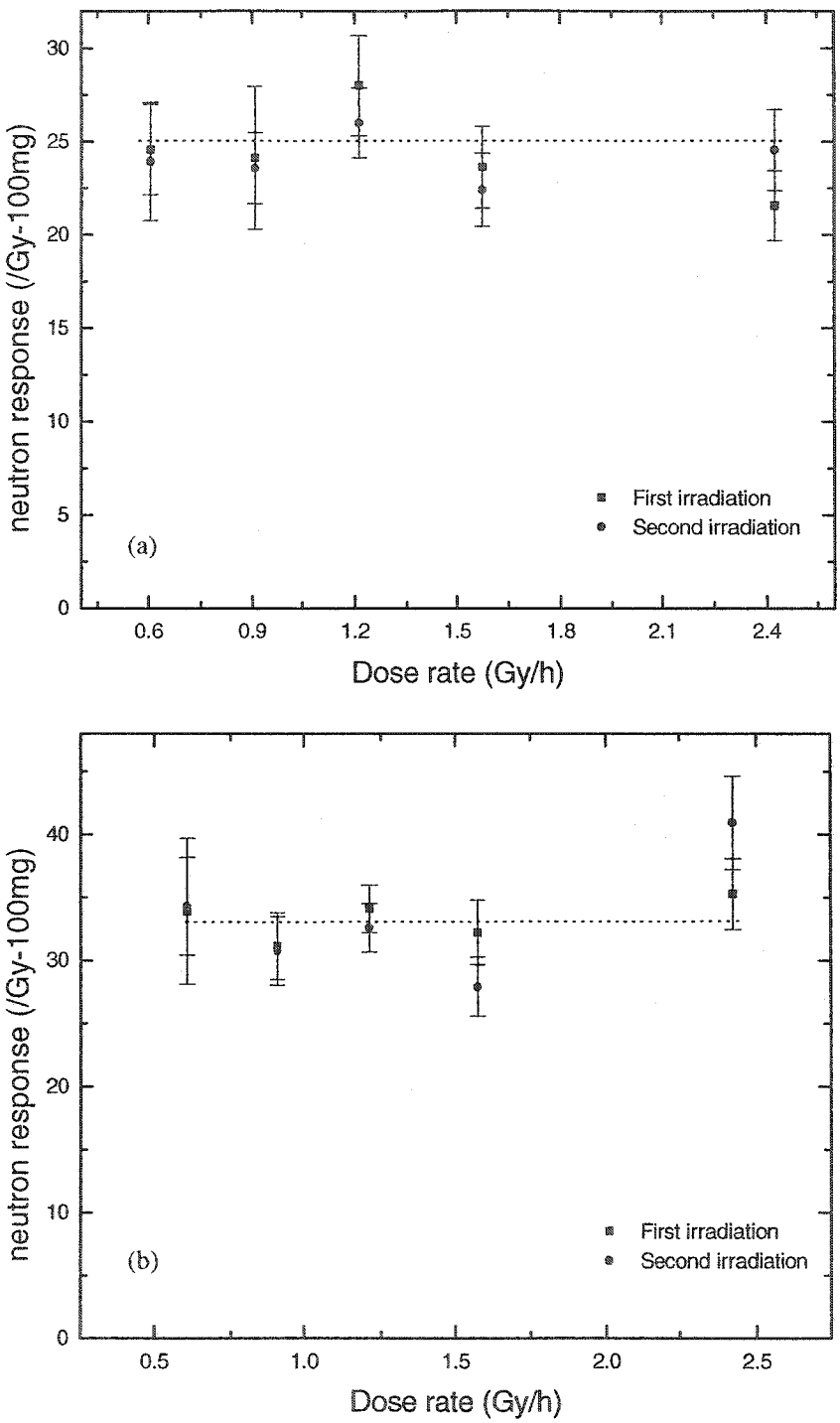

Fig. 3.8 Variation in neutron response as a function of neutron dose rate for samples a) RK02-73, RK02-67, RK02-55, RK02-69 and RK02-71 b) RK02-74, RK02-66, RK02-53, RK02-68 and RK02-70.

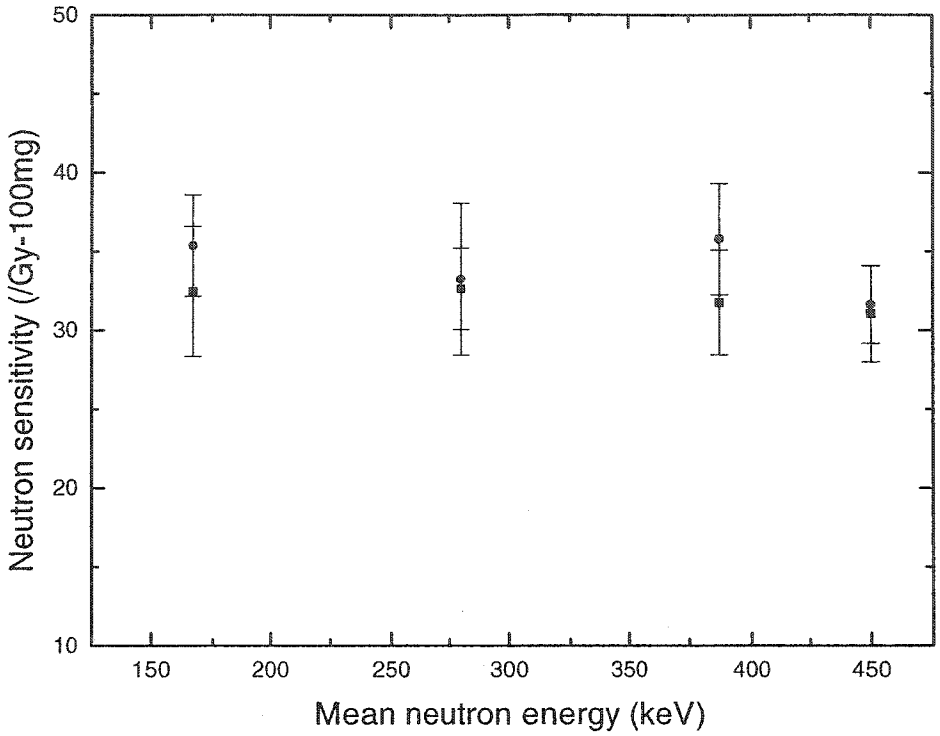

Fig. 3.9 Variation in neutron response as function of mean neutron energy for two teeth samples positioned at the same place. Samples for each mean neutron energy are listed in Table 3.4.

Theoretically, the neutron interactions in tooth can be related with the sensitivity of tooth enamel at a given energy. The total interaction probability of an incident radiation for a given energy is given by the total macroscopic cross section of the material. The total macroscopic cross-section, $\Sigma_t^n(E)$, of human tooth enamel for neutron at energy E is

$$\Sigma_t^n(E) = \sum_i N_i \, \sigma_{ti}^n(E) \tag{3.2}$$

Where N_i is atom density of the *i*th constituent element of the material (i.e. number of atoms per unit volume in units of atoms/barn-cm), and $\sigma_{ti}^n(E)$ is the total microscopic cross section of the *i*th element of enamel at energy E, in units of barn.

Tooth enamel contains 97~98 % carbonated hydroxyapatite, 2% water and <1% organic contents (mostly protein). The composition of mineral mainly hydroxyapatite with carbonates substituted both in place of hydroxyl (A-site) and phosphate groups (B-site) is given by $Ca_{10}\ [(PO_4)_{6-x}\ (CO_3)_x]\ [(OH)_{2-y}$

$(CO_3)_y$]; where x = 0.039 and y = 0.01 (Romanyukha *et al.* 2000a). In addition to this, there are also considerable amounts of various impurities like Na, and Mg present in tooth enamel (Driessens & Verbeeck 1990).

By using the continuous energy point-wise microscopic total cross section for the elements mentioned in Table 3.11 for neutrons, from Evaluated Nuclear Data Files (ENDF/ B-VI), the total macroscopic cross-section of tooth enamel for neutrons was generated as shown in Fig 3.10 (IAEA 2002). The total macroscopic cross section of enamel is essentially constant from thermal neutron energy to intermediate range up to several hundred kilo electron volts. In higher energy range up to 3 MeV there are few resonances which can result in higher interaction probability.

Table 3.11 Chemical composition of tooth enamel (% of moist weight) was used to find the atom density using $\text{Number density} = \frac{\rho N_A}{M}$; where N_A, is Avogadro's number, ρ is the density 2.92 g/cm^3, and M is the molecular weight of the compound.

Elements	**Number density (atoms/barn-cm)**
Ca	1.75×10^{-2}
O	4.55×10^{-3}
C	7.01×10^{-5}
P	1.05×10^{-2}
H	3.50×10^{-3}
Na	1.19×10^{-5}
Mg	6.20×10^{-6}

The total microscopic cross section for *i*th element consist of both elastic $\sigma^n_{elastic,i}(E)$ and non-elastic $\sigma^n_{non-elastic,i}(E)$ type of reactions, therefore for the tooth molecule the total macroscopic cross section would be sum of both macroscopic elastic cross section, $\Sigma^n_{elastic}(E) = \sum_i N_i \sigma^n_{elastic,i}(E)$, and macroscopic non-elastic cross section, $\Sigma^n_{non-elastic}(E) = \sum_i N_i \sigma^n_{non-elastic,i}(E)$.

$$\Sigma_t^n(E) = \Sigma_{elastic}^n(E) + \Sigma_{non-elastic}^n(E) \tag{3.3}$$

The elastic interaction leaves the target nucleus in the same state and the incident neutron leaves behind a recoiling nucleus. The recoiling nucleus in a crystal can form defects, out of which CO_2^- type defects give rise to the neutron induced signal in EPR spectrum. The non-elastic reactions change the state of nucleus and the result is either the production of charged particle or gamma radiation due to rearrangement of nuclear states. The contribution of elastic reactions is determined by the macroscopic elastic cross section of the enamel $\Sigma_{elastic}^n(E) = \sum_i N_i \sigma_{elastic,i}^n(E)$. The relative share of non-elastic reactions is also shown in Fig. 3.11 inset.

In Fig. 3.11 it is observed that in the tooth enamel molecule, more than 95% of total interactions are due to elastic scattering from thermal to a few MeV of incident neutron energy. The contribution of non-elastic reactions arises only after 2 MeV.

Interpretation of the cross section data at a given energy shows that non-elastic interactions of neutron are very few compared with the elastic scattering. Most of the time, the energy transfer takes place due to elastic recoil of the lattice atoms, which in turn deposit energy in the tooth and produce high density tracks in tooth. From Fig. 3.10 it is seen that for the range of neutron energy from 150 to 450 keV, there is a constant cross section except at ~ 425 keV where the total tooth cross section rises to four times of its value for other energies. This is solely due to elastic cross section as seen in Fig. 3.11. Therefore, the neutron sensitivity of enamel should remain constant up to several MeV.

It may of interest to see how much the energy is transferred by both neutrons and gamma rays, which requires the calculation of kerma. Kerma, *k*, defined by ICRU, as the quotient of sum of the initial kinetic energy of all the charged particles, dE_{tr} released by the uncharged particle in a mass dm of the material (ICRU 1999).

$$k = \frac{dE_{tr}}{dm} \tag{3.4}$$

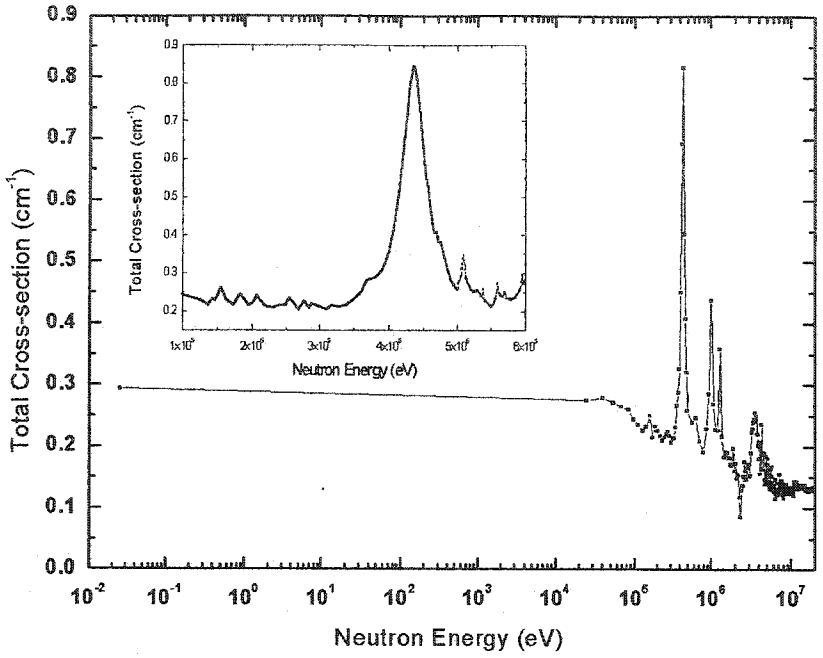

Fig. 3.10 Total macroscopic cross-section of tooth enamel for neutrons; the probability of interaction per molecule is approximately constant from thermal to intermediate neutron energies. In the inset an exaggerated view of the cross section from 100 to 600 keV is shown.

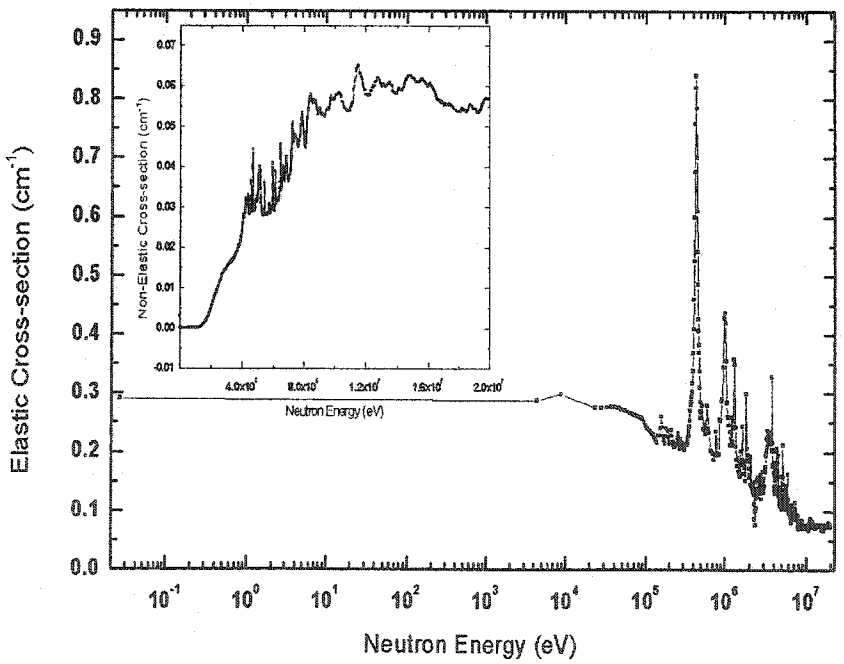

Fig. 3.11 The elastic cross-section of tooth enamel versus the neutron energy is shown; the total neutron cross-section mainly consists of the elastic cross-section; only a small contribution comes from the non-elastic nuclear reactions between 2 and 20 MeV neutron energy.

For a fluence ϕ of charged particles of energy E, the kerma is given by

$$k = \phi E \frac{\mu_{tr}}{\rho} \tag{3.4}$$

μ_{tr}/ρ is the mass energy transfer coefficient of the material for these particles. Kerma per unit fluence k/ϕ is termed as *kerma coefficient* for uncharged particle of energy E in a specified material. Kerma coefficients were evaluated for different neutron energies for tooth enamel by using data from Table 3.11, with μ_{tr}/ρ evaluated for the elastic recoil of the corresponding constituents of tooth enamel.

Table 3.12 shows that for neutrons there is not much a difference in the kerma coefficient in tooth over the neutron energy range under investigation. Kinetic energy released by neutrons in the tooth enamel is ~2.5 % of the kinetic energy released in tissue and ~ 3.5 % of the kinetic energy released in the bone. This shows that tooth enamel is inefficient in terms of energy release from neutrons compared to tissue.

Table 3.12 A comparison of kerma coefficient for tooth tissue and bone for various neutron energies. Kerma coefficients for tooth are evaluated by using tooth composition and the data for μ_{tr}/ρ for elastic recoils which comprise the majority of interactions in tooth enamel. Kerma coefficients for tissue and bone were evaluated using ICRU tissue and bone data (ICRU 1977; ICRU 1989; Caswell *et al.* 1980).

Neutron Energy (keV)	Kerma coefficient (cGy-cm^2)			Ratios		
	Tooth enamel	Tissue	Bone	Enamel: tissue	Bone: Tissue	Enamel : bone
167	1.99×10^{-11}	8.84×10^{-10}	5.79×10^{-10}	0.023	0.65	0.035
280	2.81×10^{-11}	1.19×10^{-9}	7.79×10^{-10}	0.023	0.65	0.035
387	3.63×10^{-11}	1.44×10^{-9}	9.56×10^{-10}	0.025	0.66	0.038
450	4.82×10^{-11}	1.62×10^{-9}	1.06×10^{-9}	0.029	0.65	0.045

Table 3.13 shows kerma coefficient for the irradiation of enamel, tissue and bone from ^{137}Cs gammas. The energy released by the gamma ray photons in tooth, tissue, and bone is approximately constant within 10%. This implies that the dose conversion from the enamel to equivalent dose to tissue should not be complicated. Table 3.14 shows the ratio of the neutron to gamma ray kerma coefficients for

different neutron energies. The ratio was obtained by dividing the neutron kerma coefficient data from column 2 of Table 3.12 with the gamma ray kerma coefficient 3.10×10^{-10} cGy-cm^2 for tooth enamel. A variation of 6 - 15% of equivalent gamma radiation response is observed with various energy neutrons.

Table 3.13 A comparison of kerma coefficients for tooth, tissue, and bone for ^{137}Cs gamma rays. Kerma coefficients for tissue and bone were evaluated using ICRU tissue and bone data (ICRU 1989; Attix 1986).

Gamma ray energy (keV)	Kerma coefficients (cGy-cm^2)		
	Tooth enamel	Tissue	Bone
661.6	3.10×10^{-10}	3.20×10^{-10}	3.42×10^{-10}

Table 3.14 Neutron to gamma rays kerma coefficient ratios for human tooth enamel, for various neutron energies.

Neutron energy (keV)	Enamel kerma coefficient ratio (Neutron : Gamma)
167	0.065
280	0.09
387	0.12
450	0.15

The neutron irradiation of enamel produces the same radicals as gamma, but with much less efficiency. These radicals result in the same EPR spectrum so that the two types of radiation are difficult to separate. However, tooth could still be useful as accidental dosimeter because it gives the cumulative exposure due to both neutron and gamma. The problem only arises in a mixed field for the measurement of relative contribution of one of them so that the other can be determined. In a study, polymethylene meta acrylate (PMMA) was irradiated with γ-rays and 2 MeV protons (Katsumura *et al.* 1980). The microwave power saturations for γ and proton irradiations resulted at two different saturation powers. It was concluded that the local concentration of the radicals produced by proton irradiation is at least 5.9 times higher than produced by γ -irradiation. Since neutrons are intermediate LET radiation a similar localized concentration

of radicals was expected, which could result in different power saturation characteristics. Neutron irradiated spectrum was measured at different powers for two different modulation frequencies (50 and 100 kHz) from the distal half of tooth enamel. Whereas the mesial half of the tooth was given γ dose with ^{137}Cs and power saturation was studied. In Fig. 3.12 no significant difference was seen in the power saturation characteristics for the mineralized contents of tooth at different frequencies. The failure of enamel to show different power saturation could be due to the difference in mechanism of defect formation in minerals and polymers.

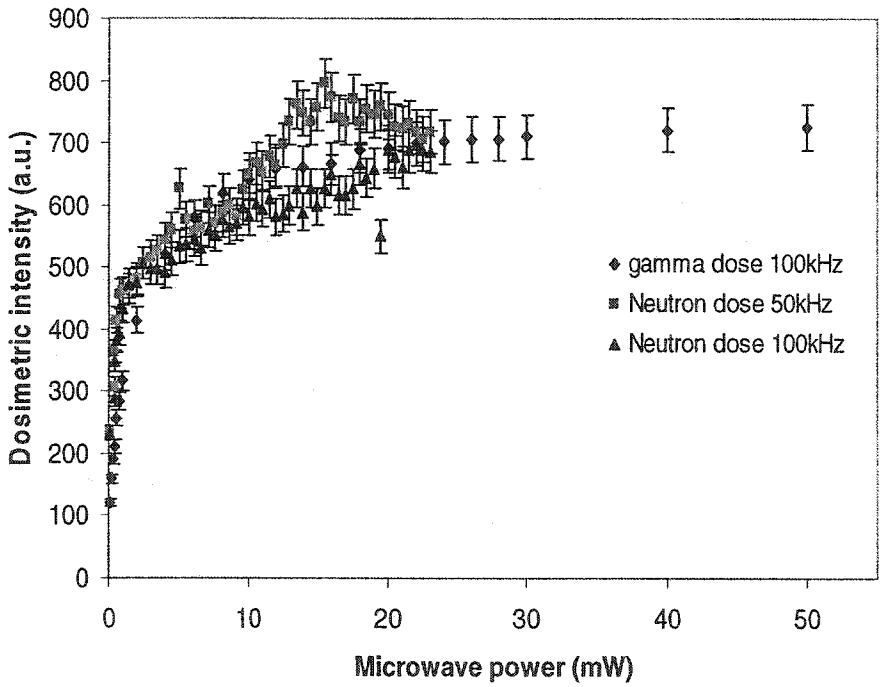

Fig. 3.12 Microwave power saturation for neutron irradiated (at two different modulation amplitudes 50 and 100 kHz) and gamma irradiated tooth enamel. No significant difference in power saturation of these signals was observed.

In an attempt to separate out the neutron induced contribution in a mix field, neutron activation analysis of tooth was done in the thermal and epithermal flux of the McMaster Nuclear Reactor (MNR). By sending samples, in a transport rabbit under pneumatic control, irradiation was done in reactor core for 60s and 180s for thermal and epithermal fluxes respectively. Tooth samples were measured at a fixed distance of 12 cm from high purity germanium HPGe detection system.

Table 3.15 Neutron irradiation of whole tooth sample in McMaster Nuclear Reactor (MNR).

Irradiation site	Markers	Counts, after irradiation (240 s)	Counts 24 h after irradiation (240 s)	Counts 6 days after irradiation (240 s)
Thermal	^{24}Na – 1.369 MeV	19522 ±223	9503 ± 98	44 ±7
(296 mg)	- 2.755 MeV	11903 ±231	5663 ± 75	32±6
	^{49}Ca - 3.049 MeV	1156 ±105	-	-
Epithermal	^{24}Na – 1.369 MeV	1165±55	5435± 74	
(251 mg)	- 2.755 MeV	676±41	4727± 69	
	^{49}Ca -3.049 MeV	74±14	-	

In the gamma radiation pulse height spectrum, ^{24}Na and ^{49}Ca show significant peaks above background. The major peaks were identified from the spectrum and net counts under the full peak are tabulated as in Table 3.15 at different time after irradiation. However, ^{49}Ca has very short half life (8.72 min), therefore it vanishes on the second day spectrum, so it can not qualify as a useful neutron marker.

^{24}Na could be a possible neutron marker for the computation of neutron component of dose with half life of 14.96 h, if the gamma spectrometry of samples is quickly performed after accident. However, due to small amount of sodium (which is only an impurity), the detection limit will be high. For example in this case with prior knowledge of ^{23}Na contents, the neutron flux of ~ 10^{13} /cm^2-s could be constructed. Only a radioactive triage, involving thousands of grays of neutrons dose, would result in a weak activation of sodium and it would be very short-lived. Also in such an accidental scenario, it would be hard to remove only a tooth from the victim, and this could only be of interest in post-mortem dosimetry. However, the possible production of ^{41}Ca, because of neutron capture of ^{40}Ca (σ_{abs} (0.0253 eV) = 0.41 barn) with half life (1.02×10^6 y) could be of use in separating thermal neutron induced component in a mixed radiation accident situation. For this purpose mass spectroscopy of calcium isotope could prove instrumental (Wieser, 2002). Other isotope separation techniques such as molecular laser isotope separation could also be useful.

3.4 CONCLUSIONS

The neutron response of human tooth enamel was studied and a number of experiments with an accelerator based neutron source were performed. The neutron beam was produced with the low gamma radiation yield, $^{7}Li(p, n)^{7}Be$ type thick target, using the 3 MV McMaster K.N. Van de Graaff accelerator. The dosimetry was done using a pre-calibrated snoopy type neutron dosimeter. Neutron irradiation induces a dosimetric signal in the tooth enamel at the same defect site as gamma ray produced damage with the same g-values ($g_{//}$ = 1.9973, width 0.4 mT $g_{\perp}$= 2.002, width 0.3 mT). The dosimetric signal grows linearly with neutron dose from 6 – 35 Gy tissue dose. Dosimetric response in two different grain sizes (0.3 – 0.5mm, and grains < 4mm) has shown increased dosimetric amplitude in the larger grains. Dose build-up effect on tooth inside the mouth due to cheek was simulated by placing a 4 mm thick paraffin wax layer between the beam and tooth, but had little effect. These results show that for mean neutron energy range from 150 - 450 keV, the relative neutron response of the human tooth enamel ranges from 8 – 12 % of the equivalent gamma ray response. Therefore, in tooth enamel one gray of neutrons produces approximately the same height of EPR dosimetric signal as 100 mGy of gamma radiation dose, demonstrating that a correction factor of 10 may possibly be suitable for neutron tooth enamel EPR biophysical dosimetry (Khan *et al.* 2003a).

Chapter 4

EPR Dosimetry using Mice Teeth

4.1 INTRODUCTION

The use of tooth enamel for radiation dosimetry has been a well established technique in different situations, like measuring environmental overexposures and retrospective accident dosimetry and in dating geological and archaeological deposits. For retrospective Electron Paramagnetic Resonance (EPR) biodosimetry using human tooth enamel, the availability of human tooth from the accident victim is a precondition. This becomes quite difficult and raises ethical issues in some instances where human involvement is not certain. For example, in high radiation background regions, or reclaimed uranium mines. In the absence of human teeth, the current practice in retrospective dosimetry for radiation accidents is to use environmental materials involved in the accident. The main requirement for such dosimeters is their ability to retain a record of the accidental exposure with negligible fading over the time interval between exposure and measurement. The dosimeters which often meet this requirement are quartz inclusions (Bailiff *et al.* 2000) found in fired ceramics such as bricks, tiles and porcelain plumbing fixtures or any other objects which can work as a transfer dosimeter. Based on the physical properties and chemical contents of these materials, EPR or thermoluminescence or optical luminescence dosimetry may be performed (Hashimoto *et al.* 2001; Haskell 1993). Several accident dose reconstructions have been published in the literature. The first dosimetric study was reported by Ikeya (1986) for the atomic bomb victims using granite rocks. Radiation exposure estimation was also done using the bones of a deceased radiation worker (Ikeya *et al.* 1996). In a radiation accident in Thailand, the general population exposure was estimated by using sugar samples collected nearby the accident site (Shiraishi *et al.* 2001). EPR dose reconstruction following the accident at the gamma irradiation facility at the Institute of Energy and Technology (Kjeller, Norway) was done using the long-lived free radicals produced in nitro-glycerol and sugar in a pharmaceutical found from one of the victims (Sagstuen *et al.* 1983). However, the main

difficulty in using the environmental materials for EPR dosimetry is in the estimation of corresponding dose to the human victims. In this chapter, an alternative method is proposed whereby the teeth extracted from animals could prove useful for the estimation of radiation exposure to humans (Khan *et al.* 2002a). Mice and rodents are a good candidate for this purpose because they offer the other extreme of tooth sizing i.e. small molars, and could often be found in the vicinity of accidental exposures. Moreover, from a biological research point of view, the knowledge of radiation response in mice could be extrapolated to human.

An estimation of radiation exposure due to nuclear vessels in Pacific Ocean was done by using walrus teeth. This was the pioneering work in determining environmental overexposure and its consequences on marine life (Hayes *et al.* 1998b). On the same lines, if the mice or rodent are collected from suspected high exposure sites or nearby radiation accidents, their teeth could be utilized to measure the exposure. The physical radiation dose to tooth can thus provide a measure of the cumulative environmental exposure or the accident dose. The only problem, using the teeth from mice or rodents, might be the turnover time of the teeth in the animals. Moreover, the rodents could be collected during only a short period because of their short life span and motility.

Another situation is that of biological risk estimation research using experimental animals where the physical dose estimate is difficult to assess. Mostly the mice and rodents, used for the radiation biology or cancer research, involve whole body laboratory doses of the order of grays (for example (Flanders *et al.* 2002; Schaffer *et al.* 2002)). These are usually delivered to a group of live animals in some type of container. Conventional dosimeters like radiochromic films and thermoluminescence dosimeter, even if attached to their bodies, could either overestimate or underestimate the dose. Tooth enamel from these experimental animals could provide a source for accurate dose measurement for these exposures. This physical dose can then be related to the biological markers, like cell killing, apoptosis, or chromosome aberrations, to measure the biological consequences of the physical radiation dose.

Mice are also very important rodents in micromammal assemblages relevant to geological deposits. Their rapid evolution renders observable changes in their dental and postcranial morphology. This

taxonomic variability through geological time renders some species excellent time markers in Quaternary deposits e.g. (Oms *et al.* 2000).

4.2 MATERIALS AND METHODS

A group of Swiss Webster mice with body weight ~ 300 g was used for this experiment. Four mice were irradiated with a ^{137}Cs gamma source with approximately 1.20 ± 0.06 Gy. They were sacrificed, skulls were separated from the rest of the body and sent to animal curation facility of Royal Ontario Museum, Toronto for soft tissue removal and cleaning by using Dermested beetles. Four incisors (weighing ~ 32 mg total) and twelve molars (weighing ~12 mg total) were extracted from the skulls of each animal (Fig. 4.1).

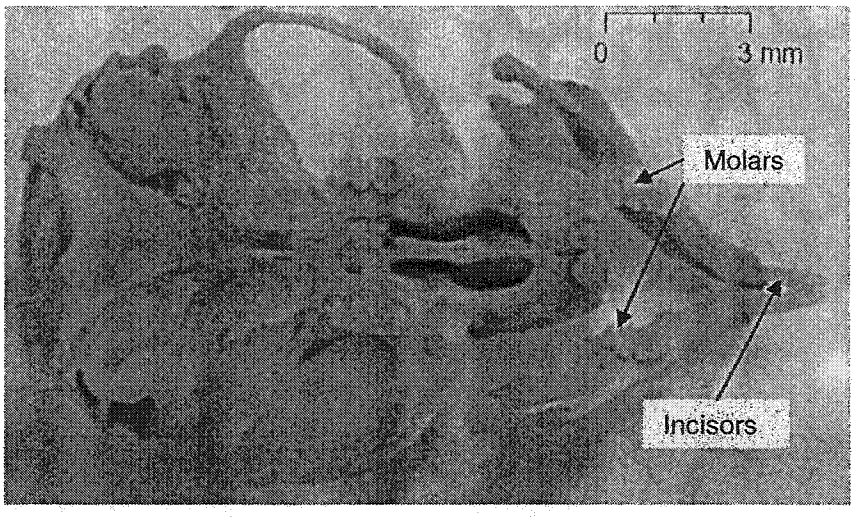

Fig. 4.1 Mouse skull cleaned, using dermested beetles, six molars and two incisors could be seen in each jaw.

The samples were put in 10 ml of supersaturated potassium hydroxide aqueous solution in polypropylene tubes and ultrasonically treated at 80 °C temperature for 5 h to remove organic contents. Then the sample was washed with de-ionized water in an ultrasonic bath for 12 h at 80° C, dried at 40 °C for 5 h and weighed.

As a result of chemical treatment, the incisor mass was significantly reduced and an interfered EPR spectrum was observed, therefore incisors were determined to be not suitable for this technique. The clean molars (4 mg per animal) resulted in an EPR spectrum devoid of any organic interference.

The EPR spectrum for the sample was collected in a JEOL JES-FA 100 EPR spectrometer operating in the X band under the conditions given in section **2.2.2.8**. The sample was rotated between measurements several times to take into account the uncertainty arising from anisotropy of the dosimetric signal due to different grain sizes. The mean intensity of the dosimetric signal was calculated.

The sample was given added laboratory doses of 2 and 5 Gy by using the ^{137}Cs source at the exposure rate of 4.27 R/min (10.97×10^{-4} C/kg-minute). The dosimetry was performed with the help of a calibrated Farmer dosimeter 2570 with a 0.6 cc chamber. The uncertainty of dose measurement was less than 5 % at the 95 % confidence interval. The irradiation was done in a specially designed acrylic rack having a 10 mm diameter, 2 mm deep cylindrical cavity for placing the samples (as mentioned in section **2.2.5**). The samples were loaded into polyethylene vials. A 3 mm thick acrylic sheet was placed between the source and sample to ensure charged particle equilibrium.

4.3 RESULTS AND DISCUSSION

The incisor and molar enamel contaminated with undissolved dentine failed to show any radiation effects in the EPR spectrum. This was due to large interfering signal characteristics of the organic contents of the tooth. As a result of chemical treatment the mass loss in the incisors was very high and very little mass was left to measure dose because in mice the enamel layer is present only on the buccal side of the incisors (Hilson 1986). Consequently, the smaller mass of incisors produced no dosimetric signal. Because the incisors have the most mass, it was expected that compared with tiny molars, they would prove to be good candidate for dose measurement. This proved to be untrue because of two possible reasons: i) the quantity of enamel (mineralized tissue) is too small to be detected, and ii) the organic components are higher and therefore as a result of laboratory irradiation there is a formation of organic radicals in the organic matrix; which interferes with the dosimetric signal. To overcome these possible variables, the sample could be prepared by combining several teeth with only mineralized contents utilized or

mineralized contents could be extracted from dentine by using soxhet apparatus, which has been extensively used in bone dosimetry (Schauer *et al.* 1993; Breen & Battista 1995).

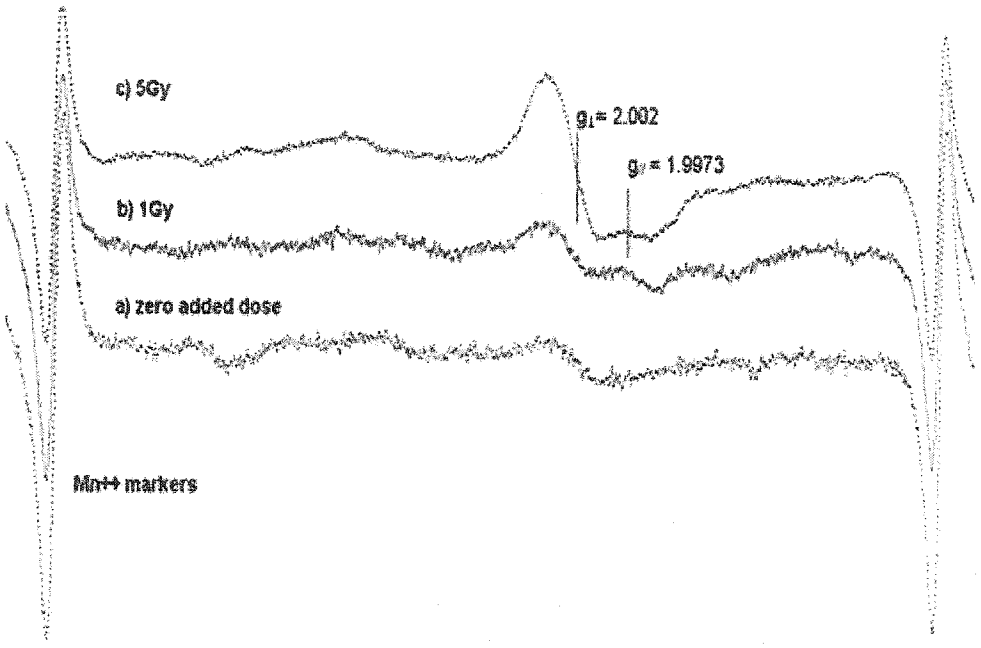

Fig. 4.2 EPR spectra (first derivative of microwave absorption vs the applied magnetic field, mT), collected for different laboratory added doses (zero, 1 and 5 Gy), in the clean molar sample of 16 mg from 4 mice (48 molars). The dosimetric signal in mice enamel is induced at the same position (i.e. at $g_{//}$ = 1.9973, $g_{\perp}$= 2.002) with the same parameters as in human enamel (shown in Table 1.2).

Therefore, the use of incisors was abandoned and only molars were selected from at least four animals and cleaned using protocol mentioned before. This yielded a dosimetric signal which was proportional to the radiation dose and similar characteristics as previously seen in human teeth (Fig. 4.2). Also the signal was located at the same g value as observed in human teeth, therefore it can be concluded that the same type of radical species (i.e. CO_2^-) is being formed as a result of radiation exposure in mice teeth. As in human tooth enamel, the dosimetric intensity increases with the added radiation dose. The dose response was linear and the backward extrapolation technique with multiple added laboratory doses resulted in a radiation dose of 1.4 Gy which is within experimental error of the previously administered laboratory dose (i.e. roughly ~1.2 Gy).

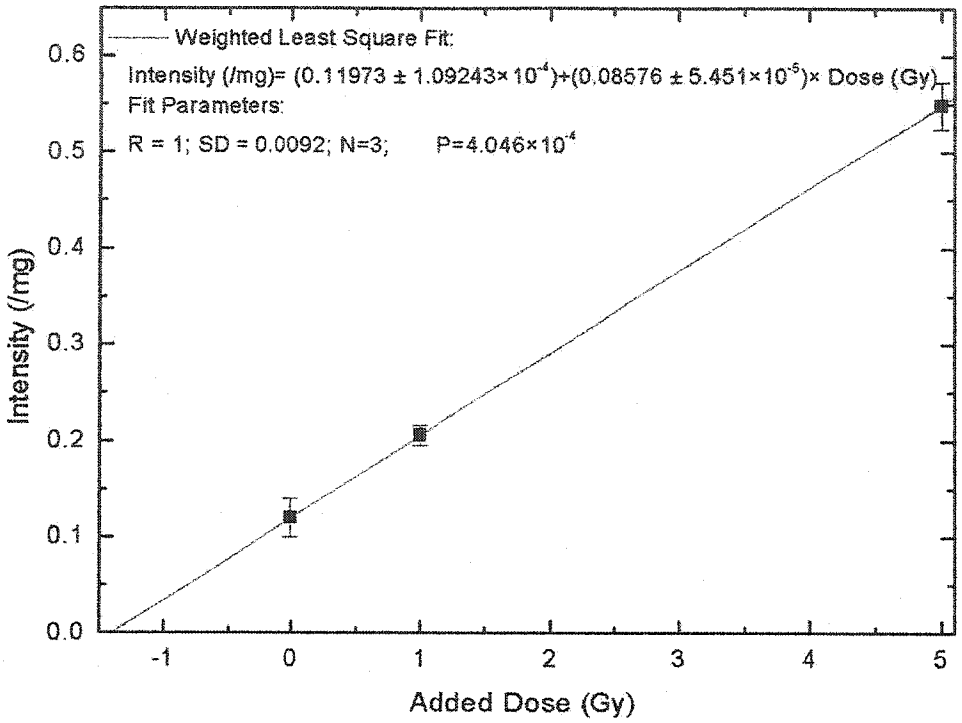

Fig. 4.3 Dose reconstruction in mice molars, (1.40 ± 0.16 Gy) was observed as the intersection of the linear plot with the dose axis for zero intensity. The error bars results from accounting the dosimetric signal anisotropy.

The dosimetric signal was followed for 42 days after the exposure to determine the stability of the signal. Though some fluctuations, not explicable, did occur, the intensity of the dosimetric signal was approximately constant over this period (Fig. 4.4). This shows that the mice molars could be collected within 45 days after the irradiation for the dose reconstruction purposes without any intensity loss.

To investigate the failure of the incisors to yield a dosimetric signal the chemically processed incisors and molars were scanned using an Environmental Scanning Electron Microscope (ESEM) and different images were obtained. The imaging of the samples showed a major structural difference in mice incisors and molars (see Fig 4.5). The incisors still had a thick layer on top of the apatite crystal bundles, while the molar images showed similar structure as found in a cleaned human tooth enamel images. The apatite crystallites in incisors were of much shorter dimension than molars, which is possibly due to the fact

that the incisors continuously grow. However, compared with the human molars the mouse molar apatite crystals were still shorter in dimensions.

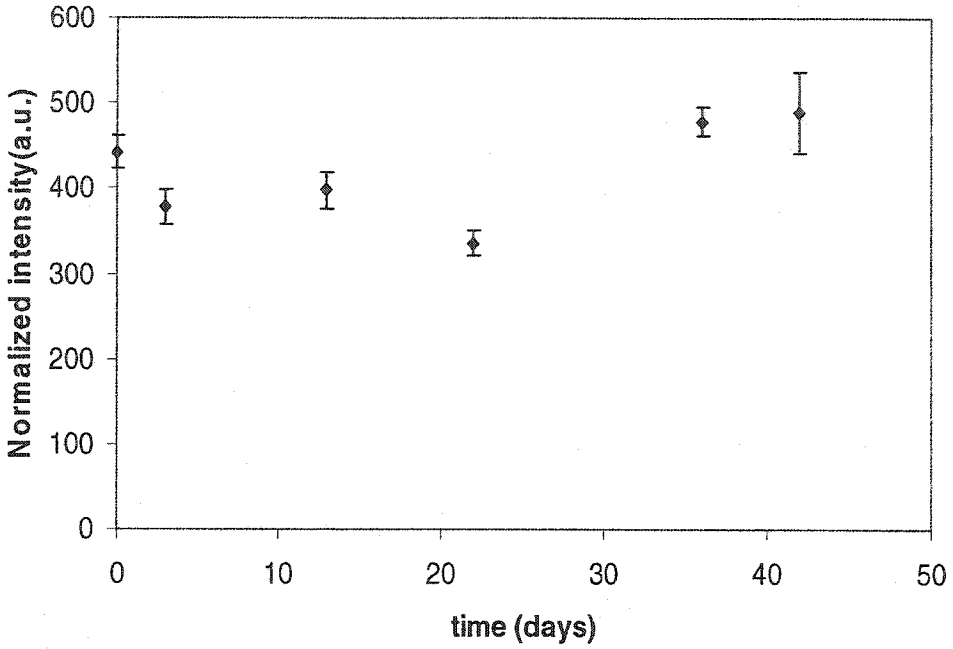

Fig. 4.4 The dosimetric signal stability in mice molars as a function of time. The uncertainly is obtained from the anisotropy of the dosimetric signal.

The main problem using this type of dosimetry could be the turnover time of teeth in the rodent or also the short lifespan of the animal itself which means that the samples may be collected only during the short available time following an exposure. All rodents have a similar dental arrangement, in each half of the jaw, a single incisor separated from the three to five cheek teeth by a wide gap. Since incisors are ever growing and their contents are ever changing. Therefore, if the mineral contents of dentine are exploited using the soxhet, they would not be useful for cumulative dose estimation.

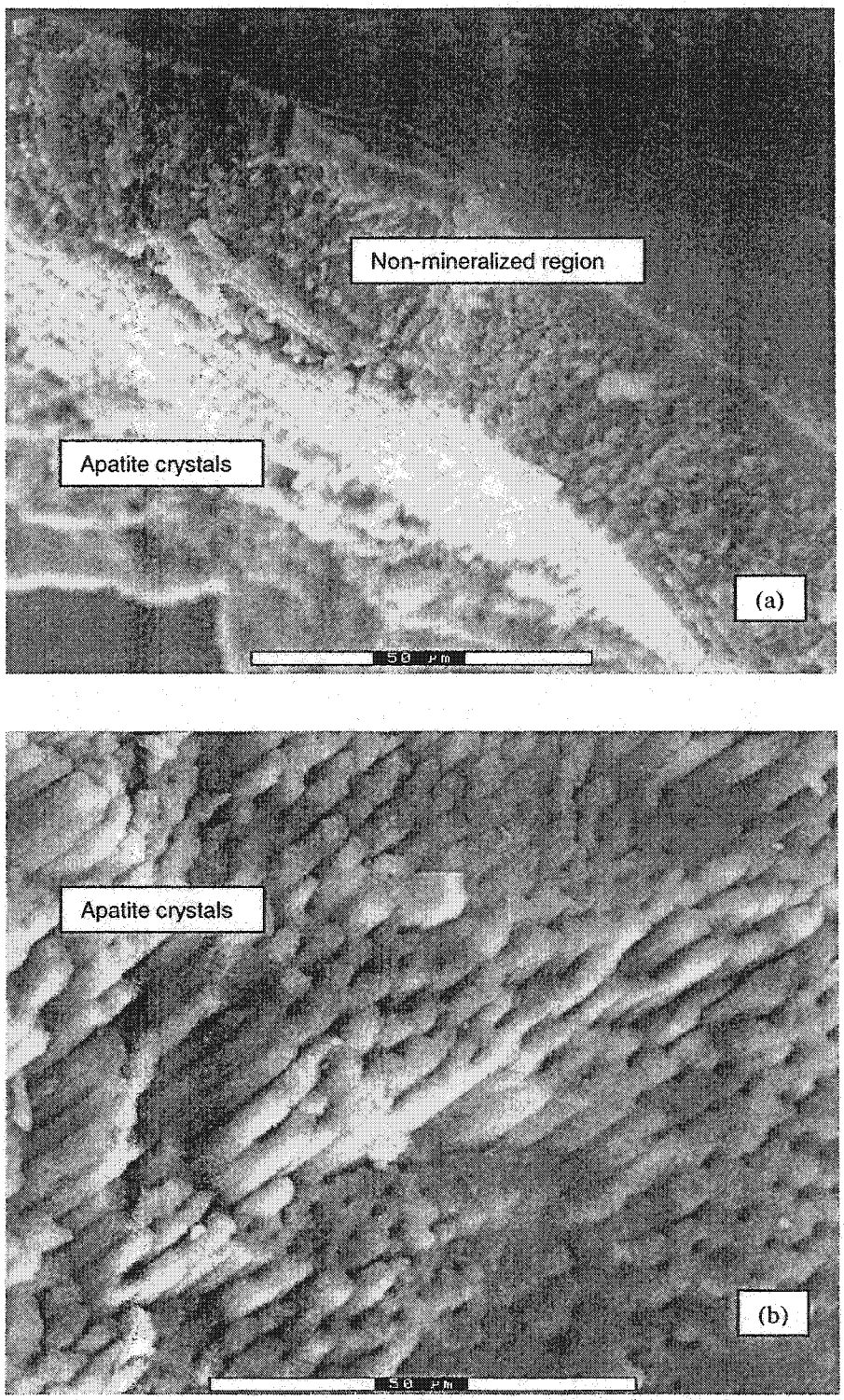

Fig. 4.5 The Environmental Scanning Electron Microscope (ESEM) image of processed incisor (a) consisting of different regions in addition to pure enamel, and processed mice molar (b) are shown.

The gamma radiosensitivity (defined as the peak-peak amplitude of the dosimetric signal per unit dose in a known mass of the sample) of mice tooth enamel was (811.18 ± 61.37) /Gy-100mg, whereas for human tooth it was (1664.42 ± 49.30) /Gy-100mg. Therefore, the mice molars have half the radiation sensitivity of that of human tooth. However, this low radiation sensitivity can not create any problem in dose reconstruction once the same species of tooth is given added doses of radiation or the calibration plot for the mice is used. This result also confirms the lower radiation sensitivity of mice enamel, as observed by others (Toyoda *et al.* 2002).

4.4 CONCLUSIONS

Electron paramagnetic resonance (EPR) dosimetry of human tooth enamel has been widely used in measuring absorbed radiation doses in various scenarios. However, for situations not involving human victim, like suspected environmental overexposures, experimental animals in radiation biology research, and for chronology of archaeological deposits, EPR dosimetry in the enamel extracted from mouse is developed. Tooth enamel from molars of previously irradiated mice was extracted and processed and the dose response resulted in reconstructing radiation doses in the 1 Gy range (1.40 ± 0.16) Gy. By using larger samples, i.e. a larger number of animals, lower doses could be determined. The gamma radiosensitivity of the mice enamel is found to be half of that of human tooth enamel. The dosimetric signal amplitude in mice enamel has been found to be stable for up to at least 42 days. Dose reconstruction was only possible in enamel extracted from molars and could not be determined in incisors. Electron micrographs showed structural variations in incisor enamel, possibly explaining the large interfering signal in non-molar teeth. This study demonstrates physical dose estimation in experimental radiation biology research and exhibits the potential for environmental exposure estimation, and age estimation for geological and archaeological deposits in higher natural dose scenarios using mice and rodents (Rink 1997; Breen & Battista 1995).

Chapter 5

A New Method for Low Dose Measurements

5.1 INTRODUCTION

At low doses in the order of 100 - 200mGy and small tooth sample masses, the concentration of radiation induced radicals (which is indicative of the amount of exposure) is very small. Therefore, in an electron paramagnetic resonance (EPR) spectrometer the amplitude of the dosimetric signal at $g_{//} = 1.9973$ and $g_{\perp} = 2.002$, (width 0.4 & 0.3 mT) is very small, too small to be visible even by using differential microwave power enhancement. To further complicate the analysis, the dosimetric signal is overshadowed by a native signal g = 2.005 (width 0.9 - 1 mT), which covers the whole region of interest from the point of view of dose reconstruction. For low dose exposures, this makes EPR dose construction impossible and may render the tooth useless in this range. In an unprocessed tooth, the native signal has amplitude corresponding to dosimetric signal of ~ 1 Gy; i.e. a dosimetric signal of even 1 Gy would be hard to realize in an unprocessed tooth. Currently, to measure the small dosimetric signal two approaches are being used:

i) Use of high sensitivity EPR cavities after visual realization of the dosimetric signal (partial elimination of native signal), and subsequent subtraction of the native signal.

ii) Complete removal of native signal, with a sample mass large enough to be measured in an EPR spectrometer (Ivannikov *et al.* 2001; Romanyukha *et al.* 2001).

Both methods rely heavily on chemical processing of tooth for partial or complete unveiling of the dosimetric signal, which has been found successful only in limited studies. The disadvantage of the first method is the sample loss due to extensive chemical treatment and long processing time (Onori *et al.* 2000). Usually a shorter time is preferred when a large number of samples are to be processed e.g. in an epidemiological or environmental study. Moreover, it requires the use of only high Q value EPR cavities, which defines the lower limit of dose measurement and is highly dependent on technological advancements. The second approach of complete native signal removal has not proven to be successful in

all different types of tooth samples especially large molars. Even if the complete organic contents are removed, the number of spins due to low exposure would be too low to show a signal in the EPR spectrum due to machine sensitivity and therefore puts a limit on the lowest detectable dose.

The most common dose reconstruction approach involves chemical treatment until the dosimetric signal (also called the zero-added-dose) due to the radiation exposure is either completely or partially revealed. Then using the fact that the dosimetric signal grows linearly with the added dose, the tooth sensitivity is determined. The unknown accident dose results from the backward extrapolation of the sensitivity line. During this procedure, it is assumed that the amplitude of the native signal does not change as a function of the added laboratory doses. Also there is a pre-condition that the zero-added-dose signal must be visible and measurable for the dose reconstruction; otherwise the dose can not be measured.

In our earlier communication (Khan *et al.* 2003b), we presented a simple modification to this dose reconstruction technique; wherein the low amplitude invisible zero-added-dose signal, due to accident or environmental exposures, is modified by a known laboratory dose to make it visible and measurable; which will henceforth be called the modified-zero-added dose, (MZAD). The rest of the multiple irradiation and dose reconstruction procedure remains the same. This technique, if carefully implemented, can be used to reconstruct radiation doses even below the currently established limit of 40 mGy (Romanyukha *et al.* 2001), without enhancing the sensitivity of spectrometer.

5.2 MATERIALS AND METHODS

Three molar tooth samples with known history were collected from the same young adult individual. Roots were removed and crowns were halved into mesial and distal parts by using a low speed water cooled diamond saw. Each mesial and distal part was further halved, and then separately placed in polypropylene vials and ultrasonically processed for 10 h in supersaturated potassium hydroxide (KOH) aqueous solution at 80 °C. The samples were intermittently washed in de-ionized water in an ultrasonic bath for 12 h, after each 5 h of KOH treatment. As a result of this processing, dentine was completely eliminated from the sample. The sample was gently crushed with the help of agate mortar and pestle and sieved into 0.2 - 0.4 mm grain distribution. The crushing was done in the presence of liquid nitrogen to

avoid localized heating in the enamel. From the mesial half of each sample, an aliquot of 100mg was taken and placed inside a 3 mm outer diameter suprasil (synthetic quartz) tube, which was then put inside a 4 mm outer diameter tube and measured in a TE_{011} mode cylindrical cavity of JEOL JES-FA100 EPR spectrometer.

The EPR spectrum was collected under the conditions provided in section **2.2.2.8**. The spectrum consisted of only the native signal due to the organic contents of enamel. For the MZAD technique, the sample was placed in small plastic pillboxes and given x mGy (~100 mGy, to mimic an "unknown" low accidental exposure) of laboratory dose from a ^{137}Cs source at 4.25 Roentgen per minute (10.94×10^{-4} C/kg-minute). The dosimetry was done using a pre-calibrated Farmer dosimeter with a 0.6cc chamber. The chamber calibration could be traced back to the primary standard laboratory at the National Research Council of Canada. The uncertainty of the dose measurement was less than 5 % at 95 % confidence interval. The irradiation was performed in a specially designed acrylic rack providing both the dose build up in all the dimensions and backscatter (see section **2.2.5**). The EPR spectrum was collected but no apparent change in native signal was seen. The sample was given a further 300 mGy (hereafter called dose modifier, y). The total dose in the sample becomes x' (hereafter called the modified-zero-added-dose), consequently the dosimetric signal is visible in the EPR spectrum. The amplitude of the signal for the modified-zero-added-dose was measured, and subsequently more added laboratory doses were given. During each measurement, the sample was manually rotated in the cavity in a complete 360° angular rotation in steps of 30° and re-measured in the EPR cavity. The spectrum at each rotation was adjusted by normalizing it with the corresponding intensity of the 3rd and 4th lines of the digital Mn^{++} marker which remained at a fixed position throughout the spectrum collection. The native component of the dosimetric signal was subtracted from the spectrum, by using the spectrum collected from the distal halves of the sample. Similarly, from the set of collected spectra at different doses, an empty EPR tube spectrum was subtracted after alignment with the help of Mn^{++} markers. For a given dose, the spectra were averaged out and the standard deviation of the mean provides the uncertainty in the dose measurements due to dosimetric signal anisotropy (Khan *et al.* 2002). Adjustments in the dosimetric intensity were made by subtracting the

native component (Table 5.1). The dose response was constructed by plotting the dosimetric intensity vs. laboratory added doses, and a weighted least square line is fitted through it (weight is provided by the uncertainty in the intensity measurement). By using backward extrapolation, the modified-zero-added-dose (x') was therefore quantified.

Table 5.1 Variation in adjusted radiogenic signal amplitude as a function of laboratory added dose. The uncertainty in intensity comes from the radiation signal anisotropy.

Additional dose (mGy)	Adjusted intensity (a.u.)
0	360±129
300.35	454±58
603.95	678±197
1104.85	1016±52
1604.84	1334±134
2605.34	1999±99
3605.84	2665±123
5606.84	4008±64
9608.84	6716±52

5.3 RESULTS AND DISCUSSION

Fig. 5.1 shows the dose response for one of these samples. The dosimetric signal intensity at zero mGy arises from both the accidental exposure, x, and dose modifier, y. The "unknown" dose due to accident x, for one of the samples, is therefore $x = x' - y = (400 \pm 18) - (300 \pm 15) = (100 \pm 23)$ mGy which matches well with the accidental dose (100 mGy chosen in this controlled experiment). The results from other samples were reproducible within 5 % of the accident dose.

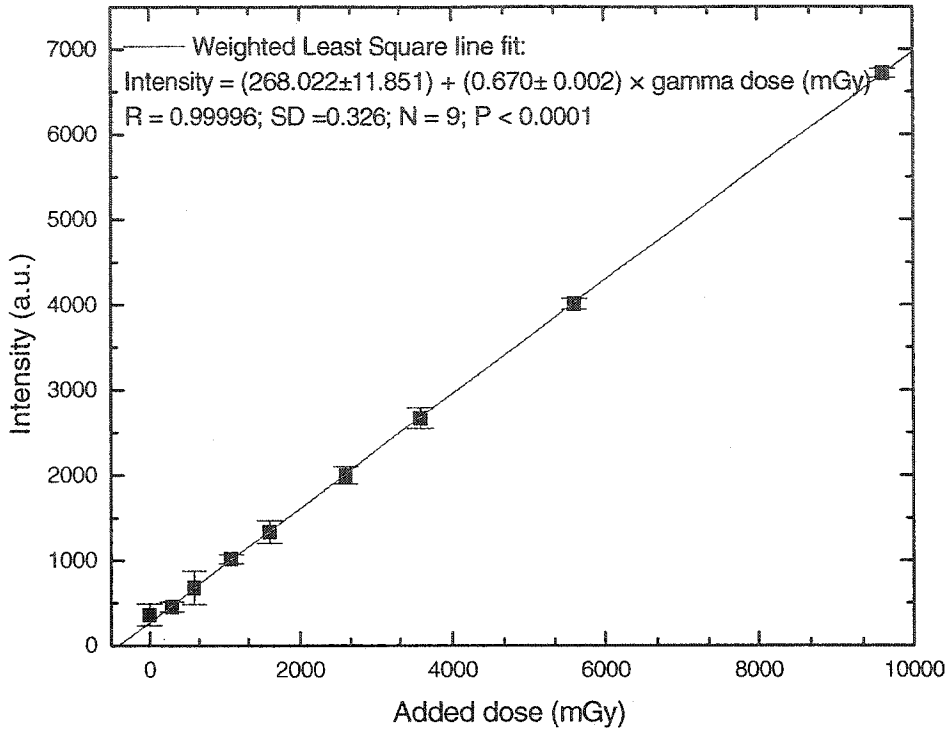

Fig 5.1 Traditional back-extrapolation technique for accidental dose reconstruction used in EPR tooth enamel dosimetry. First point at zero mGy on the plot is now (MZAD, intensity) which contains information about both the unknown accidental exposure and the dose modifier, and amounts to (400 ± 23 mGy).

This laboratory controlled experiment demonstrates the practical feasibility of MZAD concept in 100 mGy range, when the dosimetric signal was unresolvable from native signal. This dose evaluation technique is simple in approach and relies on the basic assumption of linear dose build up in teeth. The assumption of linear dose build up in the 100 mGy range is not generally unreasonable except for a few reported cases (Chumak *et al.* 1997). Very low radiation doses can be reconstructed, even if the dosimetric signal is hidden by the native signal. The contribution of the native signal can be removed from the dosimetric signal by using standard spectrum deconvolution techniques (Hayes *et al.* 1998a). This technique is well-suited for low exposure accident dosimetry, especially in situations where the organic contents of the sample can not be removed chemically and the dosimetric signal is not seen. This procedure also saves extensive chemical processing. Therefore, a large number of samples can be processed in a shorter time (Fig 5.2).

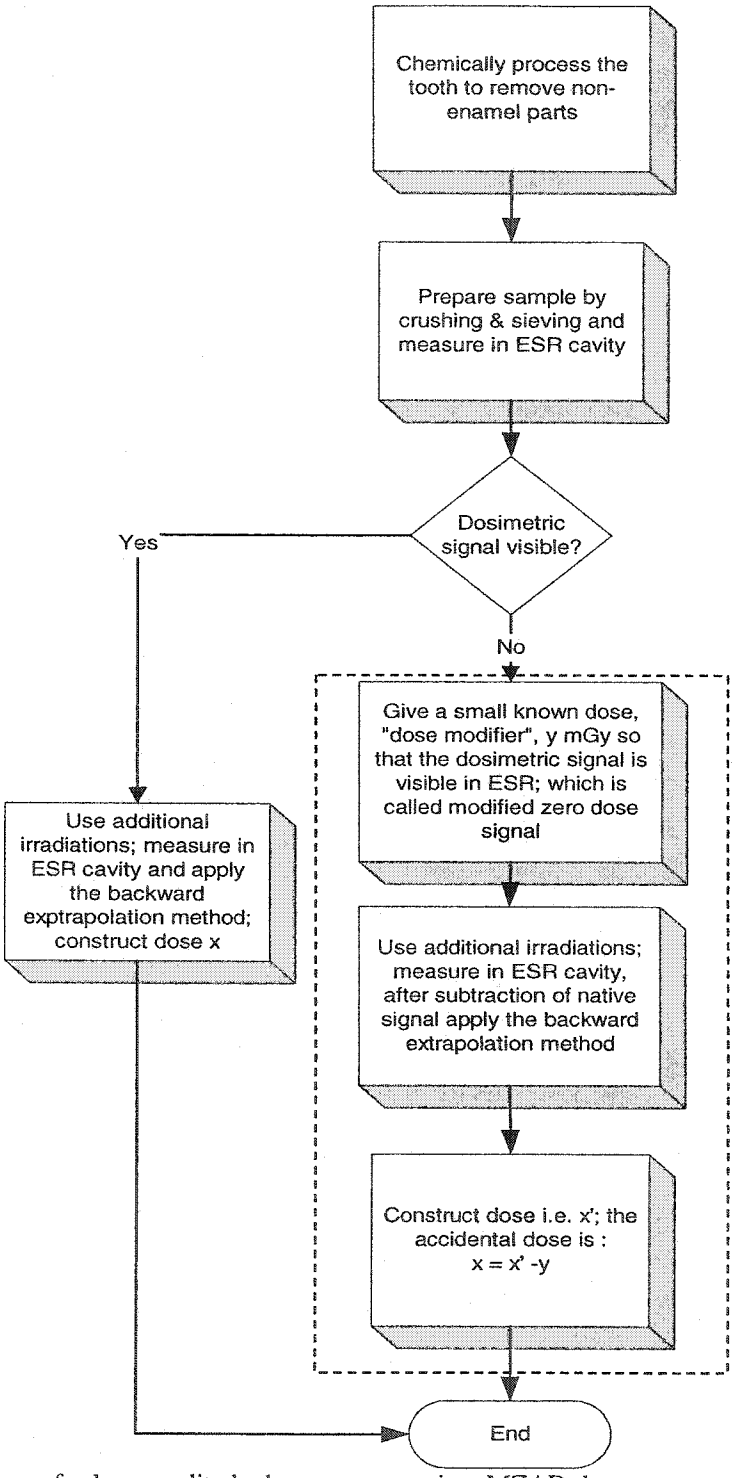

Fig 5.2 Flow diagram for low amplitude dose reconstruction, MZAD dose reconstruction is shown by the dashed box on the right, whereas the conventional protocol is shown on left of the diamond. Chemical treatment and sample preparation processes may vary from one laboratory to another.

This technique differs from others techniques only in the dose modifier. The selection of the dose modifier is important. It should be large enough to reveal the dosimetric signal but it must not be too large so that the true accident dose becomes only an uncertainty of the modified accident dose, x'. Mathematically, the whole process is equivalent to a translation of the dose calibration line by a single point in dose-intensity plane.

With the proper account of the native signal and suitable choice of the dose modifier this technique has the potential to quantify any accidental exposure even below the current limit of 40 mGy. This could pave the way for the implementation of EPR biodosimetry technique in the domain of low level suspected exposure determination and has a potential for environmental biodosimetry and epidemiological studies. For low suspected exposures, below 100 mGy, sometimes the dosimetric signal can not be visualized. Therefore, the conventional technique of dose reconstruction will render tooth useless. However, amplification with a carefully chosen dose modifier can make the signal amplitude high enough to be seen in the EPR spectrum and therefore the dose.

One of the possible problems associated with this technique could be the high uncertainty involved, due to the additional subtraction step. In the present demonstrative dose reconstruction, the relative uncertainty was 23 % which can be reduced by choosing a small dose modifier. Another disadvantage of the MZAD technique arises from the addition of dose modifier, which renders the EPR tooth dose measurement a destructive technique (Hayes *et al.* 2000a). Because, after additional irradiation, the tooth sample not only contains the history of accidental exposure but also the dose modifier. Also the MZAD method requires the correct known amount of dose modifier so it heavily relies on good laboratory irradiation facilities and precise dose measurement. However, the benefits associated with the dose modifier approach offset most of the demerits of this method.

5.4 CONCLUSIONS

We have proposed a modification to the conventional EPR dosimetry protocol used for biophysical dose measurement and reconstruction. This may prove useful for radiation exposures below 100 mGy, where the dosimetric signal in tooth enamel is too small to be measured by using the traditional

dose reconstruction procedure, and tooth dosimetry ceases to remain valid. This technique requires an additional step of laboratory irradiation to make the small dosimetric signal visible.

Mathematically, the accident dose x is modified by a known amount of exposure, y (large enough so that the signal is now visible), and the total exposure becomes $x' = x + y$, which is the modified-zero-added dose. The exposure x' is then quantified using the conventional backward extrapolation method and the accident dose can be measured.

By using a suitable mix of dose modifier and native signal subtraction, tooth enamel, in a laboratory controlled experiment, the feasibility of dose reconstruction in the 100 mGy range has been successfully demonstrated. This may make the dose measurements possible even those due to suspected low exposure in tooth enamel. Therefore, tooth would still remain useful for exposure estimation even below 40 mGy, without using the super Q value EPR cavities.

Chapter 6

Summary and Conclusions

EPR dose reconstruction using human tooth enamel is a mature technique and has been developed and been extensively utilized in the years following the Chernobyl accident. In this study, the development of the EPR dosimetry technique at McMaster University has been described which will be used as a tool for accident and emergency dose measurement. By using this technique, with conventional zero added dose (ZAD) methodology of dose reconstruction, retrospective doses well below 100 mGy can be measured. This was accomplished by developing a suitable mix of sample measurement conditions, sample positioning in the cavity, high temperature ultrasonic treatment of tooth in supersaturated potassium hydroxide aqueous solution, and well-controlled laboratory irradiations. During this investigation, it was found that the drop in the cavity Q value due to larger sample masses could be accounted for by normalizing the dosimetric signal to the intensity of the in-cavity Mn^{++} markers (located at a fixed position inside the cavity). Avoiding unnecessary crushing of sample, proper cooling of sample during inevitable crushing steps, and intermittent washing in de-ionized water during chemical preparation, can minimize the induction of undesirable preparation-induced signals in the enamel EPR spectrum. It was also observed that a grain distribution within 0.2 - 0.4 mm results in a lower dosimetric signal anisotropy, without sacrificing the dosimetric sensitivity. Higher signal sensitivity was achieved by putting the sample inside a 3 mm synthetic quartz tube, which itself is placed in another 4 mm diameter tube and allowed to have a maximum sample height of 10 mm in the inner tube, corresponding to the most sensitive volume in the EPR cavity. The dosimetric signal anisotropy could be taken into consideration by manual rotation of the sample in a 360^{o} angular range, while the cavity Q change due to the change in boundary conditions as a result of rotation is accounted for by the intensity of the Mn^{++} marker lines (located at a fixed location in the cavity). Post processing of the measured spectra is performed to remove the undesirable contribution of both

preparation-induced signals and the signals arising from the organic contents of enamel. For doses above 300 mGy, differential power saturation of the native and dosimetric signals results in quick and reliable dose reconstruction. Below 300 mGy, a more rigorous and time intensive approach has been adopted. It involved the subtraction of the empty tube spectrum, baseline shift, modeling of the native signal and simulation of dosimetric signal using three Gaussian-Lorenzian functions.

The minimum retrospective dose reconstructed by this conventional technique, subjected to visualization of zero added dose signal, was (80.21 ± 30.29) mGy. This minimum detection limit is defined by the sensitivity of the spectrometer to detect the minimum number of spins, and the efficiency of the chemical reagent in reducing the contents giving rise to non-radiogenic signals. Efficient chemical treatment, such as that developed in this protocol, sometimes results in complete de-organification of enamel, and very low doses can be measured. However, this was not observed for all types of teeth. The minimum dose reported above, is also dependent not only on the X ray exposure history of the individuals, but also on the exposure of tooth due to different environmental background doses. The real problem with human tooth enamel is, actually knowing whether a true dose has been from natural or medical X-ray irradiations (the latter can be handled to some extent). A future challenge could be to collect tooth samples from the populations with low background especially those persons who live in very low dose environments e.g. Bahamas. The Bahamas are unique because they are entirely built of coral and shell, which have very low concentrations of ^{238}U, and virtually no ^{232}Th or ^{40}K. At least in this kind of environment, one would be able to predict the maximum dose the subject received, and test whether or not the correct dose can be reconstructed in tooth enamel using EPR dosimetry. In such a study, specific information on individuals regarding their age, travel history (outside the Bahamas), and history of dental treatment would be needed.

Tooth enamel is a useful environmental dosimeter. Its response can vary within uncertainties as a function of geographic location for a given population. Although some studies have been done on geographic variability of the tooth response to radiation, a detailed and extensive study of various

populations is necessary to find the correlations between enamel sensitivity and other environmental factors such as diet and water quality.

For a person or animal involved in a radiation accident, correct knowledge about the age of the tooth is desirable to separate out the environmental exposure contribution from the accidental absorbed dose. To account for the contribution from diagnostic dental X rays, current practice is to use differential dosimetric signal amplitude measurement in the buccal and mesial parts, but this result in an approximate correction. Analogue modeling (such as Monte Carlo simulations) of the diagnostic dental X ray attenuation in adjacent tooth layers, and devising a general methodology for them could be a useful contribution in separating out their contribution.

Unlike all the biological or cytogenetic dosimetric techniques used today, only tooth enamel provides the actual physical dose at a known fixed location in the human body. An interesting cross-fertilizing study would be to reconstruct the radiation dose by using both physical and biological markers and evaluate both inter- and intra- relationships. For example, blood and tooth samples obtained from head and neck cancer patients undergoing radiation therapy (where teeth are easily available because of the treatment), can be used to reconstruct doses using biophysical means such as EPR on tooth and biological markers such as lymphocyte counting, dicentrics and stable chromosome painting. Such an effort can result not only in a biophysical dosimetric gold standard for accident dosimetry, but can be useful for radiotherapy dose verification. From the knowledge of both *in vivo* physical dose and corresponding biological response, tissue/ tumor radiation response probabilities can be obtained.

In this dissertation, the second major work reported was the response of human tooth enamel to neutron beams. This was evaluated by using an accelerator based low gamma radiation yield neutron source. For this purpose, neutron beams were produced from the 3 MV McMaster K. N. accelerator by bombarding an accelerated proton beam on to a thick lithium metal target. It was observed that, like gamma radiation, neutron irradiation produced the same stable radical species. However, the neutron response was determined to be ~ 10 % of the equivalent gamma radiation dose. Response of the tooth enamel was linearly proportional to the neutron dose from 6 to 35 Gy. Similar to gamma radiation, the neutron

radiosensitivity was found to vary as a function of grain size. The neutron radiosensitivity dropped to 20 % for grains 0.106 – 0.3 mm compared with the whole tooth samples. The enamel response to various mean neutron energies from 150 – 450 keV remained constant within experimental uncertainties. No effect of different dose rates on neutron radiosensitivity was seen, for the available dose rates from 0.6 to 2.4 Gy/h. All results indicate that tooth enamel also has the properties of a good accident dosimeter for neutron irradiations.

These set of investigations constitute the pioneering work done on the response of tooth to neutron doses. It has significant implications for accident dosimetry when tooth can be part of an accident involving a mixed neutron – gamma radiation field. A correction factor of ten is, therefore, suggested for the neutron component of mixed radiation fields for tooth enamel in the biophysical EPR dosimetry. Since as a consequence of neutron irradiation, the dosimetric signal is produced at the same g value in the EPR spectrum as for gamma, it is virtually impossible to separate out the relative contribution for the two different radiation qualities by using EPR dosimetry of tooth only. Calcium is an integral part of the bio-apatite (major constituent of tooth), the neutron irradiation can produce higher isotopes of this element such as ^{41}Ca. Therefore, techniques such as mass spectroscopy of calcium isotopes can be useful for the calculation of the neutron contribution only. With prior knowledge of the neutron correction factor (as described earlier), this in turn can be used to separate out the relative contribution of neutrons in a mixed accident scenario. Again interesting and far reaching results could be obtained for a mixed neutron-gamma field irradiation of human tissues such as tooth and blood from mock criticality accident exercises.

In certain cases, due to the problems in human tooth availability, the technique for dose construction using the tooth from mice and rodent has been devised. The teeth extracted from mice also represent the lower extreme of size and mass for this technique, which makes dose reconstruction challenging. The important features of this technique include complete removal of the organic signal in mice molars by supersaturated alkaline treatment of the sample. Dose reconstruction in mice irradiated for radiation biology research is therefore feasible. Identification of the problem giving rise to failure of the

EPR dose measurement in the incisors of mice, was done by using electron micrographs. It was ascribed to the presence of an organic layer in incisors not normally observed in molars.

Success of the mouse research opens new opportunities for the application of environmental radiation exposure assessment, and experimental radiation biology. The physical dose from mice living in a high dose-rate environment could be useful in finding the biological consequences by using different assays. Such a study could be done by collecting samples from naturally high dose-rate areas such as in the phosphate bone bed mining area of central Florida (USA), where many studies have been done associated with radon accumulation in homes, or in other high background areas such as in Ramsar (Iran), Kerala (India) and Ireland. A further improvement in dose reconstruction by bringing the minimum detectable dose to < 300 mGy could be used to construct radiation dose maps as a function of altitude, which will help to separate out the extra-terrestrial component of background radiation. High radiation exposures arising from radiation disasters have been found to have a strong impact on the ecosystem e.g. at a distance of 100 km around the Techa river (Russia) with high level gamma radiation dose-rates varying from 0.5 mR/h – 100 mR/h, could be a possible site for collection of samples.

The most conspicuous of all the work done on EPR biophysical dosimetry was the introduction of the concept of modified zero added dose (MZAD) in dose reconstruction. As mentioned earlier, due to the machine sensitivity limit or inefficient deorganification, the zero added dose signal can not be seen and tooth becomes useless for the purpose of dose reconstruction. However, a small known amount of laboratory controlled dose supplied to the tooth can modify the accident dose, and can be measured with less effort. This concept relies on the fact that the radiogenic signal is produced only by ionizing radiation, and the signal intensity increases linearly with the amount of radiation dose even below 100 mGy. This is a reasonable assumption and most of the dose reconstructions reported in the literature are in agreement with it either explicitly or implicitly.

This is a novel concept in conventional EPR dose reconstruction, which is not only simple in concept, but it is predicted that if applied to low dose measurement (< 200 mGy) it will lead to further lowering of the minimum detectable dose limit. Whereas measuring higher exposure (> 200 mGy) with the

MZAD method, will decrease the sample processing time and increase the throughput of EPR dosimetry; lowering of the limit below 20 - 30 mGy could make it useful for the measurement of annual radiation exposure in industrial radiation workers. Also this could be accomplished now without using high quality EPR cavities and any further enhancement of the EPR spectrometer technology. Since this concept is general, it will make possible measurements for the low sensitivity samples such as mice teeth and be useful for the measurement of low environmental exposure. Also it could be used to evaluate the exposures arising from the low enamel sensitivity radiations such as neutrons.

Finally, a further improvement in the understanding of radiation induced paramagnetic centre is desirable which can only be accomplished by developing simple models for the transformation of radiation induced damage in the tooth mineral to the formation of stable paramagnetic species.

References

AAPM 1983. A protocol for the determination of absorbed dose from high-energy photon and electron beams. *Medical Physics* 10: 741-771.

Aldrich, J. E. & Pass, B. 1986. Dental enamel as an *in vivo* radiation dosimeter: separation of the diagnostic X ray dose from the dose due to natural sources. *Radiation Protection Dosimetry* 17: 179-186.

Aldrich, J. E. & Pass, B. 1988. Determining radiation exposure from nuclear accidents and atomic tests using dental enamel. *Health Physics* 54: 469-471.

Aldrich, J. E., Pass, B. & Mailer, C. 1992. Changes in paramagnetic centres in irradiated and heated dental enamel studies using Electron Paramagnetic Resonance. *International Journal of Radiation Biology* 61: 433-437.

Almassy, Z., Krepinsky, A. B., Bianco, A. & Koteles, G. J. 1987. The present state and perspectives of Micronucleus assay in radiation protection - A review. *Applied Radiation and Isotopes* 38: 241-249.

Aoba, T., Doi, Y., Yagi, T., Okazaki, M., Takahashi, J. & Moriwaki, Y. 1982. Electron Spin Resonance study of sound and carious enamel. *Calcified Tissue International* 34: S88-S92.

Aragno, D., Fattibene, P. & Onori, S. 2001. Mechanically induced EPR signals in tooth enamel. *Applied Radiation and Isotopes* 55: 375-382.

Aslam, Prestwich, W. V., McNeill, F. E. & Walker, A. J. 2003a. Development of neutron source for applications in low dose radiobiological and radiochemical research. *Applied Radiation Isotopes* 58(6): 629-641.

Aslam, Prestwich, W. V., McNeill, F. E. & Walker, A. J. 2003b. Investigating the TEPC radiation quality factor response for low energy accelerator based clinical applications. *Radiation Protection Dosimetry* 103(4): 311-322.

Attix, F. H. 1986. Introduction to radiological physics and radiation dosimetry. John Wiley & Sons. New York.

Bailiff, I. K., Bùtter-Jensen, L., Correcher, V., Delgado, A., Goksu, H. Y., Jungner, H. & Petrov, S. A. 2000. Absorbed dose evaluations in retrospective dosimetry: methodological developments using quartz. *Radiation Measurements* 32: 609-613.

Becker, R. O. & Marino, A. A. 1966. Electron paramagnetic resonance spectra of bone and its major components. *Nature* 210: 583-588.

BEIR VI 1999. Committee on health risks of radon (BEIR VI). Washington, D.C.: National Research Council.

Bevington, P. R. & Robinson, D. K. 1992. Data reduction and error analysis for the physical sciences. New York: McGraw Hill.

Bochvar, I. A., Kleshchenkov, E. D., Kushnereva, K. K. & Levochkin, F. K. 1997. Sensitivity of human tooth enamel to α irradiation and neutrons. *Atomic Energy* 83: 380-383.

Bothwell, A. M., Whitehouse, C. A. & Tawn, E. J. 2000. The application of FISH for chromosome aberration analysis in relation to radiation exposure. *Radiation Protection and Dosimetry* 88: 7-14.

Brady, J. M., Norman, O. A. & Swartz, H. M. 1968. *In vivo* dosimetry by Electron Spin Resonance spectroscopy. *Health Physics* 15: 43-47.

Breen, S. L. & Battista, J. J. 1995. Radiation dosimetry in human bone using electron paramagnetic resonance. *Physics in Medicine and Biology* 40: 2065-2077.

Brik, A., Baraboy, V., Atamanenko, O., Shevchenko, Y. & Brik, V. 2000. Metabolism in tooth enamel and reliability of retrospective dosimetry. *Applied Radiation and Isotopes* 52: 1305-1310.

Brik, A., Radchuk, V., Scherbina, O., Matyash, M. & Gaver, O. 1996. Metamorphic modification and EPR dosimetry in tooth enamel. *Applied Radiation and Isotopes* 47: 1317-1319.

Brown, W. E. & Chow, L. C. 1976. Chemical properties of bone mineral. John Wiley & Sons, New York.

Callens, F., Vanhaelewyn, G., Matthys, P. & Boesman, E. 1998. EPR of carbonate derived radicals: Applications in dosimetry, dating and detection of irradiated food. *Applied Magnetic Resonance* 14: 235-254.

Callens, F. J., Verbeeck, R. M. H., Matthys, P. F. A., Martens, L. C. & Boesman, E. R. 1987. The contribution of CO_3^{3-} and CO_2^- to the ESR spectrum near g = 2 of powdered human tooth enamel. *Calcified Tissue International* 41: 124-129.

Caswell, R. S., Coyne, J. J. & Randolph, M. L. 1980. Kerma factors for neutron energies below 30 MeV. *Radiation Research* 83: 217-254.

Chang, W. P., Tsai, M. S., Hwang, J. S., Lin, Y. P., Hsieh, W. A. & Shaoyi, H. 1999. Follow-up in the micronucleus frequencies and its subsets in human population with chronic low-dose γ–irradiation exposure. *Mutation Research* 428: 99-105.

Chapman, M. R., Miller, A. G. & Stoebe, T. G. 1979. Thermoluminescence in hydroxyapatite. *Medical Physics* 6: 494-499.

Chumak, V., Bailiff, I. K., Baran, N., Bugai, A., Dubovsky, S., Fedosov, I., Finin, V., Haskell, E., Hayes, R., Ivannikov, A., Kenner, G., irillov, V., hamidova, L., olesnik, S., iidja, G., ikhtarev, I., Lippmaa, E., Maksimenko, V., Meijer, A., Minenko, V., Pasalskaya, L., Past, J., Puskar, J., Radchuk, V., Sholom, S., Skvortsov, V., Stepanenko, V., Vaher, U. & Wieser, A. 1996. The first international inter-comparison of EPR-dosimetry with teeth: First results. *Applied Radiation and Isotopes* 47: 1281-1286.

Chumak, V., Likhtarev, I., Sholom, S., Meckbach, R. & Krjuchkov, V. 1998. Chernobyl experience in field of retrospective dosimetry: Reconstruction of doses to the population and liquidators involved in the accident. *Radiation Protection Dosimetry* 77: 91-95.

Chumak, V., Sholom, S. & Pasalskaya, L. 1999. Application of high precision EPR dosimetry with teeth for reconstruction of doses to Chernobyl populations. *Radiation Protection Dosimetry* 84: 515-520.

Chumak, V. V., Likhtarev, I. A., Sholom, S. S., Pasalskaja, L. F. & Pavlenkov, Y. U. Retrospective reconstruction of radiation doses of Chernobyl liquidators by Electron Paramagnetic Resonance. (Ed.) Reeves, G. I. AAFRI 97-2. 1997. Armed Forces Radiobiology Research Institute.

Copeland, J. F., Gall, K. D., Lee, S. Y. & Shabot, G. E. 1996. Proton dosimetry in bone using Electron Spin Resonance. *Applied Radiation and Isotopes* 47: 1533-1538.

Court, L., Bassant, M., Gourmelon, P., Gueneau, G. & Psquier, C. H. 1986. Impairment of electrical functions of CNS and alterations in cell populations associated with irradiation. *British Journal of Cancer* 55: 230-231.

Dalgarno, B. G. & Mcclymont, J. D. 1989. Evaluation of ESR as a radiation accident dosimetry technique. *Applied Radiation and Isotopes* 40: 1013-1020.

Darroudi, F. 2000. Use of FISH translocations analysis for retrospective biological dosimetry: How stable are stable chromosome aberrations? *Radiation Protection and Dosimetry* 88: 101-109.

Darroudi, F. & Natarajan, A. T. 2000. Application of FISH chromosome painting assay for dose reconstruction: State of the art and Current views. *Radiation Protection and Dosimetry* 88: 51-58.

de Oliveira, L. M., de Jesus, E. F., Rossi, A. M. & Lopes, R. T. 1999. Energy dependence of EPR signal in synthetic and biological hydroxyapatite irradiated with photons. *Radiation Protection Dosimetry* 84: 511-514.

Degteva, M. O., Kozheurov, V. P. & Tolstykh, E. I. 1998. Retrospective dosimetry related to chronic environmental exposure. *Radiation Protection Dosimetry* 79: 155-160.

Degteva, M. O., Kozheurov, V. P. & Vorobiova, M. I. 1994. General approach to dose reconstruction in the population exposed as a result of radioactive wastes into the Techa river. *Science Total Environment* 142: 49-61.

Dehos, A., Hinz, G. & Schwarz, E. R. Changes in number and function of the lymphocyte populations as biological indicators for ionizing radiation. 298-301. 1986. Munchin. (In) Biological indicators for radiation dose assessment.

Desrosiers, M. F. 1991. *In vivo* assessment of radiation exposure. *Health Physics* 60: 859-861.

Desrosiers, M. F. & Schauer, D. A. 2001. Electron paramagnetic resonance (EPR) biodosimetry. *Nuclear Instruments & Methods in Physics Research Section B- Beam Interaction with Materials and Atoms* 184: 219-228.

Desrosiers, M. F., Simic, M. G., Eichmiller, F. C., Johnston, A. D. & Bowen, R. L. 1989. Mechanically-induced generation of radicals in tooth enamel. *Applied Radiation and Isotopes* 40: 1195-1197.

Driessens, F. C. M. & Verbeeck, R. M. H. 1990. Biominerals.: CRC Press Boston.

Edwards, A. A. 2000. Fluorescence *In Situ* Hybridization (FISH). *Radiation Protection and Dosimetry* 88: 5-6.

Egersdorfer, S., Wieser, A. & Muller, A. 1996. Tooth enamel as a detector material for retrospective EPR dosimetry. *Applied Radiation and Isotopes* 47: 1299-1303.

Fatome, M., Martin, A. S., Mestries, J. C. & Multon, E. 1997. Biological dosimetry after a criticality accident. *Radiation Protection and Dosimetry* 70: 445-459.

Fattibene, P., Aragno, D. & Onori, S. 1998. Effectiveness of chemical etching for background electron paramagnetic resonance signal reduction in tooth enamel. *Health Physics* 75: 500-505.

Fattibene, P., Aragno, D., Onori, S. & Pressello, M. C. 2001. Thermal induced EPR signals in tooth enamel. *Radiation Measurements* 32: 793-798.

Fischer, H. 1965. Magnetic properties of free radicals. Berlin: Springer.

Flanders, K. C., Sullivan, C. D., Fuji, M., Sowers, A., Anzano, M. A., Arabshashi, A., Major, C., Deng, C., Russo, A., Mitchell, J. B. & Robert, A. B. 2002. Mice lacking Smad3 are protected against cutaneous injury induced by ionizing radiation. *American Journal of Pathology* 160: 1057-1068.

Fowler, B. O. & Kuroda, S. 1986. Changes in heated and in laser irradiated human tooth enamel and their probable effects on solubility. *Calcified Tissue International* 38: 197-208.

Garrison, E. G., Rowlett, R. M., Cowan, D. L. & Holroyd, L. V. 1981. ESR dating of ancient flints. *Nature* 290: 44-45.

George, K., Willingham, V., Wu, H., Gridley, D., Nelson, G. & Cucinotta, F. A. 2002. Chromosome aberrations in human lymphocytes induced by 250 MeV protons: effects of dose, dose rate and shielding. *Advancements Space Research* 30: 891-899.

Gerber, G. B., Gerber, G., Kurohara, S., Altmann, K. I. & Hemplemann, L. H. 1961. Urinary excretion of several metabolites in persons accidentally exposed to ionizing radiation. *Radiation Research* 15: 314-318.

Griffith, R. V. 1998. Retrospective dosimetry needs from an IAEA perspective. *Radiation Protection and Dosimetry* 77: 3-9.

Grun, R. 1996. Errors in dose assessment introduced by the use of the "linear part" of a saturating dose response curve. *Applied Radiation and Isotopes* 26: 297-302.

Grun, R., Brink, J. S., Spooner, N. A., Taylor, L., Stringer, C. B., Franciscus, R. G. & Murray, A. S. 1996. Direct dating of Florisbad Hominid. *Nature* 382: 500-501.

Grun, R. & McDonald, P. D. M. 1989. Non-linear fitting of TL/ESR dose-response curves. *Applied Radiation and Isotopes* 40: 1077-1080.

Guo, Y., Zhu, Y. P., Ji, G. & Wu, K. 1998. Dose definition and physical dose evaluation for the human body in external radiation accident. *Radiation Protection and Dosimetry* 77: 97-100.

Hashimoto, T., Hong, D. G. & Takano, M. Retrospective dosimetry at JCO using luminescence from ceramics pieces and quartz. International symposium on new prospects of ESR dosimetry and dating , 26. 2001. Oct 25-27, Osaka University, Osaka, Japan.

Haskell, E. H. 1993. Retrospective accident dosimetry using environmental materials. *Radiation Protection Dosimetry* 47: 297-303.

Haskell, E. H., Hayes, R. B. & Kenner, G. H. 1996. Preparation induced errors in EPR dosimetry of enamel: pre- and post-crushing sensitivity. *Applied Radiation and Isotopes* 47: 1305-1310.

Haskell, E. H., Hayes, R. B. & Kenner, G. H. 1997a. Improved accuracy of EPR dosimetry using a constant rotation goniometer. *Radiation Measurements* 27: 325-329.

Haskell, E. H., Hayes, R. B., Kenner, G. H., Sholom, S. V. & Chumak, V. I. 1997b. Electron paramagnetic resonance techniques and space biodosimetry. *Radiation Research* 148: S51-S59.

Haskell, E. H., Hayes, R. B., Romanyukha, A. A. & Kenner, G. H. 2000. Preliminary report on the development of a virtually nondestructive additive dose technique for EPR dosimetry. *Applied Radiation and Isotopes* 52: 1065-1070.

Haskell, E. H., Kenner, G. H. & Hayes, R. B. 1995. Electron Paramagnetic Resonance dosimetry of dentine following removal of organic material. *Health Physics* 68: 579-584.

Hayes, R. B. Electron paramagnetic resonance dosimetry: Methodology and material characterization. 0-128. 1999. The university of Utah. Ph.D. Dissertation

Hayes, R. B., Haskell, E. H., Barrus, J. K., Kenner, G. H. & Romanyukha, A. A. 2000a. Accurate EPR radiosensitivity calibration using small sample masses. *Nuclear Instruments & Methods in Physics Research Section A- Accelerators Spectrometers Detectors and Associated Equipment* 441: 535-550.

Hayes, R. B., Haskell, E. H. & Kenner, G. H. 1997. A mathematical approach to optimal selection of dose values in the additive dose method of EPR dosimetry. *Radiation Measurements* 27: 315-323.

Hayes, R. B., Haskell, E. H., Kenner, G. H. & Barrus, J. K. 2000b. A virtually nondestructive EPR technique accounting for diagnostic X-rays. *Radiation Measurements* 32: 559-566.

Hayes, R. B., Haskell, E. H., Romanyukha, A. A. & Kenner, G. H. 1998a. Technique for increasing reproducibility in EPR dosimetry of tooth enamel. *Measurement Science & Technology* 9: 1994-2006.

Hayes, R. B., Kenner, G. H. & Haskell, E. H. 1998b. EPR dosimetry of pacific walrus (odobenus rosmarus divergens) teeth. *Radiation Protection Dosimetry* 77: 55-63.

Hennig, G. J., Herr, W., Weber, E. & Xirotiris, N. I. 1981. ESR-dating of the fossil hominid cranium from Petralona Cave, Greece. *Nature* 292: 533-536.

Hilson, S. 1986. Teeth.: Cambridge University Press New York.

Hong, D. G., Galloway, R. B., Takano, M. & Hashimoto, T. 2001. Evaluation of environmental dose at JCO using luminescence from quartz stimulated by blue light. *Radiation Protection Dosimetry* 94: 329-333.

Hutt, G., Brodski, L. & Polyakov, V. 1996. Gamma ray dose assessment after the 1994 radiation accident in Kiisa (Estonia): Preliminary results. *Applied Radiation and Isotopes* 47: 1329-1334.

IAEA . Handbook on calibration of radiation portection monitoring instruments. IAEA Technical Series No 133. 1971. Vienna, International Atomic Energy Agency.

IAEA . Biological dosimetry, Chromosomal aberration analysis for dose assessment. STI/PUB/10/260. 1986a. International Atomic Energy Agency, Vienna, Austria.

IAEA . Summary Report on the Post-Accident Review Meeting on the Chernobyl Accident. INSAG-1. 1986b. International Atomic Energy Agency, Vienna , Austria. *Safety Series No. 75.*

IAEA . The radiological accident in Goiania. STP/PUB/815. 1988. International Atomic Energy Agency, Vienna, Austria.

IAEA . The radiological accident in San Salvador. STP/PUB/847. 1990. International Atomic Energy Agency, Vienna, Austria.

IAEA . The radiological accident in Soreq. STP/PUB/925. 1993. International Atomic Energy Agency, Vienna, Austria.

IAEA . An electron accelerator accident in Hanoi, Viet Nam. STP/PUB/1008. 1996a. International Atomic Energy Agency, Vienna, Austria.

IAEA . Lessons learned from accidents in industrial irradiation facilities. STP/PUB/1015. 1996b. International Atomic Energy Agency, Vienna, Austria.

IAEA . The radiological accident at irradiation facility in Nesvizh. STP/PUB/1010. 1996c. International Atomic Energy Agency, Vienna, Austria.

IAEA . ENDF-6 Formats Manual 1997. IAEA-NDS-76. 2002. Nuclear Data Section, International Atomic Energy Agency, Vienna, Austria.

ICRU . Neutron dosimetry for biology and medicine. 1977. International Commission on Radiation Units and Measurements, Bethesa, MD.

ICRU . Tissue substitutes in radiation dosimetry and measurement. 44. 1989. International Commission on Radiation Units and Measurements, Bethesa, MD.

ICRU . Fundamental quantities and units for ionizating radiation. 60. 1999. International Commission on Radiation Units and Measurements, Bethesa, MD.

Ignatiev, E. A., Romanyukha, A. A., Koshta, A. A. & Wieser, A. 1996. Selective saturation method for EPR dosimetry with tooth enamel. *Applied Radiation and Isotopes* 47: 333-337.

Ikeya, M. & Ishii, H. 1989. Atomic bomb and accident dosimetry with ESR: Natural rocks and human tooth *in vivo* spectrometer. *Applied Radiation and Isotopes* 40: 1021-1027.

Ikeya, M., Miki, T., Kai, A. & Hoshi, M. 1986. ESR dosimetry of A-bomb radiation using tooth enamel and granite rocks. *Radiation Protection Dosimetry* 17: 181-184.

Ikeya, M., Sumitomo, H., Yamanaka, C., Lloyed, D. C. & Edwards, A. A. 1996. ESR dosimetry of a deceased radiation worker. *Applied Radiation and Isotopes* 47: 1341-1344.

Ikeya, M., Zimmerman, M. R. & Whitehead, N. 1993. New applications of Electron Spin Resonance dating, dosimetry and microscopy. World Scientific New Jersey.

Inaba, J. 2000. Radiological and environmental aspects of the criticality accident in Tokai-Mura. *Radiation Protection Dosimetry* 92: 239-246.

Ishii, H. & Ikeya, M. 1990. An Electron Spin Resonance system for *in vivo* human tooth dosimetry. *Japanese Journal of Applied Physics* 29: 871-875.

Ivannikov, A. I., Gaillard-Lecanu, E., Trompier, F., Stepanenko, V. F., Skvortsov, V. G., Yermakova, N., Tikunov, D. D. & Petin, D. V. 2003. Dose reconstruction by EPR spectroscopy of tooth enamel: Application to the population of Zaborie village exposed to high radioactive contamination after the Chernobyl accident. *Health Physics* (in press).

Ivannikov, A. I., Skvortsov, V. G., Stepanenko, V. F., Tikunov, D., Fedosov, I., Romanyukha, A. A. & Wieser, A. 1997. Wide-scale EPR retrospective dosimetry: Results and problems. *Radiation Protection Dosimetry* 71: 175-180.

Ivannikov, A. I., Skvortsov, V. G., Stepanenko, V. F., Tsyb, A. F., Khamidova, L. G. & Tikunov, D. D. 2000. Tooth enamel EPR dosimetry: sources of errors and their correction. *Applied Radiation and Isotopes* 52: 1291-1296.

Ivannikov, A. I., Tikounov, D. D., Skvortsov, V. G., Stepanenko, V. F., Khomichyonok, V. V., Khamidova, L. G., Skripnik, D. D., Bozadjiev, L. L. & Hoshi, M. 2001. Elimination of the background signal in tooth enamel samples for EPR-dosimetry by means of physical –chemical treatment. *Applied Radiation and Isotopes* 55: 701-705.

Iwasaki, M., Miyazawa, C., Uesawa, T. & Itoh, I. 1998. ESR dosimetry of human teeth enamel from a subject undergoing radiation treatment for cancer of the Epipharinx. *Radioisotopes* 47: 36-40.

Jones, I. M., Galick, H., Kato, P., Longlois, R. G., Mendelsohn, M. L., Murphy, G. A., Pleshanov, P., Ramsey, M. J., Thomas, C. B., Tucker, J. D., Tureva, L., Vorobtsova, I. & Nelson, D. O. 2002. Three somatic genetic biomarkers and covariates in radiation-exposed Russian cleanup workers of the Chernobyl nuclear reactor 6-13 years after exposure. *Radiation Research* 158: 424-442.

Katsumura, Y., Hamamoto, M., Yanagi, H. & Tabata, Y. 1980. Spatial distribution of radicals produced by fast neutron irradiation. *Radiation Physics and Chemistry* 16: 255-262.

Katsumura, Y., Tabata, Y., Seguchi, T., Morishita, N. & Kojima, T. 1986. Fast neutron irradiation effects-III sensitivity of alanine systems for fast neutron having an energy of ~ 1 MeV. *Radiation Physics and Chemistry* 28: 337-341.

Khan, R. F. H., Rink, W. J. & Boreham, D. R. Biophysical dosimetry using Electron Spin Resonance in human and rodent teeth. 49th Annual meeting of Radiation Research Society, April 20-24, 2002a, Reno (NV).

Khan, R. F. H., Rink, W. J. & Boreham, D. R. Dosimetric response evaluation of tooth enamel for the accelerator based neutron radiation, 10th international conference on Luminescence and Electron Spin Resonance Dating, June 24-28, 2002b, Reno (NV).

Khan, R. F. H., Rink, W. J. & Boreham, D. R. Biophysical dosimetry using electron paramagnetic resonances in human tooth, 29th Annual Canadian Nuclear Society/ Canadian Nuclear Association Annual conference, June 2-5, 2002c, Toronto (ON).

Khan, R. F. H., Rink, W. J. & Boreham, D. R. 2003a. Dosimetric response evaluation of tooth enamel for the accelerator based neutron radiation, *Radiation Measurements* (In press)

Khan, R. F. H., Boreham, D. R & Rink, W. J. 2003b. Quantification of low amplitude dosimetric signal in EPR teeth dosimetry – a novel approach, *Radiation Protection Dosimetry* 103 (4): 359-363.

Khan, R. F. H., Rink, W. J. & Boreham, D. R. 2003c. Biophysical dose measurement using Electron paramagnetic resonances in rodent teeth, *Applied Radiation and Isotopes* (In press).

Kirillov, V., Dubovsky, S. & Tolstik, S. 2002. Artifacts of Electron Paramagnetic Resonance dosimetry caused by a mechanical effect on samples of tooth enamel. *Radiation Protection Dosimetry* 102: 41-48.

Knoll, G. F. 2001. Radiation detection and measurement. John Wiley & Sons, New York.

Knowles, P. F., Marsh, D. & Rattle, H. W. E. 1976. Magnetic resonance of biomolecules - An introduction to the theory and practice of NMR and ESR in biological systems. John Wiley & Sons, Toronto.

Koshta, A. A., Wieser, A., Ignatiev, E. A., Bayankin, S., Romanyukha, A. A. & Degteva, M. O. 2000. New computer procedure for routine EPR-dosimetry on tooth enamel: description and verification. *Applied Radiation and Isotopes* 52: 1287-1290.

Kubelka, D., Garaj-Vrhavoc, V., Hebrang, V. & Simpraga, M. 1999. Possible discrepancies between dicentric chromosome frequencies and recorded ionizing radiation doses: *in vivo* study. *American Journal of Industrial Medicine* 36: 469-474.

Lamarsh, J. R. 1983. Introduction to Nuclear Engineering. Addison-Wesley Massachusetts.

Liidja, G., Past, J., Puskar, J. & Lippmaa, E. 1996. Paramagnetic resonance in tooth enamel created by ultraviolet light. *Applied Radiation and Isotopes* 47: 785-788.

Lushbaugh, C., Eisele, G., Burr Jr., W., Hubner, K. & Wachholz, B. 1991. Current status of biological indicators to detect and quantify previous exposures to radiation. *Health Physics* 60: 103-109.

Lyons, R. G. 1987. Alpha effectiveness in ESR dating: A preliminary note on energy dependence. *Ancient TL* 5: 4-5.

Marino, A. A. & Becker, R. O. 1968. Mechanically induced free radicals in bones. *Nature* 218: 466-467.

Mel'nichenko, E. M., Kushner, A. N., Miliutin, A. A., Mashevskii, A. A. & Muravskii, V. A. 2002. Evaluation of absorbed doses of ionizing radiation by milk teeth enamel in children living in the Belarus Republic. *Stomatologiia (Mosk)* 81: 54-56.

Moquet, J. E., Edwards, A. A., Lloyd, D. C. & Hones, P. 2000. The use of FISH chromosomes painting for assessment of old doses of ionizing radiation. *Radiation Protection and Dosimetry* 88: 27-33.

Muramatsu, Y., Noda, Y., Yonehara, H., Ishigure, N., Yoshida, S., Yukawa, M., Tagami, K., Ban-nai, T., Uchida, S., Hirama, T., Akashi, A. & Nakamura, Y. 2001. Determination of radionuclides produced by neutrons in heavily exposed workers of the JCO criticality accident in Tokaimura for estimating an individual's neutron fluence. *Journal of Radiation Research* 42: S117-S128.

Nakamura, N. & Miyazawa, C. 1997. Alkaline denaturation of dentine - A simple way to isolate human tooth enamel for electron spin resonance dosimetry. *Journal of Radiation Research* 38: 173-177.

Oduwole, A. D. & Sales, K. D. 1994. Transient ESR signals induced by γ-irradiation in tooth enamel and bone. *Quaternary Geochronology* 13: 647-650.

Oliveira, C. A. N., Farina, R., Bertelli, L., Natarajan, A. T., Ramalho, A. T. & Dantas, B. M. 1991. Measurements of ^{137}Cs in Blood from individuals exposed during the Goianian accident. *Health Physics* 60: 41-42.

Oms, O., Agusti, J., Gabs, M. & Andan, P. 2000. Lithostratigraphical correlation of micromammal sites and biostratigraphy of the Upper Pliocene to Lower Pleistcene in the northeast Guadix-Baza Basin (Southern Spain). *Journal of Quaternary Science* 15: 43-50.

Onori, S., Aragno, D., Fattibene, P., Petetti, E. & Pressello, M. C. 2000. ISS protocol for EPR tooth dosimetry. *Radiation Measurements* 32: 787-792.

Ostrowski, K., Goclawska, A. D. & Stachowicz, W. 1980. Stable radiation-induced paramagnetic entities in tissue mineral and their use in calcified tissue research. In Pryor, W. (Ed) Free radicals in Biology (pp. 321-342). NewYork: Academic Press.

Pass, B. 1997. Collective radiation biodosimetry for dose reconstruction of acute accidental exposures: A review. *Environmental Health Perspectives* 105: 1397-1402.

Pass, B. & Aldrich, J. E. 1985. Dental enamel as an *in vivo* dosimeter. *Medical Physics* 12: 305-307.

Pass, B., Wood, R. E., Liu, F. F., McLean, M. & Aldrich, J. E. 1998. High radiation doses from radiotherapy measured by Electron Spin Resonance in dental enamel. *Radiation Protection Dosimetry* 76: 239-247.

Pejovic-Milic, A. An accelerator based *in vivo* measurement of aluminum in human bone by neutron activation analysis. 1998. Ph. D. Dissertation, McMaster University, Hamilton Ontario.

Polyakov, V., Haskell, E., Kenner, G., Huett, G. & Hayes, R. 1995. Effect of mechanically induced background signal on EPR dosimetry of tooth enamel. *Radiation Measurements* 24: 249-254.

Prasanna, P. G., Kolanko, C. J., Gerstenberg, H. M. & Blakely, W. F. 1997. Premature chromosome condensation assay for biodosimetry: studies with fission-neutrons. *Health Physics* 72: 594-600.

Rink, W. J. 1997. Electron spin resonance (ESR) dating and ESR applications in quaternary science and archaeometry. *Radiation Measurements* 27: 975-1025.

Rink, W. J. & Schwarcz, H. P. 1994. Dose response of ESR signals in tooth enamel. *Radiation Measurements* 23: 481-484.

Romanyukha, A. A., Degteva, M. O., Kozheurov, V. P., Wieser, A., Jacob, P., Ignatiev, E. A., Vorobiova, M. I. & . 1996a. Pilot study of the Urals population by tooth electron paramagnetic resonance dosimetry. *Radiation Environmental Biophysics* 35: 305-310.

Romanyukha, A. A., Desrosiers, M. F. & Regulla, D. F. 2000a. Current issues on EPR dose reconstruction in tooth enamel. *Applied Radiation and Isotopes* 52: 1265-1273.

Romanyukha, A. A., Ignatiev, E. A., Degteva, M. O., Kozheurov, V. P., Wieser, A. & Jacob, P. 1996b. Radiation doses from Ural region. *Nature* 381: 199-200.

Romanyukha, A. A., Ignatiev, E. A., Vasilenko, E. K., Drozhko, E. G., Wieser, A., Jacob, P., Keirim-Markus, I. B., Kleschenko, E. D., Nakamura, N. & Miyazawa, C. 2000b. ESR dose reconstruction for Russian nuclear workers. *Health Physics* 78: 15-20.

Romanyukha, A. A., Nagy, V., Sleptchonok, O., Desrosiers, M. F., Jiang, J. & Heiss, A. 2001. Individual biodosimetry at the natural radiation background level. *Health Physics* 80: 71-73.

Romanyukha, A. A. & Regulla, D. F. 1996. Aspects of retrospective ESR dosimetry. *Applied Radiation and Isotopes* 47: 1293-1297.

Romanyukha, A. A., Regulla, D. F., Vasilenko, E. K. & Wieser, A. 1994. South Ural nuclear workers: Comparison of individual doses from retrospective EPR dosimetry and operational personal monitoring. *Applied Radiation and Isotopes* 45: 1195-1199.

Romanyukha, A. A., Regulla, D. F., Vasilenko, E. K., Wieser, A., Drozhko, E. G., Lyzlov, A. F., Koshurnikova, N. A., Shilnikova, N. S. & Panfilov, A. P. 1996c. Verification of occupational doses at the first nuclear plant in the former Soviet Union. *Applied Radiation and Isotopes* 47: 1277-1280.

Rossi, A. M. & Poupeau, G. 1990. Radiation damage in bioapatites: the ESR spectrum of irradiated dental enamel revisited. *Radiation Measurements* 17: 537-545.

Rossi, A. M., Wafcheck, C. C., de Jesus, E. F. & Pelegrini, F. 2000. Electron Spin Resonance dosimetry of teeth of Goiania radiation accident victims. *Applied Radiation and Isotopes* 52: 1297-1303.

Sagstuen, E., Theisen, H. & Henriksen, T. 1983. Dosimetry by ESR spectroscopy following a radiation accident. *Health Physics* 45: 961-968.

Saidoh, M. & Townsend, P. D. 1975. Mechanisms of defect formation. *Radiation Effects* 27: 1-12.

Schaffer, M., Schaffer, P. M., Jori, G., Corti, L., Sotti, G., Hofstetter, A. & Duhmke, E. 2002. Radiation therapy combined with photofrin or 5-ALA: effect on Lewis sarcoma tumor lines implanted in mice. Preliminary results. *Tumori* 88: 407-410.

Schauer, D. A., Coursey, B. M., Dick, C. E., McLaughlin, W. L., Puhl, J. M., Desrosiers, M. F. & Jacobson, A. D. 1993. A radiation accident at an industrial accelerator facility. *Health Physics* 65: 131-140.

Schauer, D. A., Desrosiers, M. F., Le, F. G., Seltzer, S. M. & Links, J. M. 1994. EPR dosimetry of cortical bone and tooth enamel irradiated with X and gamma rays: Study of energy dependence. *Radiation Research* 138: 1-8.

Schiff, L. I. 1968. Quantum Mechanics. McGraw-Hill, Inc, New York.

Schwarcz, H. P. 1985. ESR studies of tooth enamel. *Nuclear Tracks* 10: 865-867.

Sevan'kaev, A. V., Lloyd, D. C., Edwards, A. A., Moquet, J. E., Nugis, V. Y., Mikhailova, G. M., Potetnya, O. I., Khvostunov, I. K., Guskova, A. K., Baranov, A. E. & Nadejina, N. M. 2002. Cytogenetic investigations of serious overexposures to an industrial gamma radiography source. *Radiation Protection Dosimetry* 102: 201-206.

Shimano, T., Iwasaki, M., Miyazawa, C., Miki, T., Kai, A. & Ikeya, M. 1989. Human tooth dosimetry for gamma rays and dental X rays using ESR. *Applied Radiation and Isotopes* 40: 1035-1038.

Shiraishi, K., Iwasaki, M., Miyazawa, C., Yonehara, H. & Matsumoto, M. 2002. Dose estimation by ESR on tooth enamel from two workers exposed to radiation due to JCO accident. *Journal of Radiation Research* 43: 331-335.

Shiraishi, K., Wanitsuksombut, W., Chinudomsab, K., Suzuki, G. & Nishizawa, K. ESR dose estimation of the radiological accident in Samut Prakarn, Thailand using sugar samples and ESR method. (In) International symposium on new prospects of ESR dosimetry and dating, 70. 2001.

Sholom, S. V., Chumak, V. V. & Pasalskaja, L. F. 2000a. Some aspects of EPR dosimetry of liquidators. *Applied Radiation and Isotopes* 52: 1283-1286.

Sholom, S. V., Haskell, E. H., Hayes, R. B., Chumak, V. V. & Kenner, G. H. 1998a. Properties of light induced EPR signals in enamel and their possible interference with gamma-induced signals. *Radiation Measurements* 29: 113-118.

Sholom, S. V., Haskell, E. H., Hayes, R. B., Chumak, V. V. & Kenner, G. H. 1998b. Influence of crushing and additive irradiation procedures on EPR dosimetry of tooth enamel. *Radiation Measurements* 29: 105-111.

Sholom, S. V., Haskell, E. H., Hayes, R. B., Chumak, V. V. & Kenner, G. H. 2000b. EPR-dosimetry with carious teeth. *Radiation Measurements* 32: 799-803.

Simmons, J. A. & Bewley, D. K. 1976. The effectiveness of fast neutrons in creating stable free radicals. *Radiation Research* 65: 197-201.

Skvortsov, V. G., Ivannikov, A. I. & Stepanenko, V. F. 2000. Application of EPR retrospective dosimetry for large-scale accidental situation. *Applied Radiation and Isotopes* 52: 1275-1282.

Stratton, W. R. A review of criticality accidents. LA-3611. 1967. Los Alamos National Laboratory, NM.

Stuglik, Z., Michalik, J., Stachowicz, W., Ostrowski, K., Zvara, I. & Dziedzic-Goclawska, A. 1994. Bone powder exposed to the action of ^{12}C and ^{25}Mg ion beams as investigated by Electron Paramagnetic Resonance spectroscopy. *Applied Radiation and Isotopes* 45: 1181-1187.

Stuglik, Z. & Sadlo, A. 1996. A response of L-α-alanine and standard bone powder on 3.4MeV/ amu ^{59}Co ion beams. *Applied Radiation and Isotopes* 47: 1219-1222.

Suleiman, O. H., Stern, S. H. & Spelic, D. C. 1999. Patient dosimetry activities in the United States: the nationwide evaluation of X ray trends (NEXT) and tissue dose handbooks. *Applied Radiation and Isotopes* 50: 247-259.

Swartz, H. M., Molenda, R. P. & Lofberg, R. T. 1965. Long-lived radiation induced electron spin resonances in an aqueous biological system. *Biochemical Biophysical Research Communications* 21: 61-65.

Takahashi, F., Yamaguchi, Y., Iwasaki, M., Miyazawa, C. & Hamada, T. 2001. Relations between tooth enamel dose and organ doses for electron spin resonance dosimetry against external photon exposure. *Radiation Protection Dosimetry* 95: 101-108.

Tatsumi-Miyajima, J. 1987. ESR dosimetry for Atomic bomb survivors and radiologic technologists. *Nuclear Instruments & Methods in Physics Research Section A- Accelerators Spectrometers Detectors and Associated Equipment* 257: 417-422.

Tatsumi, J. 1986. Dose estimation of radiation exposed people by ESR. *Filmbadge News (Tokyo)* 125: 1-10.

Toyoda, S., Hoshi, M., Ueda, Y., Nitta, Y., Miyazawa, C. & Romanyukha, A. Gamma ray response of ESR signals in tooth enamel of cows and mice. 10th International Conference on Luminescence and Electron Spin Resonance Dating . 2002.

UNSCEAR . United Nations Scientific Committee on the Effects of Atomic Radiation. 1993. United Nations, New York.

Vargo, G. J. 1999. A brief history of nuclear criticality accidents in Russia - 153-1997. *Health Physics* 77: 505-511.

Voight, G. & Paretzke, H. G. 1996. Scientific recommendations of radiation doses due to reactor accidents at Chernobyl. *Radiation Environmental Biophysics* 35: 1-9.

Wang, B., Takeda, H., Gao, W. M., Zhou, X. Y., Odaka, T., Ohyama, H., Yamada, T. & Hayata, I. 1999. Induction of apoptosis by beta radiation from tritium compounds in mouse embryonic brain cells. *Health Physics* 77: 16-23.

Wertz, J. E. & Bolton, J. R. 1972. Electron spin resonance; elementary theory and practical applications. McGraw Hills Inc.

Wieser, A., Haskell, E. H., Kenner, G. H. & Bruenger, F. 1994. EPR dosimetry of bone gains accuracy by isolation of calcified tissue. *Applied Radiation and Isotopes* 45: 525-526.

Wieser, A., Mehta, K., Amira, S., Aragno, D., Bercea, S., Brik, A., Bugai, A., Callens, F., Chumak, V., Ciesielski, B., Debuyst, R., Dubovsky, S., Duliu, O. G., Fattibene, P., Haskell, E. H., Hayes, R. B., Ignatiev, E. A., Ivannikov, A., Kirillov, V., Kleschenko, E., Nakamura, N., Nather, M., Nowak, J., Onori, S., Pass, B., Pivovarov, S., Romanyukha, A., Scherbina, O., Shames, A. I., Sholom, S., Skvortsov, V., Stepanenko, V., Tikounov, D. D. & Toyoda, S. 2000. The second international inter-comparison on EPR tooth dosimetry. *Radiation Measurements* 32: 549-557.

Wieser, A.A., 2002. private communication, GSF Forschungszentrum, Institut für Strahlenschutz, Ingolstaedter Landstrasse 1 Neuherberg, Germany.

Yamanaka, C., Ikeya, M. & Hara, H. 1993. ESR cavities for in vivo dosimetry of tooth enamel. *Applied Radiation and Isotopes* 44: 77-80.